UNIVERSITY OF OKLAHOMA

GRADUATE COLLEGE

ANALYSIS OF ENERGY CONSERVING LOW-ORDER MODELS

A DISSERTATION

SUBMITTED TO THE GRADUATE FACULTY

in partial fulfillment of the requirements for the

Degree of

DOCTOR OF PHILOSOPHY

By

YUNHENG WANG
Norman, Oklahoma
2007

Downloaded from SHAREOK. Persistent Handle URL: https://hdl.handle.net/11244/1304

UMI Number: 3291937



UMI Microform 3291937

Copyright 2008 by ProQuest Information and Learning Company.
All rights reserved. This microform edition is protected against
unauthorized copying under Title 17, United States Code.

ProQuest Information and Learning Company
300 North Zeeb Road
P.O. Box 1346
Ann Arbor, MI 48106-1346

ANALYSIS OF ENERGY CONSERVING LOW-ORDER MODELS

A DISSERTATION APPROVED FOR THE
SCHOOL OF COMPUTER SCIENCE

BY

_____
S. Lakshmivarahan, Committee Chair

_____
Ming Xue

_____
Krishnaiya Thulasiraman

_____
Sudarshan Dhall

_____
John Antonio

© Copyright by YUNHENG WANG 2007
All Rights Reserved.

ACKNOWLEDGEMENTS

First, I thank my advisor Professor S. Lakshmivarahan. Without his guidance and constant encouragement throughout the Ph.D. program, this study would not have been possible. I was always inspired by his research attitude and the spirit of never giving up. Professor Lakshmivarahan has taught me the ways to approach a research problem and the need to be persistent to accomplish any goal. I also would like to thank the rest of the committee members: Dr. Xue, Dr. Thulasiraman, Dr. Dhall and Dr. Antonio for offering a lot of good comments with my study since I started the doctoral program in the school of computer science.

Special thanks go to the administration office at CAPS, including Dr. Ming Xue, Dr. Kelvin Droegemeier, Debra Farmer and Eileen Hasselwander for their support and understanding because I have maintained a full-time job at CAPS while this study was done. Debra Farmer and Eileen Hasselwander always processed the extra paper works for me on time without complaint. I am also grateful to Dr. Xue and Dr. Droegemeier for many useful discussions when initiating the research.

Last, but not least, I thank my family for their selfless love and unconditional support. In order to support my study, my wife, Haiping, has given up many good opportunities, and my son, Tony, has lost many weekends to play together with his father.

TABLE OF CONTENTS

ABSTRACT ..... **X**

CHAPTER 1 INTRODUCTION **1**

1.1 A CLASS OF LOW-ORDER MODELS 1
1.2 THE FAMILIES OF MODELS OF INTEREST 3
1.3 THE GALERKIN PROJECTION METHOD 8
1.4 NEEDS FOR ENERGERY CONSERVATION 12
1.5 COUPLED GYROSTATS AS MODELS FOR ENERGY CONSERVING SYSTEMS 13
1.6 ORGANIZATION OF THE DISSERTATION 16

CHAPTER 2 A SET OF SUFFICIENT CONDITIONS FOR CONSERVING ENERGY IN LOMS **19**

2.1 INTRODUCTION 19
2.2 A SET OF SUFFICIENT CONDITIONS FOR ENERGY CONSERVING 21
2.3 SPECIAL CASES 32
2.3.1 Simplification of Theorem 2.1 ..... *32*
2.3.2 Definition of subset SELOM(n) and examples *34*
2.4 SUMMARY 38

CHAPTER 3 ON THE RELATION BETWEEN ENERGY CONSERVING LOMS AND THE SYSTEMS OF COUPLED VOLTERRA GYROSTATS **39**

3.1 INTRODUCTION 39
3.2 A PROOF OF THE INCLUSION $\mathbf{CVG}(n) \subseteq \mathbf{SELOM}(n)$ 42
3.3 CONVERSION OF THE ENERGY CONSERVING LOM AS A SYSTEM OF COUPLED GYROSTATS: AN ALGORITHM 48
3.3.1 Properties of gyrostats used in the algorithm *49*
3.3.2 The algorithm *51*
3.3.3 Description of the algorithm *52*
3.4 CONCLUSION 56

CHAPTER 4 THE EXTENDED DEFINITION OF GYROSTATS AND ITS EQUIVALENCE WITH ENERGY CONSERVING LOMS **58**

4.1 INTRODUCTION 58
4.2 GENERALIZED VOLTERRA GYROSTATS WITH NONLINEAR FEEDBACK 60
4.3 ON THE EQUIVALENCE BETWEEN ELOM(N) AND CGVG(N) 63
4.4 CONCLUSION 69

CHAPTER 5 ANALYSIS OF VOLTERRA GYROSTATS: STABILITY OF EQUILIBRIA **71**

5.1 INTRODUCTION 71
5.2 THE FAMILY OF VOLTERRA GYROSTATS 73
5.3 STABILITY ANALYSIS OF GYROSTATS 79
5.3.1 The degenerated gyrostats *81*
5.3.2 Gyrostats with uniform properties for the equilibria *83*
5.3.3 Gyrostats with linear equilibria but the stability is not uniform *87*
5.3.4 Gyrostats with equilibrium as a 2-D curve line *98*
5.3.5 Stability of equilibrium for gyrostat in general form *106*
5.4 CONCLUSION 113

CHAPTER 6 THE HAMILTONIAN STRUCTURE OF ENERGY CONSERVING LOMS **115**

6.1 INTRODUCTION 115
6.2 THE CANONICAL HAMILTONIAN SYSTEM AND THE POISSON BRACKET 115
6.3 NON-CANONICAL HAMILTONIAN SYSTEM AND THE CASIMIR INVARIANT 118
6.4 STUDY OF COUPLED GYROSTATS AS HAMILTONIAN LOMS 122
6.4.1 Variants of the skew symmetric matrix J for SELOM(n) 123
6.4.2 Verification of Jacobin identity 125
6.4.3 Examples of the coupled gyrostats as Hamiltonian systems 128
6.5 LOMS FOR BURGER'S EQUATION AS HAMILTONIAN SYSTEMS 133
6.5.4 Kinetic energy as Hamiltonian 133
6.5.5 Hamiltonian function as a cubic function 134
6.6 CONCLUSIONS 135

CHAPTER 7 CONCLUSION 137

BIBLIOGRAPHY 142

APPENDIX A REGROUPING OF THE NONLINEAR TERMS IN ODES 148

APPENDIX B VOLTERRA GYROSTAT: AN OVERVIEW 150

APPENDIX C CARDAN'S FORMULA FOR THE ROOTS OF A CUBIC POLYNOMIAL 154

LIST OF TABLES

Table 3.1 An enumeration of distinct (k, l, m)-gyrostats for LOM with order n. 44
Table 3.2 Four types of gyrostats used in the algorithm.....50
Table 3.3 A listing of gyrostats with non-zero linear terms 54
Table 3.4 Distribution – the number and the types of gyrostats 55
Table 4.1 Special cases of the GVG(3) corresponding to the triplet (k, l, m) in (4.14) 66
Table 5.1 A listing of the special gyrostats and their number of equilibrium sets 77
Table 5.2 Properties of equilibria – Case 5.....84
Table 5.3 Specification of Equilibria – General gyrostat 107
Table 5.4 The shapes of the equilibria in the state space for each case.....113
Table B.1 Special Cases of Volterra gyrostat 152
Table B.2 A representation of the gyrostats used in the main body 153
Table C.1 The roots of a cubic polynomial.....157

LIST OF FIGURES

Figure 2.1 Low-order model hierarchy arising from Galerkin projection 36
Figure 3.1 Patterns of assignment of linear terms into the gyrostats 54
Figure 4.1 Two classes of models: (a) low-order models arising from Galerkin projection59
Figure 5.1 The relation between the various special cases of the Volterra Gyrostat. It is assumed that $a \neq 0$ and $b \neq 0$. Number of different sets of equilibria is given in brackets. Red numbers in parenthesis denote the number of nonlinear terms and green numbers for the number of linear terms. Background colors are used to distinguish the stability properties of the equilibria. 79
Figure 5.2 An illustration of the heteroclinic orbit starting from $\boldsymbol{\omega}(0) = \boldsymbol{\omega}^* + \boldsymbol{\delta}$, $\boldsymbol{\omega}^* = (0.7, 0, 0)^{\mathrm{T}}$, $\boldsymbol{\delta} = (0, 0.001, 0)^{\mathrm{T}}$, $\mathbf{I} = (4, 3, 7)^{\mathrm{T}}$ and $\mathbf{h} = (0, 0, 0)^{\mathrm{T}}$ for Case 5. $\boldsymbol{\omega}^* \in \boldsymbol{\varepsilon}_1$ is a saddle point. 85
Figure 5.3 An illustration of the orbit starting from $\boldsymbol{\omega}(0) = \boldsymbol{\omega}^* + \boldsymbol{\delta}$, $\boldsymbol{\omega}^* = (0.7, 0, 0)^{\mathrm{T}}$, $\boldsymbol{\delta} = (0, 0.001, 0)^{\mathrm{T}}$, $\mathbf{I} = (3, 7, 4)^{\mathrm{T}}$ and $\mathbf{h} = (0, 0, 0)^{\mathrm{T}}$ for Case 5. $\boldsymbol{\omega}^* \in \boldsymbol{\varepsilon}_1$ is a center...86
Figure 5.4 Relative disposition of the three equilibria for Case 6. $\boldsymbol{\varepsilon}_1 = (\omega_1, 0, 0)^{\mathrm{T}}$, $\boldsymbol{\varepsilon}_2 = (-\frac{d_{13}}{c}, \omega_2, 0)^{\mathrm{T}}$ and $\boldsymbol{\varepsilon}_3 = (\frac{d_{12}}{b}, 0, \omega_3)^{\mathrm{T}}$. $\mathbf{I} = (4, 3, 7)^{\mathrm{T}}$, $\mathbf{h} = (0.8, 0, 0)^{\mathrm{T}}$, a = -1, b = 1, c = 0.14286, d_{12} = 0.2667, d_{13} =0.1143. Every point along the ω_1–axis that are in the interval (α, β) is a center. Points along the ω_1-axis outside of the interval (α, β) are saddle points. 88
Figure 5.5 An illustration of the homoclinic orbits for Case 6 with equilibria affixed. The parameters are $\mathbf{I} = (4, 3, 7)^{\mathrm{T}}$ and $\mathbf{h} = (0.8, 0, 0)^{\mathrm{T}}$. Both orbits starts from $\boldsymbol{\omega}(0) = \boldsymbol{\omega}^* + \boldsymbol{\delta}$ with $\boldsymbol{\delta} = (0, 0.001, 0)^{\mathrm{T}}$ and $\boldsymbol{\omega}^* \in \boldsymbol{\varepsilon}_1$ is a saddle point. (a) $\boldsymbol{\omega}^* = (0.7, 0, 0)^{\mathrm{T}}$ (b) $\boldsymbol{\omega}^* = (2, 0, 0)^{\mathrm{T}}$ 91
Figure 5.6 Relative disposition of the two equilibria for the Lorenz gyrostat. $\boldsymbol{\varepsilon}_1 = \{(\omega_1, 0, 0)^{\mathrm{T}}, \omega_1 \in \mathrm{R}\}$ and $\boldsymbol{\varepsilon}_3 = \{(\omega_1 = -\frac{d_{12}}{a}, 0, \omega_3)^{\mathrm{T}}, \omega_3 \in \mathrm{R}\}$. The parameters are $\mathbf{I} = (4, 4, 7)^{\mathrm{T}}$, $\mathbf{h} = (0.8, 0, 0)^{\mathrm{T}}$, a = -0.75, c = 0, d_{12} = 0.2, d_{13} = 0.1143 and α = 0.2667 94
Figure 5.7 A relative disposition of the two equilibria in case 7. The parameters used are $\mathbf{I} = (4,3,7)^{\mathrm{T}}$ and $h = (0.8,0.3,0)^{\mathrm{T}}$ 99
Figure 5.8 A plot of the numerator of $\mathrm{P}(\omega_1)$ for Case 7. 102
Figure 5.9 An illustration of the closed orbit that is homoclinic for Case 7. The orbit starting from $\boldsymbol{\omega}(0) = \boldsymbol{\omega}^* + \boldsymbol{\delta}$ with $\boldsymbol{\omega}^* = (0.7, 0.140, 0)^{\mathrm{T}}$ and $\boldsymbol{\delta} = (0, 0.001, 0)^{\mathrm{T}}$. The parameters used are $\mathbf{I} = (4,3,7)^{\mathrm{T}}$, $h = (0.8,0.3,0)^{\mathrm{T}}$. 102
Figure 5.10 A plot of the equilibrium curve in the (ω_1, ω_3)-plane ($\omega_2 = 0$) for Case 3...103
Figure 5.11 A plot of the numerator of $P(\omega_1)$ for Case 3. 105
Figure 5.12 A plot of the projection of the equilibrium curve $\boldsymbol{\varepsilon}_1$ on plane (ω_1, ω_2) and plane (ω_1, ω_3) respectively for the general Volterra gyrostat. 109
Figure 5.13 A plot of the discriminant $\Delta(\omega_1)$ for the Volterra gyrostat.....111

Figure 5.14 A plot of the discriminant $\Delta(\omega_1)$ for Case 4. 111
Figure 5.15 An illustration of the homoclinic orbit starting from $\boldsymbol{\omega}(0) = \boldsymbol{\omega}^* + \boldsymbol{\varepsilon}$ with $\boldsymbol{\omega}^* = (1.7, 0.204, -0.32692)^T$ and $\boldsymbol{\varepsilon} = (0, 0.001, 0)^T$. Parameters used are $\mathbf{I} = (5,4,7)^T$ and $h = (0.8,0.3,0.5)^T$. 112

ABSTRACT

Low-order models of order n, denoted by LOM(n), naturally arise in the application of Galerkin type projection techniques to a system of partial differential equations of interest in geophysical domain. In order for the LOM(n) to represent physically meaningful solution, it is necessary that LOM(n) conserves energy. The Galerkin projection technique does not incorporate any explicit criteria for the choice of the order and the modes to guarantee energy conservation. With this study, we derive a new set of sufficient conditions on the structural parameter of LOM(n) for conserving energy.

It is well known in Mathematical Physics that the Volterra gyrostat and many of its special cases including the Euler gyroscope represent a prototype of energy conserving dynamical systems. It is formally proved in this dissertation that the systems of coupled Volterra gyrostats are special cases of LOMs that satisfies the new sufficient conditions. We also introduce the definition of the generalized Volterra gyrostats that contains nonlinear feedback. Exploiting the inherent relation between the energy conserving LOMs satisfying the sufficient conditions and the systems of coupled generalized Volterra gyrostats, it turns out that these two sets of systems are equivalent. Using the class of generalized Volterra gyrostats as basic building block, any energy conserving low-order model that routinely arise in fluid dynamics, turbulence and atmospheric sciences can be converted into a system of coupled generalized gyrostats. An algorithm for doing such a transformation is provided.

Motivated by the importance and the central role played by the Volterra gyrostat in studying LOMs, this study also analyze the stability properties of the classical Volterra gyrostat and all of its special cases.

Chapter 1
Introduction

1.1 A CLASS OF LOW-ORDER MODELS

Starting with the pioneering work of Saltzman (1959), Platzman (1962), and Lorenz (1960, 1963), great strides have been made in the analysis of complex (fluid) dynamical systems using the lower order (spectral) models (with and without dissipation and forcing). Lorenz (1960) using one of the simplest lower order models explained the transfer of energy between the zonal flow and the disturbances thereby describing the phenomenon of index cycles (Namias (1950)) as observed in a real atmosphere. For a thorough review of the analysis and application of the lower order models refer to the monographs by De Swart (1989) and Krishnamurti et al. (1998) and paper by Wiin-Nielson (1992).

In this study, our purpose is to analyze the properties of a class of Low-Order Models (LOM) of interest in geophysical fluid dynamics. The structure of LOM (of order *n*) of interest in this domain is given by

$$\dot{\mathbf{x}} = \mathbf{A}(\mathbf{x}, \mathbf{x}) + B\mathbf{x} + \mathbf{c} \tag{1.1}$$

where $\mathbf{x} = (x_1, x_2, \cdots, x_n)^T \in \Re^n$ is called the **state vector**, representing the different **modes** in the **spectral expansion** of a chosen meteorological field, such as velocity, pressure, temperature, *etc*; $\mathbf{A}(\mathbf{x}, \mathbf{x}) = (\mathbf{x}^T A^{(1)}\mathbf{x}, \mathbf{x}^T A^{(2)}\mathbf{x}, \cdots, \mathbf{x}^T A^{(n)}\mathbf{x}) \in \Re^n$ is a vector of *n* quadratic forms with $A^{(i)} \in \Re^{n \times n}$ is an *n* x *n* matrix for *i* = 1, 2,…,*n*; $B \in \Re^{n \times n}$ is a *n* x *n*

matrix and $\mathbf{c} = (c_1, c_2, \cdots, c_n)^T \in \Re^n$ is a vector. Expressed in the component form (1.1) becomes

$$\begin{aligned} \dot{x}_i &= \mathbf{x}^T A^{(i)} \mathbf{x} + B_i \mathbf{x} + c_i \\ &= \sum_{p=1}^{n} \sum_{q=1}^{n} x_p a_{pq}^{(i)} x_q + \sum_{q=1}^{n} b_{iq} x_q + c_i \end{aligned} \tag{1.2}$$

where B_i in (1.2) denotes the ith row of B. In this model (1.2), the first term $\mathbf{x}^T A^{(i)} \mathbf{x}$ denotes the nonlinear interaction between the various modes; the diagonal elements of the matrix B denotes the frictional terms and the off-diagonal elements of B represents the coefficients of the linear feed-back between the states. The components of the vector $\boldsymbol{c}$ denotes the external forcing.

Let LOM(n) denote the set of all n^{th} order nonlinear coupled systems of ODEs of the type (1.1). To avoid excessive notation, we will use LOM(n) to denote both the set defined above as well as the member of this set.

LOM(n) of the type (1.1) often arise as a result of applying the well-known Galerkin projection technique (Saltzman 1962, Lonrenz 1960, 1963) to a system of partial differential equations of interest in a number of application areas – in the analysis of multi-flow equilibrium and blocking in the atmosphere (Charney and DeVore (1979)), in atmospheric circulation studies (DeSwart (1988)), in atmospheric predictability (Legras and Ghil (1985)), in climate study (Roebber (1995)) and the strongly coupled tropical atmospheric / ocean system associated with El-Niño-Southern Oscillation (ENSO) (Peña and Kalnay (2004)). The low-order models are also known as the low-dimensional models in fluid mechanics and turbulence (Holmes *et al.* (1996)). Depending

on the phenomenon in question, the order of the LOM (also known as the degrees of freedom of the reduced order model) varies from three for the analysis of atmospheric index cycles by Lorenz (1960) to an order of hundred for the fully developed three dimensional turbulence (Bohr *et al.* (1998)).

1.2 THE FAMILIES OF MODELS OF INTEREST

Many models of interest in engineering and scientific applications arise as a special case of the Navier-Stokes equations or the primitive equations (Pedlosky (1987), Kundu (1990)). These models consist of a set of coupled nonlinear partial differential equations (PDEs) describing the space-time evolution of field variables including velocity, pressure, temperature, water content in all of its three phases, *etc*. Some of the typical models of interest in geophysical domain include the Burgers equation, geostrophic potential vorticity equation with forcing, topography and dissipation, and the Rayleigh-Bénard convection equations.

Burgers' equation (Platzman 1964). Let u = u(t, x) denotes the velocity as a function of time t and space variable x, where $t \geq 0$. It is assumed that $u(t, x)$ is periodic in x with $0 \leq x \leq 1$. Then $u(t, x)$ evolves according to

$$\frac{\partial u}{\partial t} + u\frac{\partial u}{\partial x} = \kappa \frac{\partial^2 u}{\partial x^2} \tag{1.3}$$

where κ is called the diffusion coefficient, and the nonlinear term $u\dfrac{\partial u}{\partial x}$ is called the nonlinear advection term that is responsible for the nonlinear interaction terms in (1.1). The initial and boundary conditions are specified as

$$u(0,x) = f(x)$$

and (1.4)

$$u(t,0) = \alpha \text{ and } u(t,1) = \beta \cdot$$

Geostrophic vorticity equation (Charney and DeVore 1979, De Swart 1988). Let $\psi(x,y)$ denote the stream function, then

$$u = -\frac{\partial \psi}{\partial x} \text{ and } v = \frac{\partial \psi}{\partial y} \tag{1.5}$$

denote the x component (east-west) and the y component (north-south) of the two dimensional velocity vector **v**. Thus, the vorticity ζ is given by

$$\zeta = \frac{\partial v}{\partial y} - \frac{\partial u}{\partial x} = \frac{\partial^2 \psi}{\partial x^2} + \frac{\partial^2 \psi}{\partial y^2} = \nabla^2 \psi \, . \tag{1.6}$$

Then the geostrophic vorticity equation relates to the evolution of vorticity $\zeta = \nabla^2 \psi$ given by

$$\frac{\partial}{\partial t}\left(\nabla^2 \psi - \frac{\psi}{\lambda^2} \right) + \mathrm{J}\left(\psi, \nabla^2 \psi - \frac{\psi}{\lambda} + f_0 \frac{h}{H} + \beta y \right) = f_0 \left(\frac{D_E}{2H} \right) \nabla^2 \left(\psi - \psi^* \right) \tag{1.7}$$

where

$$\mathrm{J}(a,b) = \begin{vmatrix} \dfrac{\partial a}{\partial x} & \dfrac{\partial a}{\partial y} \\ \dfrac{\partial b}{\partial x} & \dfrac{\partial b}{\partial y} \end{vmatrix} = \frac{\partial a}{\partial x}\frac{\partial b}{\partial y} - \frac{\partial a}{\partial y}\frac{\partial b}{\partial x} \tag{1.8}$$

is called the Jacobian (determinant),

$$\lambda^2 = \frac{gH}{f_0}$$

$f_0 = 2\Omega \sin \phi_0$, corriolis factor

$$\beta = \frac{2\Omega}{a} \cos \phi_0$$

Ω is the angular velocity of the earth rotation

a is the radius of the earth

ϕ_0 is the central lattitude.

Equation (1.7) represents the atmospheric flow between two horizontal walls separated by a distance πL apart, where h = h(x,y) denotes the lower boundary elevation (mountains and valleys). That is, $h(x,y)$ denotes the topography of the terrain over which the flow is modeled. Let H be the mean height confined between the boundaries. It is assumed that

$$|h(x,y)| \ll H \text{ and } \pi L \ll 2a .$$

The coefficient

$$D_E = \left(\frac{2\nu_E}{f_0} \right)^{1/2}$$

is called the Ekman depth and ν_E is the bulk eddy viscosity with the frictional boundary layer. The factor $f_0 \frac{D_E}{2H} \nabla^2 \psi$ represents the frictional term and $f_0 \frac{D_E}{2H} \nabla^2 \psi^*$ denotes the vorticity source which in the baroclinic case arises due to the thermal wind driven by radiation.

This equation has been be the basis for numerous investigation including those by Charney and DeVore (1979), DeSwart (1988), Lorenz (1960, 1963) to name a few.

Rayleigh-Bénard convection (Tong and Gluhovsky 2002). Let $\mathbf{x} = (x, y, z)^T$ denote the standard three dimensional space coordinates and t the time. $\mathbf{v} = \mathrm{v}(t, x) = (v_1(t, x), v_2(t, x), v_3(t, x))^T$ denote the velocity of the fluid element at time t and point x. It is assumed that the layer of fluid is confined between stress-free horizontal surfaces at $z \equiv 0$ and $z \equiv h$. The behavior of the fluid is periodic with period $2L$ in both x and y (horizontal) direction. Let $a = h/L$ define the aspect ratio for the problem. The bottom layer ($z = 0$) is at constant temperature T_0 and the top layer ($z = h$) is at temperature $T_0 - \delta T$ with $\delta T > 0$. The Oberbeck-Boussinesq equation that relates the hydrodynamic variable **v**-velocity, p – pressure and T – temperature is given by

$$\frac{\partial \mathbf{v}}{\partial t} + (\mathbf{v} \cdot \nabla)\mathbf{v} = -\frac{\nabla p}{\rho_0} - [1 - \alpha(T - T_0)]g\hat{z} + \nu\nabla^2\mathbf{v} \tag{1.9}$$

$$\frac{\partial T}{\partial t} + (\mathbf{v} \cdot \nabla)T = \kappa\nabla^2 T \tag{1.10}$$

and

$$\nabla \cdot \mathbf{v} = 0 \tag{1.11}$$

where ν is the kinematic viscosity, κ is the thermal diffusivity, α is the thermal expansion coefficient of the fluid, g is acceleration due to gravity and ρ_0 is the density of the fluid at $T = T_0$.

Equation (1.9) is called the momentum equation, (1.10) thermal energy conservation equation and (1.11) is the mass conservation.

It is convenient to normalize (1.9) - (1.11) to a dimensionless form as follows:

x, y, z are normalized by $\frac{h}{\pi}$

Temperature T by δT

Time t by $\tau = \sqrt{\frac{h}{g\alpha\delta T}}$

Pressure p by $\frac{\rho_0 h^2}{\pi^2 \tau^2}$

Kinematic viscosity (ν) and thermal diffusivity κ are by $\frac{h^2}{\pi^2 \tau}$.

The transformed system is given in the vorticity form where $\nabla \times \mathbf{v} = \zeta$ is the vorticity

$$\frac{\partial \zeta}{\partial t} = (\zeta \cdot \nabla)\mathbf{v} - (\mathbf{v} \cdot \nabla)\zeta + \nu \nabla^2 \zeta + \left(x \frac{\partial \theta}{\partial y} - y \frac{\partial \theta}{\partial x} \right) \tag{1.12}$$

$$\frac{\partial \theta}{\partial t} = -\mathbf{v} \cdot \nabla \theta + v_3 + \kappa \nabla^2 \theta \tag{1.13}$$

$$\nabla \cdot \mathbf{v} = 0 \tag{1.14}$$

where θ / π denotes the temperature deviation from the conductive steady state distribution. This flow is characterized by the Rayleigh number $R = \frac{\pi^4}{\nu\kappa}$, and Prandtl number $\sigma = \frac{\nu}{\kappa}$. The stress free boundary conditions are given by

$$v_3\big|_{\substack{z=0 \\ z=\pi}} = \left.\frac{\partial v_1}{\partial z}\right|_{\substack{z=0 \\ z=\pi}} = \left.\frac{\partial v_2}{\partial z}\right|_{\substack{z=0 \\ z=\pi}} = \theta\big|_{\substack{z=0 \\ z=\pi}} = 0 .$$

The fluid satisfies horizontal boundary conditions with period $\frac{2\pi}{a}$ along both x and y directions.

1.3 THE GALERKIN PROJECTION METHOD

It is well known that these infinite dimensional models described by the PDEs can be approximated by a set of n coupled nonlinear ordinary differential equations (ODEs) using, for example, the Galerkin type projection method. In the classical (so called spectral) method, the standard Fourier modes consisting of the trigonometric functions or the spherical harmonics (which are the eigen functions of differential operators) are used as the basis. Refer to the papers by Silberman (1954), Saltzman (1962), Platzman (1964), Lorenz (1960), (1962), (1963) and (1982) and the books by Canuto *et al.* (1988) and Krishnamurti *et al*. (2006) for details. With the ever increasing desire to produce realistic results with as few degrees of freedom as possible, it leads to the development of several alternatives to the classical Fourier basis functions.

The empirical orthogonal functions (EOF) which are eigen functions of the covariance operator became a popular basis in meteorology (Rinne and Karhilla (1975), and Crommelin and Majda (2004)). EOF based analysis is also known as the principal component analysis (PCA) and as Karhunen-Loéve expansion. In fluid dynamics and turbulence literature, EOF based approach is also known as proper orthogonal decomposition (POD). Refer to Chapter 3 in Holmes *et al*. (1996) for details. A recent tutorial by Smith *et al*. (2005) provides an excellent overview of the model reduction process using POD. The special issue on "Dimension Reduction of Dynamical Systems: Methods, Models, Application" edited by Rega and Troger (2005) provides an up-to-date

coverage of topics in this area. More recently, other bases including the principal interaction patterns (PIP) by Achatz *et al*. (1995), Kwasniok (1996), (2001) and (2004), and optimal persistent patterns (OPP) by DelSole (2001) have been introduced. Crommelin and Majda (2004) contains an interesting comparison of these bases. Also refer to Farell and Ioannou (2001).

It turns out that irrespective of the basis used, the resulting low-order model takes the same general form of type (1.1). The LOM(n) obtained from the above projection process describes the time evolution of the amplitudes of the modes used to capture the spatial variation of the field variables. Mathematically speaking, the modes denote the basis function used in the Galerkin projection method. For a given set of PDEs and for a chosen set of basis functions, the size and the structure of the matrices $A^{(i)}$ (i = 1, 2,…,n), the matrix B and the vector **c** in (1.1) depend on the number n and the type of the subset of modes (such as $\{\sin x, \sin 3x\}$ or $\{\sin x, \sin 2x\}$, when n = 2 in the case of Fourier modes) that define the subspace onto which the given PDE is projected.

In the following, we illustrate the Galerkin projection method with the typical partial differential equations mentioned in Section 1.2.

Burger's equation Consider the general Fourier transformation

$$u(x,t) = \frac{a_0}{2} + \sum_{n=1}^{\infty} a_n(t)\cos nx + \sum_{n=1}^{\infty} b_n(t)\sin nx\,. \tag{1.15}$$

Substitute (1.15) into (1.3) with an arbitrary truncation number n, we get

$$
\begin{aligned}
\dot{a}_0 &= 0 \\
\dot{a}_i &= -\frac{i}{2}\left(a_0 b_i + \sum_{k=1}^{i-1} a_{i-k} b_k + \sum_{k=1}^{n-i} a_k b_{i+1} - \sum_{k=1}^{n-i} a_{i+k} b_k \right) - \kappa i^2 a_i \\
\dot{b}_i &= \frac{i}{2}\left(a_0 a_i + \frac{1}{2}\sum_{k=1}^{i-1} a_k a_{i-k} + \sum_{k=1}^{n-i} a_k a_{i+k} - \frac{1}{2}\sum_{k=1}^{i-1} b_k b_{i-k} + \sum_{k=1}^{n-i} b_k b_{i+k} \right) - \kappa i^2 b_i
\end{aligned}
\tag{1.16}
$$

for i = 1,2,3,..,n. When the diffusion term is dropped from the right-hand side of (1.3) and the initial velocity is a pure sinusoid, (1.16) can be written in a simpler form as that in Platzmen (1964),

$$
\dot{u}_i = \frac{i}{4}\sum_{k=1}^{i-1} u_k u_{i-k} - \frac{i}{2}\sum_{k=1}^{n} u_k u_{i+k} \tag{1.17}
$$

where u_i corresponds to just $-b_i$ in (1.16).

Geostrophic vorticity equation Expand ψ, ψ* and h in (1.7) with orthonormal eigenfunctions,

$$
\begin{aligned}
(\psi, \psi^*) &= L^2 f_0 \sum_{i=1}^{\infty} (\psi, \psi^*) F_i \\
h &= H \sum_{i=1}^{\infty} h_i F_i
\end{aligned}
\tag{1.18}
$$

where F_i is just a simple trigonometric function as

$$
\begin{aligned}
F_1 &= \sqrt{2}\cos\frac{y}{L}, & F_2 &= 2\cos\frac{nx}{L}\sin\frac{y}{L} \\
F_3 &= 2\sin\frac{nx}{L}\sin\frac{y}{L}, & F_4 &= \sqrt{2}\cos\frac{2y}{L} \\
F_5 &= 2\cos\frac{nx}{L}\sin\frac{2y}{L}, & F_6 &= 2\sin\frac{nx}{L}\sin\frac{2y}{L}.
\end{aligned}
$$

Substitute (1.18) into (1.7), we get the following LOM (with number of truncated modes, n = 6):

$$
\begin{aligned}
\dot{\psi}_1 &= -k_{01}(\psi_1 - \psi_1^*) + h_{01}\psi_3 \\
\dot{\psi}_2 &= -k_{n1}(\psi_2 - \psi_2^*) - (\alpha_{n1}\psi_1 - \beta_{n1})\psi_3 - \delta_{n1}\psi_4\psi_6 \\
\dot{\psi}_3 &= -k_{n1}(\psi_3 - \psi_3^*) - h_{n1}\psi_1 + (\alpha_{n1}\psi_1 - \beta_{n1})\psi_2 + \delta_{n1}\psi_4\psi_5 \\
\dot{\psi}_4 &= -k_{02}(\psi_4 - \psi_4^*) + h_{02}\psi_6 + \in_n (\psi_2\psi_6 - \psi_3\psi_5) \\
\dot{\psi}_5 &= -k_{n2}(\psi_5 - \psi_5^*) - (\alpha_{n2}\psi_1 - \beta_{n2})\psi_6 - \delta_{n2}\psi_4\psi_3 \\
\dot{\psi}_6 &= -k_{n2}(\psi_6 - \psi_6^*) + h_{n2}\psi_4 - (\alpha_{n2}\psi_1 - \beta_{n2})\psi_5 - \delta_{n2}\psi_4\psi_2
\end{aligned}
\tag{1.19}
$$

where

$$
\alpha_{nm} = \frac{n^2 + m^2 - 1}{n^2 + m^2 + \lambda^{-2}}\gamma_{nm} \qquad \beta_{nm} = \frac{n}{n^2 + m^2 + \lambda^{-2}}\frac{L}{a}\cos\phi_0
$$

$$
\delta_{nm} = \frac{n^2 - m^2 + 1}{n^2 + m^2 + \lambda^{-2}}\gamma_{n3} \qquad \in_n = \frac{3\gamma_{n3}}{4 + \lambda^{-2}}
$$

$$
k_{nm} = \frac{n^2 + m^2}{n^2 + m^2 + \lambda^{-2}}k \qquad h_{01} = \frac{\gamma_{n1}}{1 + \lambda^{-2}}\frac{h_0}{2H}
$$

$$
h_{02} = \frac{\gamma_{n3}}{4 + \lambda^{-2}}\frac{h_0}{2H} \qquad h_{n1} = \frac{\gamma_{n1}}{n^2 + 1 + \lambda^{-2}}\frac{h_0}{2H}
$$

$$
h_{n2} = \frac{\gamma_{n3}}{n^2 + 4 + \lambda^{-2}}\frac{h_0}{2H} \qquad \text{and}
$$

$$
\frac{\gamma_{n1}}{5} = \frac{\gamma_{n2}}{4} = \frac{\gamma_{n3}}{8} = \frac{8\sqrt{2}}{15\pi}n\cdot
$$

Rayleigh-Bérnard convection Consider the following expansion in (truncated) Fourier series:

$$
\begin{aligned}
v_1 &= x_1(t)\sin(ax)\cos(z) + w_1(t)\sin(ax)\cos(ay)\cos(2z) \\
v_2 &= y_1(t)\sin(ay)\cos(z) + w_1(t)\cos(ax)\sin(ay)\cos(2z) \\
v_3 &= -ax_1(t)\cos(ax)\sin(z) - ay_1(t)\cos(ay)\sin(z) - aw_1(t)\cos(ax)\cos(ay)\sin(2z) \\
\theta &= \theta_{101}(t)\cos(ax)\sin(z) + \theta_{011}(t)\cos(ay)\sin(z) \\
&\quad + \theta_{002}(t)\sin(2z) + \theta_{112}(t)\cos(ax)\cos(ay)\sin(2z) + \theta_{004}(t)\sin(4z)\cdot
\end{aligned}
\tag{1.20}
$$

Substitute (1.20) into (1.12) - (1.14) will result in the following LOM:

$$
\begin{aligned}
\dot{x}_1 &= -\nu(1+a^2)x_1 - \frac{a}{1+a^2}\theta_{101} - \frac{a}{4}w_1 y_1 \\
\dot{y}_1 &= -\nu(1+a^2)y_1 - \frac{a}{1+a^2}\theta_{011} - \frac{a}{4}w_1 x_1 \\
\dot{w}_1 &= -2\nu(2+a^2)w_1 - \frac{a}{2+a^2}\theta_{112} + a\frac{1+a^2}{2+a^2}x_1 y_1 \\
\dot{\theta}_{101} &= -\kappa(1+a^2)\theta_{101} - ax_1 - ax_1\theta_{002} - \frac{a}{4}\theta_{112}y_1 \\
\dot{\theta}_{011} &= -\kappa(1+a^2)\theta_{011} - ay_1 - ay_1\theta_{002} - \frac{a}{4}\theta_{112}x_1 \\
\dot{\theta}_{002} &= -4\kappa\theta_{002} + \frac{a}{2}\theta_{101}x_1 + \frac{a}{2}\theta_{011}y_1 \\
\dot{\theta}_{112} &= -2\kappa(2+a^2)\theta_{112} - aw_1 + \frac{a}{2}\theta_{011}x_1 + \frac{a}{2}\theta_{101}y_1 - 2a\theta_{004}w_1 \\
\dot{\theta}_{004} &= -16\kappa\theta_{004} + \frac{a}{2}\theta_{112}w_1
\end{aligned}
\tag{1.21}
$$

1.4 NEEDS FOR ENERGERY CONSERVATION

Granted that (1.1) is only an approximation to the original physical problem under consideration, for it to be useful in the analysis, it is required that the resulting LOM(*n*) in (1.1) inherits several of the basic properties of the physical model described by the PDEs. These include symmetry and conservation of physical quantities such as kinetic energy, enstrophy, or vorticity which ever is applicable. Holmes *et al*. (1996) contains a succinct discussion of the symmetry in LOM(*n*) and its implications. In this paper our main concern is with the conservation of kinetic energy by the LOM(*n*) in (1.1) and their relation to other well known energy conserving systems.

It is well known that if the original physical model consists of only the momentum equation, then the resulting LOM(*n*) conserves kinetic energy for any *n* (Platzman (1964), Holmes *et al*. (1996), Smith *et al*. (2005)). The story is quite different if the original physical model contains the momentum equations and the interaction

between temperature and velocity leading to thermally induced convection as it happens in the celebrated Rayleigh-Bérnard convection equations. In this case, LOM(n) in general, (after dropping the frictional and external forces) does not conserve energy for any n. For example, the LOM(6) used by Howard and Krishnamurti (1986) did not conserve energy and is known to lead to non-physical solutions. Modifications of the Howard and Krishnamurti model to conserve vorticity and energy are discussed in Hermiz *et. al.* (1995) and Thiffeault and Horton (1996) respectively. Refer to Gluhovsky and Tong (1999) and Gluhovsky *et. al*. (2002) for an excellent discussion of these and other related results.

Despite the wide spread popularity of this framework for the analysis of complex systems, except for the several illuminating examples contained in Gluhovsky (1982), (2006), Gluhovsky and Tong (1999), Gluhovsky *et al*. (2002) and Tong and Gluhovsky (2002), there are still no known criteria for the choice of a subset of modes (that is, $\{\sin x$, $\sin 3x$ and $\sin 5x\}$ or $\{\sin x$, $\sin 2x$, $\sin 4x\}$, *etc*) that will guarantee the conservation of energy in LOM(n) in (1.1). One goal of this study is to examine the structure of LOM(n) that guarantees conservation of energy.

1.5 COUPLED GYROSTATS AS MODELS FOR ENERGY CONSERVING SYSTEMS

In classical physics, the Volterra gyrostat and its special case Euler gyroscope are mechanical systems studied greatly in rigid body dynamics. Mathematically, the system is described by a system of three coupled non-linear systems (with quadratic nonlinearity)

of ordinary differential equations, denoted by VG(3) in this study (Refer to Appendix B for a quick overview of Volterra gyrostat),

$$\left.\begin{aligned} \dot{x}_1 &= px_2x_3 + h_{12}x_2 + h_{13}x_3 \\ \dot{x}_2 &= qx_1x_3 + h_{21}x_1 + h_{23}x_3 \\ \dot{x}_3 &= rx_1x_2 + h_{31}x_1 + h_{32}x_2 \end{aligned}\right\} \tag{1.22}$$

where p, q, r and h_{ij}, $1 \le i \ne j \le 3$ are all real coefficients. The coefficients h_{ij} on the right hand side of (1.22) denote the fixed angular momenta caused by the relative motion of the rotor (Wittenberg (1977)). Denoting $\mathbf{x} = (x_1, x_2, x_3)^T$, it can be verified that VG(3) in (1.22) conserves energy $\mathrm{E}_1(\mathbf{x}) = \frac{1}{2}\mathbf{x}^T\mathbf{x}$ when

$$\alpha + \beta + \gamma = 0,$$

and

$$h_{ij} + h_{ji} = 0, 1 \le i \ne j \le 3.$$

If $h_{ij} \equiv 0$ for $1 \le i \ne j \le 3$ in (1.22), the resulting dynamical system is known as the Euler gyroscope and is given by

$$\begin{aligned} \dot{x}_1 &= px_2x_3 \\ \dot{x}_2 &= qx_1x_3 \\ \dot{x}_3 &= rx_1x_2. \end{aligned} \tag{1.23}$$

The classical gyroscopic dynamics constitutes a prototype of energy conserving systems (see Chapter 5 for details).

It turns out that many copies of VG(3) in (1.22) and its special cases can be coupled to arrive at a system of coupled Volterra gyrostats. The set of all coupled Volterra gyrostats of order n is denoted by **CVG(*n*)** in this study. If $S \in \mathrm{CVG}(n)$ has k component gyrostats, since it is required that each of these components conserves energy,

it follows that every member of CVG(n) is a conservative system (Refer to Chapter 3 for the formal proof). One example of a CVG(5) is found in Gluhovsky and Tong (1999), which naturally arises in modeling Rayleigh-Bérnard convection in an electrically conducting fluid:

$$\left.\begin{array}{lll|l|l} \dot{y}_1 = & -\alpha_1 y_2 y_3 & & & -\lambda_1 y_1 + f \\ \dot{y}_2 = & \alpha_1 y_1 y_3 - h y_3 & & & -\lambda_2 y_2 \\ \dot{y}_3 = & +h y_2 & & \alpha_2 y_4 y_5 & -\lambda_3 y_3 \\ \dot{y}_4 = & & & \beta_2 y_3 y_5 & -\lambda_4 y_4 \\ \dot{y}_5 = & & & \gamma_2 y_3 y_4 & -\lambda_5 y_5 \end{array}\right\} \quad (1.24)$$

A special case of Volterra gyrostat | Euler gyroscope | Extenal forces

By setting all the external forces to zero ($\lambda_i = 0$ for $i = 1, 2, \cdots, 5$ and $f = 0$) in (1.24), it reduces to a system of coupled Volterra gyrostats of order 5 consisting of a special case of VG(3) and the Euler gyroscope.

Historically, Lorenz (1960) and Obukhov (1973) represent early attempts to show that there exists a close connection between the energy conserving low-order models and a system of coupled Euler gyroscopes. Gluhovsky (1982), (2006) and Gluhovsky and his collaborators (1999), (2002) extended this idea and showed using several examples that if a given low-order model can be rewritten as a system of coupled Volterra gyrostats, then the low-order model in question conserves energy. Another goal of this study is to establish a formal relationship between energy conserving low-order models in question and the systems of coupled gyrostats.

Motivated by the important role of gyrostat and its special cases as a prototype for energy conserving systems, the third goal of this study is to analyze the stability properties of Volterra gyrostats and all of its special cases.

1.6 ORGANIZATION OF THE DISSERTATION

In Chapter 2, we first derive a set of sufficient conditions on the structural parameter of the LOM(n) in (1.1) to conserve energy of the form

$$\mathrm{E}(\mathbf{x}) = \frac{1}{2}\mathbf{x}^T\mathbf{K}\mathbf{x} \tag{1.25}$$

where $\mathbf{K} = \mathrm{Diag}(K_1, K_2, \cdots, K_n) \in \Re^{n\times n}$ is a diagonal matrix with $K_i > 0$ for $i = 1,2,\ldots,n$. Low-order models of the type (1.1) satisfying these energy conserving conditions defines a proper subset of LOM(n) and it is named as ELOM(n) in this study.

While exploiting the relation between energy conserving LOMs and systems of coupled gyrostats, we isolated an interesting subset of ELOM(n) called the special case of energy conserving low-order models and denoted by SELOM(n). We prove formally the relation between set SELOM(n) and CVG(n) in Chapter 3. An algorithm is also provided for converting any system in SELOM(n) as a system of coupled gyrostats. This is a generalization of the results due to Lorenz (1960), Obukhov (1973), Gluhovsky (1982), and Gluhovsky *et al*. (1997, 1999, 2002).

The formal development in Chapter 3 defined a natural hierarchy of low-order models as follows:

$$\mathrm{CVG}(n) = \mathrm{SELOM}(n) \subset \mathrm{ELOM}(n) \subset \mathrm{LOM}(n)\,. \tag{1.26}$$

To further examine the relation between the energy conserving model and the system of coupled gyrostats based on the modular approach for constructing physical meaningful LOMs of interest in various fluid dynamical problems (Brown and Chua (1992), Gluhovsky (1999, 2002 *etc*.)), the traditional Volterra gyrostat is not useful any more to act as the basic building block for the general energy conserving model, say systems not inside SELOM(n).

To this end, we extend the concept of Volterra gyrostats to the **generalized Volterra gyrostats** GVG(3), which includes nonlinear feedback. Let CGVG(n) denote the set of all coupled generalized Volterra gyrostats of order n. Using this class of gyrostats as the building block, we then describe an algorithm in Chapter 4 for rewriting any system in ELOM(n) as a system in CGVG(n) and prove the equivalence

$$\text{ELOM}(n) = \text{CGVG}(n). \tag{1.27}$$

These results complete the journey of exploring the intimate relation between the mechanical system of energy conserving coupled Euler gyroscopes and Volterra gyrostats on one hand and the energy conserving low-order model, LOM(n) of the type (1.1) derived by applying the Galerkin type projection methods to well known fluid dynamical models on the other. It further helps to focus attention on the important role played by the coupled gyrostats in the analysis of fluid dynamical systems.

Given that gyrostat is the elementary module for constructing energy conserving LOMs of interest in various fluid dynamics, we analyze the stability of the equilibria of Volterra gyrostat and all of its special cases in Chapter 5.

Since retaining the Hamiltonian structure of the original equations in geophysical fluid dynamics is also desired with LOMs to avoid unphysical behaviors, we study the instrumental role of gyrostatic LOMs plays in constructing Hamiltonian multi-mode LOMs in Chapter 6.

Finally, a summary of this study along with associated open questions is discussed in the last Chapter (Chapter 7).

Chapter 2

A Set of Sufficient Conditions for Conserving Energy in LOMs

2.1 INTRODUCTION

Let $\mathbf{x} = (x_1, x_2, \cdots, x_n)^T \in \Re^n$ be a (real) column vector denoting the state of a dynamical system whose time evolution is governed by a system of nonlinear (quadratic type) coupled ordinary differential equations (ODEs) given by

$$\dot{x}_i = \mathbf{x}^T A^{(i)} \mathbf{x} + B_i \mathbf{x} + c_i \tag{2.1}$$

where $\dot{x}_i = \dfrac{dx_i}{dt}$, $A^{(i)} \in \Re^{n \times n}$ is a (real) matrix, $B_i \in \Re^{1 \times n}$ is a (real) row vector and $c_i \in \Re$ is a (real) constant. Equivalently, in vector form (2.1) can be written as

$$\dot{\mathbf{x}} = A(\mathbf{x}, \mathbf{x}) + B\mathbf{x} + C \tag{2.2}$$

where $A(\mathbf{x}, \mathbf{x}) = (\mathbf{x}^T A^{(1)} \mathbf{x}, \mathbf{x}^T A^{(2)} \mathbf{x}, \cdots, \mathbf{x}^T A^{(n)} \mathbf{x})^T \in \Re^n$ is a vector of quadratic forms in $\mathbf{x}$, $B \in \Re^{n \times n}$ is a matrix with B_i as its ith row and $C = (c_1, c_2, \cdots, c_n)^T \in \Re^n$. An example of a typical system that arises in rigid body mechanics and in meteorology is given by

$$\begin{aligned} \dot{x}_1 &= a_1 x_2 x_3 - \sum_{j=1}^{3} b_{1j} x_j + c_1 \\ \dot{x}_2 &= a_2 x_1 x_3 - \sum_{j=1}^{3} b_{2j} x_j + c_2 \\ \dot{x}_3 &= a_3 x_1 x_2 - \sum_{j=1}^{3} b_{3j} x_j + c_3 \end{aligned} \tag{2.3}$$

where

$$A^{(1)} = \begin{pmatrix} 0 & 0 & 0 \\ 0 & 0 & a_1 \\ 0 & 0 & 0 \end{pmatrix}, A^{(2)} = \begin{pmatrix} 0 & 0 & a_2 \\ 0 & 0 & 0 \\ 0 & 0 & 0 \end{pmatrix}, A^{(3)} = \begin{pmatrix} 0 & a_3 & 0 \\ 0 & 0 & 0 \\ 0 & 0 & 0 \end{pmatrix}.$$

Let $\mathrm{E} : \Re^n \to \Re$ be given by

$$\mathrm{E}(\mathbf{x}) = \frac{1}{2}\sum_{i=1}^{n} K_i x_i^2 = \frac{1}{2}\mathbf{x}^T \mathbf{K}\mathbf{x} \tag{2.4}$$

where $K_i > 0$ and **K** is a diagonal matrix

$$\mathbf{K} = \mathrm{Diag}(K_1, K_2, \cdots, K_n)\,. \tag{2.5}$$

As a positive definite quadratic form, E(**x**) in (2.4) denotes (generalized) energy.

Statement of the problem: Our goal is to derive a set of sufficient conditions on the structural parameters – matrix $A^{(i)}$, row vector B_i and the scalar c_i for $i = 1,2,\ldots,n$ of the system (2.1) such that the time derivative $\dot{\mathrm{E}}(\mathbf{x})$ of E(**x**) evaluated along the trajectory of (2.1) vanishes (identically in **x**). That is, we are seeking conditions under which (2.1) conserves the energy.

A little reflection would reveal that we can assume one of the K_i's is a fixed constant. Without loss of generality, it is assumed that $K_1 = 1$. All the formulas for K_i are conditioned on this assumption. If, instead, we assume that $K_i = 1$ for $i \neq 1$, we would obtain a corresponding equivalent set of formulas. Refer to Example 2.5.

Motivation for this work: Equation of the type (2.2) are called low-order models (LOM) and routinely arise from the application of Galerkin type projection techniques (Silberman (1954)) to the standard models of interest in fluid mechanics and atmospheric sciences including the Rayleigh-Bérnard convection equations (Saltzman (1962),

Gluhovsky (2006)), quasi-geostrophic potential vorticity equation (Charney and Devore (1979), De Swart (1998), Lorenz (1962), (1963), (1982), Legras and Ghil (1985)) and Burgers' equation (Platzman (1964)). Refer to Chapter 1 for further discussion. It is well known that while the order n of the resulting LOM depends on the number of modes, the structure of the resulting matrices $\mathrm{A}^{(i)}$ (i =1,2,…,n), B and the vector **c** depends critically on the type of modes (sin 2x or sin 4x) in the orthogonal expansion of the field variable.

Despite this wide popularity of LOMs, it seems that there is no guiding principle for the choice of the order of LOMs that will preserve energy. One example is the Howard-Krishnamurti (1986) model mentioned in last chapter. Our goal in this chapter is to replace the *ad hoc* approach in LOM construction by a systematic methodology by which one can test if a given LOM conserves energy. This involves testing for simple conditions on the parameters – matrices $A^{(i)}$, matrix B and the vector C in (2.2).

Section 2.2 contains the derivation of the sufficient conditions for conserving energy. The resulting subset of LOMs is defined as ELOM(n). A specific set of ELOM(n) of great interest in geophysical application with its examples are given Section 2.3. At last, a summary of this chapter is discussed in Section 2.4.

2.2 A SET OF SUFFICIENT CONDITIONS FOR ENERGY CONSERVING

It can be verified by direct computation that

$$\begin{aligned}\dot{\mathrm{E}}(\mathbf{x}) &= \mathbf{x}^T\mathbf{K}\dot{\mathbf{x}} \\ &= \mathbf{x}^T\mathbf{K}\mathbf{A}(\mathbf{x},\mathbf{x}) + \mathbf{x}^T(\mathbf{K}B)\mathbf{x} + \mathbf{x}^T\mathbf{K}C\end{aligned} \tag{2.6}$$

$$= \sum_{i=1}^{n} x_i K_i A^{(i)}(\mathbf{x},\mathbf{x}) + \sum_{i=1}^{n} x_i K_i \left(\sum_{j=1}^{n} b_{ij} x_j \right) + \sum_{i=1}^{n} x_i K_i c_i \,. \tag{2.7}$$

A sufficient condition for $\dot{E}(\mathbf{x}) \equiv 0$ is that each of the three terms on the right-hand side. of (2.6) or (2.7) in turn must vanish uniformly for all $\mathbf{x} \in \Re^n$. Let us start from right to left in equation (2.7).

1). **Linear term** $\mathbf{x}^T \mathbf{K} C$: This linear term vanishes exactly when $\mathbf{K}\boldsymbol{C} = 0$. Since $\mathbf{K}$ is positive definite matrix, this leads to the following:

Condition C: The energy is conserved exactly when $\boldsymbol{C} = 0$

The constant term $\boldsymbol{C}$ on the right-hand side of (2.2) denotes the external forcing. It is all but natural to require that the forcing be zero to conserve the energy.

2). **Quadratic term** $\mathbf{x}^T(\mathbf{K}B)\mathbf{x}$: We begin by additively decomposing $\boldsymbol{B}$ as

$$B = B_d + B_n \tag{2.8}$$

where

$$B_d = \text{Diag}(b_{11}, b_{22}, \cdots, b_{nn}) \tag{2.9}$$

is the diagonal part of $\boldsymbol{B}$ and

$$B_n = B - B_d \tag{2.10}$$

denotes the non-diagonal part of $\boldsymbol{B}$. Hence,

$$\mathbf{x}^T(\mathbf{K}B)\mathbf{x} = \mathbf{x}^T(\mathbf{K}B_d)\mathbf{x} + \mathbf{x}^T(\mathbf{K}B_n)\mathbf{x} \tag{2.11}$$

where

$$\mathbf{x}^T(\mathbf{K}B_d)\mathbf{x} = \sum_{i=1}^{n} b_{ii} K_i x_i^2 \tag{2.12}$$

and

$$\mathbf{x}^T(\mathbf{K}B_n)\mathbf{x} = \sum_{\substack{i=1 \\ j>i}}^{n} x_i x_j (K_i b_{ij} + K_j b_{ji}) . \tag{2.13}$$

Consider the first term on the right-hand side of (2.11). Since $K_i x_i^2 \geq 0$ for all x, the first term on the right-hand side of (2.11) vanishes exactly when

$$b_{ii} = 0 \text{ for all } i = 1, 2, \cdots, n . \tag{2.14}$$

That is, ***B*** must be a matrix with zero diagonal entries.

Recall that the term $b_{ii}x_i$ in (2.1) denotes the friction or the dissipative term. Hence it is only natural to require that there be no friction or dissipation to conserve the energy.

The second term on the right-hand side of (2.11) vanishes exactly when

$$K_i b_{ij} + K_j b_{ji} = 0 \tag{2.15}$$

for all i = 1,2,…,n and $j > i$. Since K_i's are all positive, (2.15) requires that b_{ij} and b_{ji} must be of opposite sign, that is

$$\text{sgn}(b_{ij})\,\text{sgn}(b_{ji}) = -1 \tag{2.16}$$

where

$$\left.\begin{aligned} \text{sgn}(y) = \;& 1 \quad \text{if } y > 0 \\ = \;& -1 \quad \text{if } y < 0 \end{aligned}\right\} . \tag{2.17}$$

Since $K_1 = 1$, from (2.15) we get

$$K_r = -\frac{b_{1r}}{b_{r1}} \text{ for } 1 < r \le n \tag{2.18}$$

and for $1 < i \le n$ and $j > i$

$$\frac{K_j}{K_i} = -\frac{b_{ij}}{b_{ji}} \tag{2.19}$$

Since K_r's defined in (2.18) must satisfy (2.19), combining these we obtain a set of **consistency** condition for the elements of the matrix $\boldsymbol{B}$ as

$$\frac{K_j}{K_i} = -\frac{b_{ij}}{b_{ji}} = \left(\frac{b_{1j}}{b_{j1}}\right)\left(\frac{b_{i1}}{b_{1i}}\right)$$

or

$$b_{1i}b_{ij}b_{j1} + b_{1j}b_{ji}b_{i1} = 0 \tag{2.20}$$

for $1 < i \le n$ and $j > i$.

Combining (2.14) and (2.16), it can be verified that (2.20) is indeed the determinant of the 3x3 principal submatrix $B(1,i,j)$ of $\boldsymbol{B}$ formed by the rows and columns at positions 1, i and j. That is,

$$B(1,i,j) = \begin{pmatrix} 0 & b_{1i} & b_{1j} \\ b_{i1} & 0 & b_{ij} \\ b_{j1} & b_{ji} & 0 \end{pmatrix} \tag{2.21}$$

and by (2.20)

$$\text{Det}\left(B(1,i,j)\right) = b_{1i}b_{ij}b_{j1} + b_{1j}b_{ji}b_{i1} = 0$$

We now summarize the above discussion in the following:

Condition B: Given that $\boldsymbol{K}$ is a diagonal matrix with positive diagonal elements, the quadratic term $\mathbf{x}^T(\mathbf{K}B)\mathbf{x}$ vanishes identically exactly when the matrix $\boldsymbol{B} = [b_{ij}]$ is such that

$$b_{ii} = 0 \quad 1 \le i \le n$$
$$\operatorname{sgn}(b_{ij})\operatorname{sgn}(b_{ji}) = -1 \text{ for } i \ne j$$

and every principal submatrix $B(1,i,j)$ formed by the elements at the intersection of the rows and columns at positions 1, i and j for $2 \le i \le n$ and $j > i$ must be singular. In this case the values for $\boldsymbol{K}_i$'s are given by (2.18).

Recall that if $b_{ij} = -b_{ji}$, then matrix $\boldsymbol{B} = [b_{ij}]$ is called a skew symmetric matrix. Since (2.16) is a generalization of this condition, matrices defined by the condition B are called **generalized skew symmetric matrices** which includes the skew symmetric matrices as a proper subset.

It is well known (Bellman (1995)) that the determinant of a skew symmetric matrix of odd order is always zero. Condition (2.20) is an extension of this property of skew symmetric matrices and the principal submatrices $B(1,i,j)$ of $\boldsymbol{B}$ which are themselves generalized skew symmetric matrices of order 3.

Example 2.1 An example of a matrix $\boldsymbol{B}$ satisfying the condition B is given by

$$b_{ij} = \begin{cases} b_j & \text{if } j > i \\ 0 & \text{if } j = i \\ -b_j & \text{if } j < i \end{cases} \tag{2.22}$$

Thus, when $n = 4$ we get

$$B = \begin{pmatrix} 0 & b_2 & b_3 & b_4 \\ -b_1 & 0 & b_3 & b_4 \\ -b_1 & -b_2 & 0 & b_4 \\ -b_1 & -b_2 & -b_3 & 0 \end{pmatrix}$$

In this case, $K_1 = 1$,

$$K_r = \left| \frac{b_r}{b_1} \right| \qquad r = 2,3,4$$

and

$$\frac{K_j}{K_i} = -\frac{b_{ij}}{b_{ji}} = \left| \frac{b_j}{b_i} \right| = \left| \frac{b_j}{b_1} \right| \left| \frac{b_1}{b_i} \right| .$$

3). **Higher order term $\mathbf{x}^T \mathbf{K} \mathbf{A}(\mathbf{x}, \mathbf{x})$**:

Let

$$A^{(i)} = \left[a_{pq}^{(i)} \right] \tag{2.23}$$

Then

$$\mathbf{x}^T A^{(i)} \mathbf{x} = \sum_{p,q=1}^{n} a_{pq}^{(i)} x_p x_q \, . \tag{2.24}$$

Substituting this and simplifying by collecting the like terms (see Appendix A for details), we obtain

$$\mathbf{x}^T\mathbf{K}\mathbf{A}(\mathbf{x},\mathbf{x}) = \sum_{i=1}^{n} x_i K_i (\mathbf{x}^T \mathbf{A}^{(i)} \mathbf{x})$$

$$= \underbrace{\sum_{i=1}^{n} K_i a_{ii}^{(i)} x_i^3}_{\text{Group I}} + \underbrace{\sum_{i=1}^{n}\sum_{p\neq i} x_i^2 x_p \left[K_p a_{ii}^{(p)} + K_i \left(a_{ip}^{(i)} + a_{pi}^{(i)} \right) \right]}_{\text{Group II}} \tag{2.25}$$

$$+ \underbrace{\sum_{i<p<q} x_i x_p x_q \left[K_i \left(a_{pq}^{(i)} + a_{qp}^{(i)} \right) + K_p \left(a_{iq}^{(p)} + a_{qi}^{(p)} \right) + K_q \left(a_{ip}^{(q)} + a_{pi}^{(q)} \right) \right]}_{\text{Group III}} \cdot$$

The right-hand side of (2.25) is the sum of n^3 polynomial terms (each of degree three) in the components of the vector **x.** The first term (group I) has n polynomials (each with one coefficient), the second term (group II) has $n(n\text{-}1)$ polynomials (each containing the sum of three coefficients) and the third term (group III) has $\binom{n}{3} = \frac{n(n-1)(n-2)}{6}$ polynomials (each containing the sum of six coefficients). Thus, these three groups together have

$$n + n(n-1) + \frac{n(n-1)(n-2)}{6} = \frac{n(n+1)(n+2)}{6}$$

distinct third degree polynomials and account for $n + 3n(n-1) + n(n-1)(n-2) = n^3$ terms. Note that $\binom{n}{r}$ denotes the number of combinations of r items taken out of n objects.

In view of this algebraic complexity, in the following, to illustrate the basic patterns of ideas we consider the case when $n = 3$.

Example 2.2 By collecting the like terms, the 27 terms on the right-hand side of (2.25) can be expressed as the sum of 10 polynomials (three with one variables, six with two variables and one with three variables) as follows:

$$
\begin{aligned}
\mathbf{x}^T\mathbf{K}\mathbf{A}(\mathbf{x},\mathbf{x}) = {} & x_1^3 K_1 a_{11}^{(1)} + x_2^3 K_2 a_{22}^{(2)} + x_3^3 K_3 a_{33}^{(3)} \\
& + x_1^2 x_2 \left[K_2 a_{11}^{(2)} + K_1 \left(a_{12}^{(1)} + a_{21}^{(1)} \right) \right] \\
& + x_1^2 x_3 \left[K_3 a_{11}^{(3)} + K_1 \left(a_{13}^{(1)} + a_{31}^{(1)} \right) \right] \\
& + x_1 x_2^2 \left[K_1 a_{22}^{(1)} + K_2 \left(a_{12}^{(2)} + a_{21}^{(2)} \right) \right] \\
& + x_1 x_3^2 \left[K_1 a_{33}^{(1)} + K_3 \left(a_{13}^{(3)} + a_{31}^{(3)} \right) \right] \\
& + x_2^2 x_3 \left[K_3 a_{22}^{(3)} + K_2 \left(a_{23}^{(2)} + a_{32}^{(2)} \right) \right] \\
& + x_2 x_3^2 \left[K_2 a_{33}^{(2)} + K_3 \left(a_{23}^{(3)} + a_{32}^{(3)} \right) \right] \\
& + x_1 x_2 x_3 \left[K_1 \left(a_{23}^{(1)} + a_{32}^{(1)} \right) + K_2 \left(a_{13}^{(2)} + a_{31}^{(2)} \right) + K_3 \left(a_{12}^{(3)} + a_{21}^{(3)} \right) \right].
\end{aligned}
\tag{2.26}
$$

A sufficient condition of $\mathbf{x}^T\mathbf{K}\mathbf{A}(\mathbf{x},\mathbf{x})$ to vanish is that the coefficients of each of the $\frac{n(n+1)(n+2)}{6}$ polynomials on the right-hand side of (2.25) must vanish. This observation leads to the following set of conditions on the elements of $\mathbf{A}^{(i)}$, $i = 1, 2 \ldots, n$.

Condition A1: Considering the n polynomials in single variables (group I), it is required that

$$
a_{ii}^{(i)} = 0 \text{ for } i = 1, 2, \cdots, n . \tag{2.27}
$$

Condition A1 implies that all the terms in group I on the right-hand side of (2.26) vanish. Referring to the example 2.2, this condition requires $a_{11}^{(1)} = a_{22}^{(2)} = a_{33}^{(3)} = 0$.

To understand the naturalness of this condition, recall that the three coefficients in (2.27) correspond to the terms $a_{ii}^{(i)} x_i^2$ on the right-hand side of $\dot{x}_i$ in (2.1). Since it is well known that the solution

$$
y(t) = \frac{1}{1-t}
$$

of the scalar O.D.E $\dot{y} = y^2$ goes to infinity in finite time, condition (2.27) prevent the solution of (2.6) from being unbounded which is necessary for conserving the kinetic energy.

Condition A2: The coefficients of the $n(n\text{-}1)$ polynomials in group II must vanish. That is, for all $i = 1, 2, \ldots, n$ and for all $p \neq i$

$$K_i \left(a_{ip}^{(i)} + a_{pi}^{(i)} \right) = -K_p a_{ii}^{(p)} . \tag{2.28}$$

Referring to the example 2.2, this condition requires for $n = 3$ (assuming $K_1 = 1$)

$$\begin{aligned} (a_{12}^{(1)} + a_{21}^{(1)}) &= -K_2 a_{11}^{(2)} \\ (a_{12}^{(2)} + a_{21}^{(2)}) &= -\frac{1}{K_2} a_{22}^{(1)} \end{aligned} \tag{2.29}$$

$$\begin{aligned} (a_{13}^{(1)} + a_{31}^{(1)}) &= -K_3 a_{11}^{(3)} \\ (a_{13}^{(3)} + a_{31}^{(3)}) &= -\frac{1}{K_3} a_{33}^{(1)} \end{aligned} \tag{2.30}$$

and

$$\begin{aligned} (a_{23}^{(2)} + a_{32}^{(2)}) &= -\frac{K_3}{K_2} a_{22}^{(3)} \\ (a_{23}^{(3)} + a_{32}^{(3)}) &= -\frac{K_2}{K_3} a_{33}^{(2)} \cdot \end{aligned} \tag{2.31}$$

The following remarks are in order.

1. Since K_i's are defined by the condition B, there are infinitely many choices for $\left(a_{ip}^{(i)} + a_{pi}^{(i)} \right)$ and $a_{ii}^{(p)}$ satisfying (2.28).

2. Condition (2.28) states that the sum of the (symmetric) pair of elements $a_{ip}^{(i)}$ (p^{th} element of the ith row) and $a_{pi}^{(i)}$ (p^{th} element of the ith column) of $\mathrm{A}^{(i)}$ is a negative multiple of $a_{ii}^{(p)}$, the ith diagonal element of $\mathrm{A}^{(p)}$ for $p \neq i$. That is, (since K_i's are positive) the sum $\left(a_{ip}^{(i)} + a_{pi}^{(i)}\right)$ is of sign opposite to that of $a_{ii}^{(p)}$.

3. In the special case when

$$a_{ii}^{(p)} = 0 \quad i = 1, 2, \cdots, n, \quad p \neq i \tag{2.32}$$

condition (2.28) requires that

$$a_{ip}^{(i)} = -a_{pi}^{(i)}. \tag{2.33}$$

That is, elements on the ith row and i^{th} column of $\mathrm{A}^{(i)}$ must satisfy the standard skew symmetric condition.

Condition A3: The coefficients of the $\binom{n}{3}$ polynomials in group III must also vanish. That is, for $i < p < q$, we obtain an orthogonality condition

$$K_i\left(a_{pq}^{(i)} + a_{qp}^{(i)}\right) + K_p\left(a_{iq}^{(p)} + a_{qi}^{(p)}\right) + K_q\left(a_{ip}^{(q)} + a_{pi}^{(q)}\right) = 0. \tag{2.34}$$

Referring to Example 2.2, this condition requires that

$$K_1\left(a_{23}^{(1)} + a_{32}^{(1)}\right) + K_2\left(a_{13}^{(2)} + a_{31}^{(2)}\right) + K_3\left(a_{12}^{(3)} + a_{21}^{(3)}\right) = 0. \tag{2.35}$$

That is, the vector $\left(\left(a_{23}^{(1)} + a_{32}^{(1)}\right), \left(a_{13}^{(2)} + a_{31}^{(2)}\right), \left(a_{12}^{(3)} + a_{21}^{(3)}\right)\right)^T$ must be orthogonal to $\left(K_1, K_2, K_3\right)^T$. Clearly, there are infinitely many choices satisfying (2.34). Condition (2.34), quite similar to condition (2.28), only defines that the sum of the (symmetric)

pairs $\left(a_{pq}^{(i)}+a_{qp}^{(i)}\right)$, $\left(a_{iq}^{(p)}+a_{qi}^{(p)}\right)$ and $\left(a_{ip}^{(q)}+a_{pi}^{(q)}\right)$. Thus, there is a wide latitude for the choice of the individual elements $a_{pq}^{(i)}$ and $a_{qp}^{(i)}$ of the sum $\left(a_{pq}^{(i)}+a_{qp}^{(i)}\right)$.

We now summarize the above developments in the following.

Theorem 2.1: The low-order dynamical system given by (2.2) conserves the energy in (2.4) when the parameters of the system consisting of the n matrices $A^{(i)} \in \Re^{n\times n} \quad i=1,2,\cdots,n$, the matrix $B \in \Re^{n\times n}$, the vector $C \in \Re^{n}$ and the diagonal matrix $K \in \Re^{n\times n}$ with positive diagonal entries satisfy the following conditions:

Condition A: The matrices $A^{(i)}$ are such that

(A1) $a_{ii}^{(i)}=0 \quad \text{for } i=1,2,\cdots,n$

(A2) $K_i\left[a_{ip}^{(i)}+a_{pi}^{(i)}\right]=-K_p a_{ii}^{p} \quad \text{for all } p\neq i$

(A3) $K_i\left[a_{pq}^{(i)}+a_{qp}^{(i)}\right]+K_p\left[a_{iq}^{(p)}+a_{qi}^{(p)}\right]+K_q\left[a_{ip}^{(q)}+a_{pi}^{(q)}\right]=0 \quad \text{for all } i<p<q$

Condition B: The matrix B is such that

$$\begin{aligned} &b_{ii}=0 \quad \text{for } i=1,2,\cdots,n \\ &\operatorname{sgn}(b_{ij})\operatorname{sgn}(b_{ji})=-1 \quad \text{for } i\neq j \\ &\det\left[B(1,i,j)\right]=0 \quad \text{for } i\neq j \end{aligned}$$

where $B(1,i,j)$ is the 3x3 principal submatrix formed by the rows and columns at position 1, i and j.

Condition C: $c_i=0 \quad \text{for all } 1\le i\le n$

In this dissertation, we use **ELOM(*n*)** to denote the set of all energy conserving low-order models that satisfy Theorem 2.1. Obviously, ELOM(n) is a proper subset of LOM(n), *i.e.* $\text{ELOM}(n) \subset \text{LOM}(n)$. The properties of the class ELOM(n) will be further analyzed in later chapter by exploring its relation to other known conservative systems.

2.3 SPECIAL CASES

In this section, we demonstrate several well known LOMs of interest in geophysical fluid dynamics and rigid body mechanics using examples. Then a special case of Theorem 2.1 that usually arises in geophysical application is isolated.

2.3.1 Simplification of Theorem 2.1

If **K** (= **I**) is the identity matrix, then, while condition C and A1 remain the same in Theorem 2.1, condition B, A2 and A3 take a simplified form as

Condition (A2): $a_{ip}^{(i)} + a_{pi}^{(i)} = -a_{ii}^{p}$ for all $p \neq i$

Condition (A3): $\left(a_{pq}^{(i)} + a_{qp}^{(i)}\right) + \left(a_{iq}^{(p)} + a_{qi}^{(p)}\right) + \left(a_{ip}^{(q)} + a_{pi}^{(q)}\right) = 0$ for all $i<p<q$.

Condition (B): $b_{ij} = -b_{ji}$ for $i \neq j$. That is, ***B*** is a skew-symmetric matrix.

Actually, it can be verified that any system in ELOM(n) with $\mathbf{K} \neq \mathbf{I}$ can be transferred into a system with $\mathbf{K} = \mathbf{I}$ with proper linear transformation of the state variable, **x**. Note that when all the matrices $A^{(i)}$ (i = 1,2,…,n) are skew-symmetric matrices, all of the energy conserving conditions are satisfied directly.

Example 2.3 Charney and DeVore (1979) and De Swart(1988) model. This model is given by

$$\begin{aligned}\dot{x}_1 &= r_{11}^* x_3 - c(x_1 - x_1^*)\\ \dot{x}_2 &= -\alpha_{11} x_1 x_3 + \beta_{11} x_3 - c x_2\\ \dot{x}_3 &= \alpha_{11} x_1 x_2 - \beta_{11} x_2 - r_{11} x_1 - c x_3 .\end{aligned} \tag{2.36}$$

Rewriting (2.36) using the matrix notation, we get

$$A^{(1)} \equiv 0, A^{(2)} = \begin{bmatrix} 0 & 0 & -\alpha_{11} \\ 0 & 0 & 0 \\ 0 & 0 & 0 \end{bmatrix}, A^{(3)} = \begin{bmatrix} 0 & \alpha_{11} & 0 \\ 0 & 0 & 0 \\ 0 & 0 & 0 \end{bmatrix}$$

$$B = \begin{bmatrix} -c & 0 & r_{11}^* \\ 0 & -c & \beta_{11} \\ -r_{11} & -\beta_{11} & -c \end{bmatrix}, C = \begin{pmatrix} c x_1^* \\ 0 \\ 0 \end{pmatrix}.$$

Clearly, $c = 0$ for conserving the energy. With this condition, it can be verified that Det($\boldsymbol{B}$) = 0. Now using (2.18)-(2.19), we get

$$\frac{K_1}{K_3} = -\frac{b_{31}}{b_{13}} = \frac{r_{11}}{r_{11}^*} \text{ and } \frac{K_3}{K_2} = -\frac{b_{23}}{b_{32}} = 1 .$$

Thus, choosing $K_1 = \frac{r_{11}}{r_{11}^*}, K_2 = K_3 = 1$, We can readily verify the condition A3 as well. We may also directly verify that

$$\mathrm{E}(\mathbf{x}) = \frac{1}{2}\left[\left(\frac{r_{11}}{r_{11}^*} \right) x_1^2 + x_2^2 + x_3^2 \right].$$

is conserved when $c = 0$.

Now, consider a linear transformation of the variables

$$\begin{cases} x_1 = y_1 \\ x_2 = \sqrt{K_1}\, x_2 \\ x_3 = \sqrt{K_2}\, x_3 \end{cases}$$

Substituting it into (2.36) with the energy conserving condition $c = 0$, we get

$$\begin{cases} \dot{y}_1 = \sqrt{r_{11}^* r_{11}}\, y_3 \\ \dot{y}_2 = -\alpha_{11} y_1 y_3 + \beta_{11} y_3 \\ \dot{y}_3 = \alpha_{11} y_1 y_2 - \beta_{11} y_2 - \sqrt{r_{11} r_{11}^*}\, y_1 \end{cases}$$

Obviously, this system satisfies the simplified condition B, condition (A2) and (A3).

Since most of the LOMs arose from systems of partial differential equations of interest in geophysical domain are not readily satisfying the simplified conditions above without complicate linear transformations, we would like remain Theorem 2.1 as it is. So the condition in Theorem 2.1 and those simplifications will be used interchangeably without notice throughout the dissertation.

2.3.2 Definition of subset SELOM(*n*) and examples

Referring to the condition A2 in Theorem 2.1, let $A^{(i)}$ be such that for all $i = 1,2, \ldots, n$ and $p \neq i$

$$\left.\begin{array}{l} a_{ii}^{(p)} = 0 \\ a_{ip}^{(i)} = a_{pi}^{(i)} = 0 \end{array}\right\}. \tag{2.37}$$

This when combined with the condition A1, implies that all the elements of $A^{(i)}$ along the principal diagonal, and along the ith row and i^{th} column are zero. Thus, for $n = 3$, we have

$$A^{(1)}=\begin{bmatrix}0 & 0 & 0\\ 0 & 0 & a_{23}^{(1)}\\ 0 & a_{32}^{(1)} & 0\end{bmatrix}, A^{(2)}=\begin{bmatrix}0 & 0 & a_{13}^{(2)}\\ 0 & 0 & 0\\ a_{31}^{(2)} & 0 & 0\end{bmatrix}, A^{(3)}=\begin{bmatrix}0 & a_{12}^{(3)} & 0\\ a_{21}^{(3)} & 0 & 0\\ 0 & 0 & 0\end{bmatrix}$$

and (2.2) becomes

$$\begin{aligned}\dot{x}_1 &= \left(a_{23}^{(1)}+a_{32}^{(1)}\right)x_2x_3+b_{12}x_2+b_{13}x_3\\ \dot{x}_2 &= \left(a_{13}^{(2)}+a_{31}^{(2)}\right)x_1x_3+b_{21}x_1+b_{23}x_3\\ \dot{x}_3 &= \left(a_{12}^{(3)}+a_{21}^{(3)}\right)x_1x_2+b_{31}x_1+b_{32}x_2\,.\end{aligned} \tag{2.38}$$

It can be verified that under condition B and A3, this system (2.38) conserves the kinetic energy. The system is the well known **Volterra gyrostat** that preserves kinetic energy. Refer to Gluhovsky and Tong (1999),

Systems satisfies the additional condition (2.37) consists of an interesting subset of ELOM(n) denoted by SELOM(n). The set SELOM(n) plays an important role in the study of energy conserving LOMs and it connects the energy conserving LOMs to the coupled gyrostats studied by Obukhov (1973) and Gluhovsky *etc*. (1982, 1999, 2002 and 2006). Details are provided in next chapter.

Until now, a natural hierarchy of low-order models is defined as

$$\text{SELOM}(n) \quad \subset \quad \text{ELOM}(n) \quad \subset \quad \text{LOM}(n) \tag{2.39}$$

Graphically, it is showing as Figure 2.1.

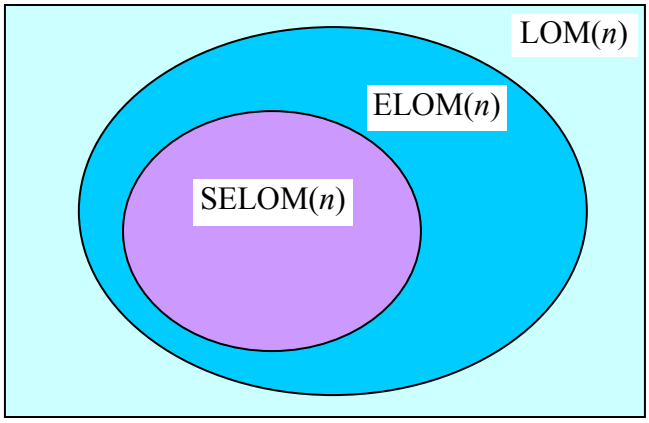

Figure 2.1 Low-order model hierarchy arising from Galerkin projection

Example 2.4 Euler gyroscope and Lorenz's maximum simplification equation: By setting $b_{ij} = 0$ in (2.38), we obtain (after redefining the parameters)

$$\begin{aligned} \dot{x}_1 &= a_1 x_2 x_3 \\ \dot{x}_2 &= a_2 x_1 x_3 \\ \dot{x}_3 &= a_3 x_1 x_2 \,. \end{aligned} \tag{2.40}$$

which represents the Euler gyroscope and the famous maximum simplification equation of Lorenz (1960). Also refer to Lakshmivarahan et. al (2006) for details. Obviously, Euler gyroscope is in the set SELOM(n).

Also note that system in Example 2.3 is also in set SELOM(n).

Now we consider a system that is in the set ELOM(n), but not in the set SELOM(n). The general form of the nth order LOM for Burgers equation is given by (Platzman (1964))

$$\dot{u}_i = \frac{i}{4}\sum_{k=1}^{i-1} u_k u_{i-k} - \frac{i}{2}\sum_{k=1}^{n-i} u_k u_{i+k} \text{ for } i = 1,2,\cdots,n\,. \tag{2.41}$$

By rewriting it in the matrix notation and identifying the n matrices $A^{(i)}$ i = 1,2,…,n, we can easily verify that all conditions in Theorem 2.1 are satisfied. So for any n, the system (2.41) is in ELOM(n).

Example 2.5 Platzman's LOM for Burgers equation (Platzman (1964)): Consider the third order LOM of the Burgers equation derived from (2.41)

$$\left.\begin{aligned} \dot{u}_1 &= -\frac{1}{2}(u_1u_2 + u_2u_3) \\ \dot{u}_2 &= \frac{1}{2}u_1^2 - u_1u_3 \\ \dot{u}_3 &= \frac{3}{2}u_1u_2 \end{aligned}\right\}. \tag{2.42}$$

Let $\mathbf{u} = (u_1, u_2, u_3)^T$. Rewriting in the matrix notation (with $B = 0$ and $C = 0$)

$$\begin{aligned} \dot{u}_1 &= \mathbf{u}^T A^{(1)}\mathbf{u} \\ \dot{u}_2 &= \mathbf{u}^T A^{(2)}\mathbf{u} \\ \dot{u}_3 &= \mathbf{u}^T A^{(3)}\mathbf{u} \end{aligned} \tag{2.43}$$

where

$$A^{(1)} = \begin{bmatrix} 0 & -\frac{1}{2} & 0 \\ 0 & 0 & -\frac{1}{2} \\ 0 & 0 & 0 \end{bmatrix}, A^{(2)} = \begin{bmatrix} \frac{1}{2} & 0 & -1 \\ 0 & 0 & 0 \\ 0 & 0 & 0 \end{bmatrix}, A^{(3)} = \begin{bmatrix} 0 & \frac{3}{2} & 0 \\ 0 & 0 & 0 \\ 0 & 0 & 0 \end{bmatrix}.$$

It can be verified that these matrices satisfy condition (A1)-(A3) and it conserves $\mathrm{E}(\mathbf{u}) = \frac{1}{2}\left(u_1^2 + u_2^2 + u_3^2\right)$. However, the matrix $\mathrm{A}^{(1)}$ does not satisfy condition (2.37). So it is not in the set SELOM(n).

2.4 SUMMARY

In the chapter, we have derived a set of sufficient conditions on the structural parameters of a class of LOM to conserve the energy. This set of conditions provides a systematic method for testing if a given LOM conserves energy. Furthermore, a subset of LOM(n) is also isolated with these conditions as ELOM(n) and it is demonstrated that many low-order models of interest in geophysical applications fall in this set. A subclass of this set is also identified as SELOM(n). It turns out that there is an intrinsic relation between SELOM(n) and the class of systems of coupled gyrostats. The relation is examined with more details in Chapter 3. However, there are also systems of great interest in geophysical domain that do not belong to SELOM(n). One example is provided with Example 2.5 and this kind of system is studied in Chapter 4.

Chapter 3
On the Relation between Energy Conserving LOMs and the Systems of Coupled Volterra Gyrostats

3.1 INTRODUCTION

In mathematical physics, it has been known since the days of Euler and Volterra that gyroscopic dynamics constitutes a prototype of energy conserving systems. Refer to Landau and Lifshitz (1960) and Wittenberg (1977) for details. The classical Volterra gyrostat, denoted by VG(3), is a third order nonlinear dynamical system given by (Refer to Appendix B for a quick overview of Volterra gyrostat)

$$\left.\begin{aligned} \dot{y}_1 &= \alpha y_2 y_3 + h_{12} y_2 + h_{13} y_3 \\ \dot{y}_2 &= \beta y_1 y_3 + h_{21} y_1 + h_{23} y_3 \\ \dot{y}_3 &= \gamma y_1 y_2 + h_{31} y_1 + h_{32} y_2 \end{aligned}\right\} \tag{3.1}$$

where α, β, γ and h_{ij}, $1 \le i \ne j \le 3$ are all real coefficients. The coefficients h_{ij} on the right hand side of (3.1) denote the fixed angular momenta caused by the relative motion of the rotor (Wittenberg (1977)). Denoting $\mathbf{y} = (y_1, y_2, y_3)^T$, it can be verified that VG(3) in (3.1) conserves energy

$$\mathrm{E}_1(\mathbf{y}) = \frac{1}{2}\mathbf{y}^T\mathbf{y} \tag{3.2}$$

when

$$\begin{aligned} &\alpha + \beta + \gamma = 0, \\ \text{and} \quad &h_{ij} + h_{ji} = 0, 1 \le i \ne j \le 3. \end{aligned} \tag{3.3}$$

If $h_{ij} \equiv 0$ for $1 \le i \ne j \le 3$ in (3.1), the resulting dynamical system is known as the Euler gyroscope and is given by

$$\begin{aligned} \dot{y}_1 &= \alpha y_2 y_3 \\ \dot{y}_2 &= \beta y_1 y_3 \\ \dot{y}_3 &= \gamma y_1 y_2 . \end{aligned} \tag{3.4}$$

Further, if $\gamma = 0$, then y_3 is a constant and we obtain the degenerate gyroscope given by

$$\begin{aligned} \dot{y}_1 &= \alpha y_2 y_3 \\ \dot{y}_2 &= \beta y_1 y_3 \end{aligned} \tag{3.5}$$

with $\alpha+\beta = 0$. Besides fluid dynamics and turbulence, Volterra type gyroscopes routinely arise in several application domains including magnetohydrodynamics, dynamics of solid bodies with fluid filled cavities, DNA molecules, to name a few. Refer to Tong and Gluhovsky (2002) for details and references.

It turns out that many copies of VG(3) in (3.1) and its special cases can be coupled to arrive at a system of coupled Volterra gyrostats. Let **CVG(*n*)** denote the set of all coupled Volterra gyrostats of order *n*. The following is an example of a CVG(5) that naturally arises in modeling Rayleigh-Bérnard convection in an electrically conducting fluid (Gluhovsky and Tong (1999)):

$$\left.\begin{array}{lll|l|l} \dot{y}_1 = & -\alpha_1 y_2 y_3 & & & -\lambda_1 y_1 + f \\ \dot{y}_2 = & \alpha_1 y_1 y_3 - h y_3 & & & -\lambda_2 y_2 \\ \dot{y}_3 = & +h y_2 & \alpha_2 y_4 y_5 & & -\lambda_3 y_3 \\ \dot{y}_4 = & & \beta_2 y_3 y_5 & & -\lambda_4 y_4 \\ \dot{y}_5 = & & \gamma_2 y_3 y_4 & & -\lambda_5 y_5 \end{array}\right\} \tag{3.6}$$

A special case of Volterra gyrostat | Euler gyroscope | Extenal forces

By setting all the external forces to zero ($\lambda_i = 0$ for $i = 1, 2, \cdots, 5$ and $f = 0$) in (3.6), it reduces to a system of coupled Volterra gyrostats of order 5 consisting of a special case of VG(3) and the Euler gyroscope. If $S \in \mathrm{CVG}(n)$ has *k* component gyrostats, since it is required that each of these components conserves energy, it follows that every member of CVG(*n*) is a conservative system.

Historically, Lorenz (1960) and Obukhov (1973) represent early attempts to show that there exists a close connection between the energy conserving low-order models and a system of coupled Euler gyroscopes. Gluhovsky (1982), (2006) and Gluhovsky and his collaborators (1999), (2002) extended this idea and showed using several examples that if a given low-order model can be rewritten as a system of coupled Volterra gyrostats, then the low-order model in question conserves energy.

In previous chapter, we have identified an interesting subset of energy-conserving LOMs denoted as SELOM(*n*) that is the special case of energy conserving low-order models denoted by ELOM(*n*). In Section 3.2 of this chapter, we first prove that every member of CVG(*n*) is indeed satisfies the special conditions for conserving energy. That is

$$\mathrm{CVG}(n) \subset \mathrm{SELOM}(n). \tag{3.7}$$

We then provide an algorithm in Section 3.3 for rewriting any member of SELOM(*n*) as a member of CVG(*n*) thereby proving the converse connection between the SELOM(*n*) and the CVG(*n*) families,

$$\mathrm{SELOM}(n) \subset \mathrm{CVG}(n), \tag{3.8}$$

which in turn proves the equivalence $\mathrm{SELOM}(n) = \mathrm{CVG}(n)$. A summary of this chapter is provided in Section 3.4.

3.2 A PROOF OF THE INCLUSION $\mathbf{CVG}(n) \subseteq \mathbf{SELOM}(n)$

As the first step to prove the equivalence between CVG(n) and SELOM(n), we first prove $\mathrm{CVG}(n) \subset \mathrm{SELOM}(n)$ in this section.

In Section 2.3, we have mentioned that any system with $\mathbf{K} \neq \mathbf{I}$ can be converted into a system with $\mathbf{K} = \mathbf{I}$ with proper linear transformation. In this section, we begin by examining the effect of a class of linear transformations on the prototype VG(3) in (3.1). Let $K_i > 0$ for $i = 1, 2, 3$ and define

$$\left.\begin{aligned} y_1 &= \sqrt{K_1}\,x_1 \\ y_2 &= \sqrt{K_2}\,x_2 \\ y_3 &= \sqrt{K_3}\,x_3 \end{aligned}\right\}. \tag{3.9}$$

Substituting (3.9) in (3.1), the latter becomes

$$\left.\begin{aligned} \dot{x}_1 &= \alpha\sqrt{\tfrac{K_2K_3}{K_1}}\,x_2x_3 + h_{12}\sqrt{\tfrac{K_2}{K_1}}\,x_2 + h_{13}\sqrt{\tfrac{K_3}{K_1}}\,x_3 \\ \dot{x}_2 &= \beta\sqrt{\tfrac{K_1K_3}{K_2}}\,x_1x_3 + h_{21}\sqrt{\tfrac{K_1}{K_2}}\,x_1 + h_{23}\sqrt{\tfrac{K_3}{K_2}}\,x_3 \\ \dot{x}_3 &= \gamma\sqrt{\tfrac{K_1K_2}{K_3}}\,x_1x_2 + h_{31}\sqrt{\tfrac{K_1}{K_3}}\,x_1 + h_{32}\sqrt{\tfrac{K_2}{K_3}}\,x_2 \end{aligned}\right\}. \tag{3.10}$$

It can be verified that, under the condition (3.3), this new set of equations in (3.10) conserves energy of the form $\mathrm{E}(\mathbf{x}) = \frac{1}{2}\mathbf{x}^T\mathbf{K}\mathbf{x}$. Stated in other words, the prototype VG(3) in (3.1) with (3.3) conserving $\mathrm{E}(\mathbf{y}) = \frac{1}{2}\mathbf{y}^T\mathbf{y}$ is equivalent to (3.10) conserving $\mathrm{E}(\mathbf{x}) = \frac{1}{2}\mathbf{x}^T\mathbf{K}\mathbf{x}$. Hence, in the following analysis, without loss of generality, we will only

consider the system of coupled gyrostats CVG(n) composed of copies of VG(3) satisfying (3.2) and (3.3).

We start by generalizing the prototype VG(3) in (3.1) for any set of three distinct integers (k, l, m) as

$$\left.\begin{aligned} \dot{y}_k &= \alpha_{lm}^{(k)} y_l y_m + h_{kl} y_l + h_{km} y_m \\ \dot{y}_l &= \alpha_{km}^{(l)} y_k y_m + h_{lk} y_k + h_{lm} y_m \\ \dot{y}_m &= \alpha_{kl}^{(m)} y_k y_l + h_{mk} y_k + h_{ml} y_l \end{aligned}\right\} \tag{3.11}$$

where

$$\begin{aligned} &\alpha_{lm}^{(k)} + \alpha_{km}^{(l)} + \alpha_{kl}^{(m)} = 0 \\ \text{and} \quad &h_{ij} + h_{ji} = 0 \quad \text{for} \quad i, j \in \{k, l, m\} \quad \text{and} \quad i \neq j. \end{aligned} \tag{3.12}$$

For easy reference, we denote the VG(3) in (3.11) as (k, l, m)-gyrostat.

Given any LOM with order $n \geq 3$, our goal is to first characterize the total number of distinct (k, l, m)-gyrostats that are possible, where it is required that

$$1 \leq k, l, m \leq n\,. \tag{3.13}$$

It can be verified that there are a total of $n(n\text{-}1)(n\text{-}2)$ distinct (k, l, m)-triplets satisfying (3.13). Now, given a triplet (k, l, m), there are 3! = 6 different permutations {(k,l,m), (k,m,l), (l,k,m), (l,m,k), (m,k,l), (m,l,k)}, each corresponding to distinct ordering of the three equations in (3.11). However, since the structural relationship between the state variable y_k, y_l and y_m remain **invariant** with respect to these six permutations, it follows that each triplet defines an equivalence class. Without loss of generality, we can pick the triplet (k, l, m) with the constraint

$$k < l < m \tag{3.14}$$

as the representative of this equivalence class. It can be verified that the number of distinct triplets satisfying (3.13) and (3.14) is given by

$$N_g(n) = \frac{1}{6} n(n-1)(n-2). \tag{3.15}$$

Refer to Table 3.1 for an enumeration of these triplets for $3 \le n \le 5$. A little reflection immediately reveals that for a given n, the set CVG(n) is to be synthesized using only the $N_g(n)$ distinct Volterra gyrostats or their special cases.

Table 3.1 An enumeration of distinct (k, l, m)-gyrostats for LOM with order n.

n	$N_g(n)$	A listing of the triplets
3	1	(1,2,3)
4	4	(1,2,3), (1,2,4), (1,3,4), (2,3,4)
5	10	(1,2,3), (1,2,4), (1,3,4), (1,2,5), (1,3,5), (1,4,5), (2,3,4), (2,3,5), (2,4,5), (3,4,5)

We now list the properties of the set of coupled gyrostats in CVG(n).

1) Any member in CVG(n) must contain a minimum of $\left\lceil \frac{n}{3} \right\rceil$ and a maximum of $N_g(n)$ copies of the Volterra gyrostats. Let G(n) denote the unique member of CVG(n) that contains all the $N_g(n)$ copies of VG(3)s. We call G(n) the **maximally coupled systems**.

2) G(n) exhibits a very nice **recursive** structure given by

$$G(n+1) = G(n) \cup S_{n+1} \tag{3.16}$$

where S_{n+1} consists of all new triplets given by

$$S_{n+1} = \begin{Bmatrix} (1,2,n+1),(1,3,n+1),\cdots,(1,n,n+1), \\ (2,3,n+1),(2,4,n+1),\cdots,(2,n,n+1) \\ \vdots \\ (n-1,n,n+1) \end{Bmatrix} \tag{3.17}$$

and

$$\left|S_{n+1}\right| = N_g(n+1) - N_g(n) = \frac{n(n-1)}{2}. \tag{3.18}$$

3) The structure of G(n) is such that each index $1 \le k \le n$ occurs in exactly $\frac{1}{2}(n-1)(n-2)$ triplets. Further, in each of the n equations in G(n), there are exactly $\frac{1}{2}(n-1)(n-2)$ nonlinear terms (α-coefficients) and (n-1)(n-2) linear terms (h-coefficients).

Against this back drop, we now move on to proving the inclusion of CVG(n) in SELOM(n) by induction using G(n) as the representative for the set CVG(n). Since all the other members of CVG(n) are obtained as a special case of G(n), it is sufficient to prove the claim using G(n).

Base case n = 3. For the triplet (1,2,3) we can write (3.11) in the vector form as $\dot{\mathbf{y}} = (1,2,3)$ or equivalently as

$$\dot{\mathbf{y}} = \boldsymbol{\alpha}(\mathbf{y},\mathbf{y}) + \mathbf{H}(3)\mathbf{y} \tag{3.19}$$

where $\mathbf{y} = (y_1, y_2, y_3)^T$, $\boldsymbol{\alpha}(\mathbf{y},\mathbf{y}) = \left(\mathbf{y}^{\mathbf{T}}\boldsymbol{\alpha}^{(1)}(3)\mathbf{y}, \mathbf{y}^{\mathbf{T}}\boldsymbol{\alpha}^{(2)}(3)\mathbf{y}, \mathbf{y}^{\mathbf{T}}\boldsymbol{\alpha}^{(3)}(3)\mathbf{y}\right)^T$

$$\boldsymbol{\alpha}^{(1)}(3)=\begin{bmatrix}0&0&0\\0&0&\alpha_{23}^{(1)}\\0&0&0\end{bmatrix},\quad \boldsymbol{\alpha}^{(2)}(3)=\begin{bmatrix}0&0&\alpha_{13}^{(2)}\\0&0&0\\0&0&0\end{bmatrix},\quad \boldsymbol{\alpha}^{(3)}(3)=\begin{bmatrix}0&\alpha_{12}^{(3)}&0\\0&0&0\\0&0&0\end{bmatrix}$$

and
$$\mathbf{H}(3)=\begin{bmatrix}0&h_{12}^{(123)}&h_{13}^{(123)}\\h_{21}^{(123)}&0&h_{23}^{(123)}\\h_{31}^{(123)}&h_{32}^{(123)}&0\end{bmatrix}.$$

The superscript (123) for the elements of **H**(3) indicates that these *h*-elements are contributed by the triplet (1,2,3).

In view of the condition (3.12), it readily follows that the matrices $\boldsymbol{\alpha}^{(1)}(3),\boldsymbol{\alpha}^{(2)}(3),\boldsymbol{\alpha}^{(3)}(3)$ and **H**(3) associated with (3.19) satisfy the special conditions for SELOM(3) with **K** = **I**. Hence, in view of the equivalence between (3.1) and (3.10) the claim $\text{CVG}(n)\subset\text{SELOM}(n)$ is true for $n = 3$.

Inductive Step: We now verify that the claim is true for (*n*+1) given that it is true for *n*. This involves recursively constructing a new set of (*n*+1)x(*n*+1) α-matrices denoted by $\boldsymbol{\alpha}^{(1)}(n+1),\boldsymbol{\alpha}^{(2)}(n+1),\cdots,\boldsymbol{\alpha}^{(n+1)}(n+1)$ and the new (*n*+1)x(*n*+1) **H**(*n*+1) matrix using the given set of *n*x*n* α-matrices $\boldsymbol{\alpha}^{(1)}(n),\boldsymbol{\alpha}^{(2)}(n),\cdots,\boldsymbol{\alpha}^{(n)}(n)$, the *n*x*n* **H**(*n*) matrix and using all the $\frac{1}{2}n(n-1)$ new triplets given in (3.17).

To save space and for added simplicity and elegance in presentation, we now illustrate this dynamics using $n = 3$. The ideas verbatim carry over to all *n*.

The equation describing G(4) in CVG(4) may be succinctly written as

$$\dot{\mathbf{y}}=(1,2,3)\,|\,(1,2,4)\,|\,(1,3,4)\,|\,(2,3,4) \tag{3.20}$$

with $\mathbf{y} = (y_1, y_2, y_3, y_4)^T$ and each triplet represents the right hand side of (3.11) and the vertical bar separating the triplet represents the union of these four triplets that describe G(4). We now describe the structure of the resulting α and H matrices for G(4) using those of G(3).

$$\boldsymbol{\alpha}^{(1)}(4) = \left[\begin{array}{ccc|c} 0 & 0 & 0 & 0 \\ 0 & 0 & \alpha_{23}^{(1)} & \alpha_{24}^{(1)} \\ 0 & 0 & 0 & \alpha_{34}^{(1)} \\ \hline 0 & 0 & 0 & 0 \end{array}\right], \quad \boldsymbol{\alpha}^{(2)}(4) = \left[\begin{array}{ccc|c} 0 & 0 & \alpha_{13}^{(2)} & \alpha_{14}^{(2)} \\ 0 & 0 & 0 & 0 \\ 0 & 0 & 0 & \alpha_{34}^{(2)} \\ \hline 0 & 0 & 0 & 0 \end{array}\right],$$

$$\boldsymbol{\alpha}^{(3)}(4) = \left[\begin{array}{ccc|c} 0 & \alpha_{12}^{(3)} & 0 & \alpha_{14}^{(3)} \\ 0 & 0 & 0 & \alpha_{24}^{(3)} \\ 0 & 0 & 0 & 0 \\ \hline 0 & 0 & 0 & 0 \end{array}\right], \quad \boldsymbol{\alpha}^{(4)}(4) = \begin{bmatrix} 0 & \alpha_{12}^{(4)} & \alpha_{13}^{(4)} & 0 \\ 0 & 0 & \alpha_{23}^{(4)} & 0 \\ 0 & 0 & 0 & 0 \\ 0 & 0 & 0 & 0 \end{bmatrix}$$

and

$$\mathbf{H}(4) = \begin{bmatrix} 0 & h_{12}^{(123)} + h_{12}^{(124)} & h_{13}^{(123)} + h_{13}^{(134)} & h_{14}^{(124)} + h_{14}^{(134)} \\ h_{21}^{(123)} + h_{21}^{(124)} & 0 & h_{23}^{(123)} + h_{23}^{(234)} & h_{24}^{(124)} + h_{24}^{(234)} \\ h_{31}^{(123)} + h_{32}^{(134)} & h_{32}^{(123)} + h_{32}^{(234)} & 0 & h_{34}^{(134)} + h_{34}^{(234)} \\ h_{41}^{(124)} + h_{41}^{(134)} & h_{42}^{(124)} + h_{42}^{(234)} & h_{43}^{(134)} + h_{43}^{(234)} & 0 \end{bmatrix}.$$

In view of the fact that each of the triplets on the right hand side of (3.20) satisfy the condition similar to (3.12), it can be verified that the matrices $\boldsymbol{\alpha}^{(1)}(4), \boldsymbol{\alpha}^{(2)}(4), \boldsymbol{\alpha}^{(3)}(4), \boldsymbol{\alpha}^{(4)}(4)$ and $\mathbf{H}(4)$ satisfy the special conditions for SELOM(4) with $\mathbf{K} = \mathbf{I}$.

Since the above pattern of arguments can be readily extended to any *n*, the inclusion of CVG(*n*) in SELOM(*n*) is proved.

3.3 CONVERSION OF THE ENERGY CONSERVING LOM AS A SYSTEM OF COUPLED GYROSTATS: AN ALGORITHM

In this section, we prove the converse of $\text{CVG}(n) \subset \text{SELOM}(n)$ which in turn proves the equivalence $\text{CVG}(n) = \text{SELOM}(n)$. We provide an algorithm to convert any system in SELOM(n) into a system of coupled gyrostats by analyzing the properties of the energy conserving LOM defined in SELOM(n). If any system in SELOM(n) can be converted to a system in CVG(n), then the converse of inclusion $\text{SELOM}(n) \subset \text{CVG}(n)$ is proved.

The set SELOM(n) consists energy conserving nonlinear systems with state vector $\mathbf{x} = (x_1, x_2, \cdots, x_n)^T \in \Re^n$ as

$$\dot{x}_i = \mathbf{x}^T A^{(i)} \mathbf{x} + B_i \mathbf{x} \qquad \text{for } i = 1, 2, \cdots, n \tag{3.21}$$

where $\dot{x}_i = \dfrac{dx_i}{dt}$, $A^{(i)} \in \Re^{n \times n}$ is a (real) matrix, $B_i \in \Re^{1 \times n}$ is a (real) row vector. In order for the energy ($\text{E}(\mathbf{x}) = \frac{1}{2}\mathbf{x}^T\mathbf{x}$) to conserve (with **K** = **I**), matrices $\mathbf{A}^{(1)}, \mathbf{A}^{(2)}, \cdots, \mathbf{A}^{(n)}$ and **B** must satisfy the following conditions:

Condition A1: $a_{ii}^{(i)} = 0$ for $i = 1, 2, \cdots, n$

Condition A2 plus the special conditions for SELOM(n): $\begin{cases} a_{pp}^{(i)} \\ a_{ip}^{(i)} = a_{pi}^{(i)} = 0 \end{cases}$ (3.22)

Condition A3: $\left(a_{pq}^{(i)} + a_{qp}^{(i)}\right) + \left(a_{iq}^{(p)} + a_{qi}^{(p)}\right) + \left(a_{ip}^{(q)} + a_{pi}^{(q)}\right) = 0$ for all $i < p < q$

Condition B: $\begin{cases} b_{ii} = 0 & \text{for } i = 1, 2, \cdots, n \\ b_{ij} = -b_{ji} & \text{for } i \neq j \end{cases}$

That is the elements along the principal diagonal and those along the ith row and i^{th} column of matrix $A^{(i)}$ are zero for $i = 1, 2, \ldots, n$, and the matrix **B** is a skew-symmetric matrix. An example of such a matrix $A^{(i)}$ for $n = 4$ and $i = 1$ is

$$A^{(1)} = \begin{bmatrix} 0 & 0 & 0 & 0 \\ 0 & 0 & a_{23}^{(1)} & a_{24}^{(1)} \\ 0 & a_{32}^{(1)} & 0 & a_{34}^{(1)} \\ 0 & a_{42}^{(1)} & a_{43}^{(1)} & 0 \end{bmatrix}. \tag{3.23}$$

To simplify our notation, define (for $q > p$)

$$A_{pq}^{(i)} = \left(a_{pq}^{(i)} + a_{qp}^{(i)} \right). \tag{3.24}$$

Combining these with the conditions in (3.22), the dynamics in (3.21) reduces to

$$\dot{x}_i = \sum_{\substack{p=1 \\ q>p \\ p\neq i}}^{n} A_{pq}^{(i)} x_p x_q + \sum_{\substack{j=1 \\ j\neq i}}^{n} b_{ij} x_j \tag{3.25}$$

for $i = 1, 2 \ldots, n$. The right hand side of (3.25) contains $\frac{(n-1)(n-2)}{2}$ nonlinear terms and (n-1) linear terms. Hence, in all of the n equations there are $\frac{n(n-1)(n-2)}{2}$ nonlinear terms and $n(n$-1) linear terms.

3.3.1 Properties of gyrostats used in the algorithm

Our algorithm seeks to rewrite (3.25) as a system of coupled gyrostats. Actually, it has been revealed that our algorithm uses only four types of gyrostats or their special cases. The four types of gyrostats are listed in Table 3.2 and the general description of the Volterra gyrostats and nine of its special cases are given in Appendix B. For easy

reference, the three nonlinear terms with $\alpha_{lm}^{(k)}, a_{km}^{(l)}$ and $a_{kl}^{(m)}$ as coefficients in (3.11) are call α-terms. Similarly, the six linear terms with h_{kl}, h_{lk}, h_{km}, h_{mk}, h_{ml}, and h_{lm} as coefficients in (3.11) are call h-terms.

Table 3.2 Four types of gyrostats used in the algorithm

Case	Triplet (k, l, m)	Coefficients of the h-terms on the right hand side of						Total number of non-zero h-terms in (3.11)
		$\dot{x}_k$ in (3.11)		$\dot{x}_l$ in (3.11)		$\dot{x}_m$ in (3.11)		
		h_{kl}	h_{km}	h_{lk}	h_{lm}	h_{mk}	h_{ml}	
Type A VG(3)	(k, l, m)	1	1	1	1	1	1	6
Type B	(k, l, m)	0	1	0	1	1	1	4
Type C	(k, l, m)	0	0	0	1	0	1	2
Type D (Euler gyroscope)	(k, l, m)	0	0	0	0	0	0	0

As before, we refer to the gyrostat of the type VG(3) in (3.11) involving the three state variables (x_k, x_l, x_m) by the triplet (k, l, m). Gyrostats of **Type A** in Table 3.2 is the general Volterra gyrostats and the right hand side of each of the three equations contains two non-zero h-terms. For simplicity in notation, in Table 3.2, an entry 1 in the column for h_{kl} denotes that $h_{kl} \neq 0$ and an entry of 0 denotes $h_{kl} = 0$ in (3.11). Thus, referring to the Table 3.2, the gyrostat (k, l, m) described in the first line has a total of six 1 entries corresponding to the six non-zero h-terms on the right hand side of (3.11) and hence it is of Type A. At the other extreme, a gyrostat (k, l, m) is said to be of **Type D**, if there are no h-terms on the right hand side of (3.11). A gyrostat of Type D is also known as the **Euler gyroscope** is represented by the fourth line with all six zero entries in Table 3.2. A triplet (k, l, m) is a gyrostat of **Type B** (**Type C**) if two (four) of the symmetric h-terms

on the right hand side of (3.11) are zeros. Thus, in the Type B triplet, the pair $h_{kl} = h_{lk} = 0$ and in the Type C triplet, $h_{kl} = h_{lk} = 0$ and $h_{km} = h_{mk} = 0$.

3.3.2 The algorithm

Since we have *a priori* decided to use only the four types of gyrostats (Table 3.2) in our construction, the problem now reduces to one of deciding on the number of gyrostats of each of these four types to be used in the synthesis.

To this end, first recall that there are $\frac{1}{2}(n-1)(n-2)$ α-terms and (n-1) h-terms in (3.25). Hence, in all of the n equations (i = 1, 2, …, n), there are a total of $\frac{1}{2}n(n-1)(n-2)$ α-terms and $n(n$-1) h-terms. In view of the identity $\frac{1}{2}n(n-1)(n-2) = 3\binom{n}{3}$, we first divide the set of all α-terms into $\binom{n}{3}$ gyrostats. In distributing the h-terms across these gyrostats, let $W_j^{(n)}$ be the number of gyrostats that have j h-terms assigned to each of them, where j is confined to the set $\mathbf{I} = \{6,4,2,0\}$. As the number of gyrostats and the number of h-terms are fixed, a little reflection reveals that $W_j^{(n)}$ must satisfy the following two conditions:

$$\left.\begin{aligned} W_6^{(n)} + W_4^{(n)} + W_2^{(n)} + W_0^{(n)} &= \binom{n}{3} \\ 6W_6^{(n)} + 4W_4^{(n)} + 2W_2^{(n)} &= n(n-1) \end{aligned}\right\} \tag{3.26}$$

Clearly, there is no unique solution to (3.26). If $(W_6^{(n)}, W_4^{(n)}, W_2^{(n)}, W_0^{(n)})^T$ denotes a solution of (3.26), it can be verified that $(2,2,0,6)^{\mathrm{T}}$ and $(1,2,3,4)^{\mathrm{T}}$ are both solutions of (3.26) for n = 5.

The essential of the algorithm is based on a **greedy strategy** which is one of the basic arsenals in the design of deterministic algorithms. A greedy algorithm, by definition, makes a choice that "looks best at that moment". Surprisingly, this simple myopic strategy can often lead to optimal solutions. Refer to chapter 16 in Cormen *et al.* (2004) for details.

In applying this strategy, we first create as many triplets of Type A as possible by assigning six *h*-terms to each. We then create as many triplets of Type B as possible by assigning four *h*-terms to each, followed by the creation of as many triplets of Type C as possible by assigning two *h*-terms to each. Once all the *h*-terms are assigned, the rest of the triplets are of Type D.

3.3.3 Description of the algorithm

Against this background, we now describe our algorithm using an example of $n = 7$. These ideas readily carry over to any n.

The algorithm is described in three steps.

Step 1 Referring to Figure 3.1 (a) for $n = 7$, we first identify three Volterra gyrostats corresponding to the triplets (1,2,3), (3,4,5) and (5,6,7) of Type A. These three gyrostats are enclosed within the dotted squares in Figure 3.1 (a) and together account for a total of 18 *h*-terms. These three gyrostats are also represented (using notation in Table 3.2) in the first three rows in Table 3.3.

Step 2 Again referring to Figure 3.1 (a), we identify six gyrostats given by the triplets (1,2,4), (1,2,5), (1,2,6), (1,2,7), (3,4,6) and (3,4,7) (of Type B) each carrying four *h*-terms. Refer to next six entries in Table 3.3.

Notice that these nine gyrostats identified in steps 1 and 2 together account for all the 42 *h*-terms that are present for the case $n = 7$. Thus, the rest of the 26 gyrostats must be of Type D (Euler gyroscopes).

Step 3 The rest of the 26 Euler gyroscopes defined by the 26 triples are given in Table 3.3.

The distribution – number vs. type, of the gyrostat resulting from this algorithm is given in Table 3.4.

	1	**2**	**3**	**4**	**5**	**6**	**7**
1	x	2	3	4	5	6	7
2	1	x	3	4	5	6	7
3	1	2	x	4	5	6	7
4	1	2	3	x	5	6	7
5	1	2	3	4	x	6	7
6	1	2	3	4	5	x	7
7	1	2	3	4	5	6	x

(a) $n = 7$

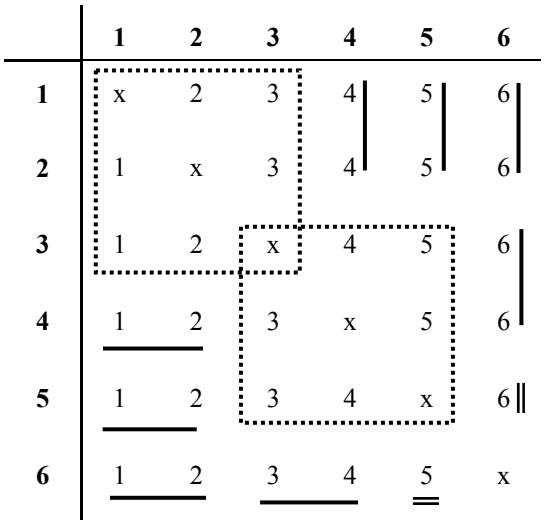

	1	2	3	4	5	6
1	x	2	3	4	5	6
2	1	x	3	4	5	6
3	1	2	x	4	5	6
4	1	2	3	x	5	6
5	1	2	3	4	x	6
6	1	2	3	4	5	x

(b) $n = 6$

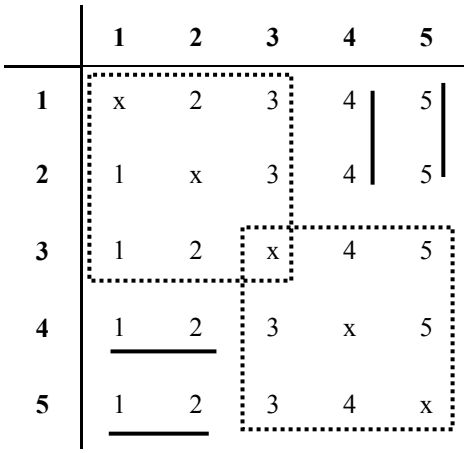

	1	2	3	4	5
1	x	2	3	4	5
2	1	x	3	4	5
3	1	2	x	4	5
4	1	2	3	x	5
5	1	2	3	4	x

(c) $n = 5$

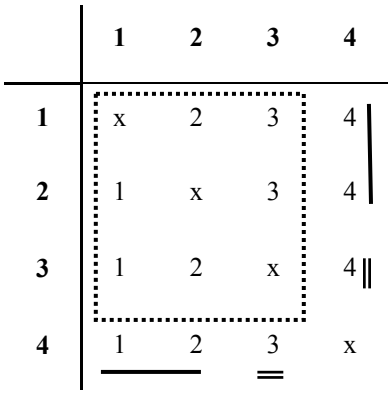

	1	2	3	4
1	x	2	3	4
2	1	x	3	4
3	1	2	x	4
4	1	2	3	x

(d) $n = 4$

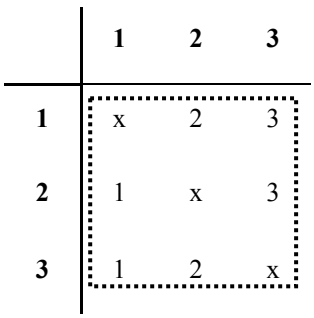

	1	2	3
1	x	2	3
2	1	x	3
3	1	2	x

(e) $n = 3$

Figure 3.1 Patterns of assignment of linear terms into the gyrostats

Table 3.3 A listing of gyrostats with non-zero linear terms

n	The triplets corresponding to the Euler gyroscopes			
7	(1 3 4) (1 3 5) (1 3 6) (1 3 7) (1 4 5) (1 4 6) (1 4 7) (1 5 6) (1 5 7) (1 6 7)	(2 3 4) (2 3 5) (2 3 6) (2 3 7) (2 4 5) (2 4 6) (2 4 7) (2 5 6) (2 5 7) (2 6 7)	(3 5 6) (3 5 7) (3 6 7)	(4 5 6) (4 5 7) (4 6 7)
6	(1 3 4) (1 3 5) (1 3 6) (1 4 5) (1 4 6)	(2 3 4) (2 3 5) (2 3 6) (2 4 5) (2 4 6) (2 5 6)	(3 5 6)	(4 5 6)
5	(1 3 4) (1 3 5) (1 4 5)	(2 3 4) (2 3 5) (2 4 5)		
4		(2 3 4)		
3				

Table 3.4 Distribution – the number and the types of gyrostats

n	$W_6^{(n)}$ (Type A)	$W_4^{(n)}$ (Type B)	$W_2^{(n)}$ (Type C)	$W_0^{(n)}$ (Type D)	$\sum W_j^{(n)}$ (Total # of coupled)	$\sum jW_j^{(n)}$ (Total linear terms)
7	3	6	0	26	35	42
6	2	4	1	13	20	30
5	2	2	0	6	10	20
4	1	1	1	1	4	8
3	1	0	0	0	1	6

The following observations are in order.

1) The set of all triplets of different Types for $n = 6$ can be obtained by applying the basic principles described above to the array for $n = 6$ in Figure 3.1 (b). Clearly there are two Type A triplets given by (1,2,3) and (3,4,5). The triplets (1,2,4), (1,2,5), (1,2,6), (3,4,6) (of Type B) each carries four *h*-terms. The last triplet (1,5,6) (of the Type C) carries two *h*-terms. The rest of the 13 gyrostats are of Type D. Refer to Table 3.2, Table 3.3 and Table 3.4 for details.

2) Referring to Figure 3.1, a similar procedure when used for case n =5, 4 and 3 leads to the decomposition described in Table 3.2, Table 3.3 and Table 3.4.

3) From Table 3.4, it follows that our decomposition algorithm uses only three types – Types A, B and D when n is odd, but uses all the four types when n is even.

4) Referring to Table 3.2 and Table 3.3, it follows that the triplets for $n = 6$ can be easily obtained from those for $n = 7$ by deleting all the triplets containing the symbol 7 and adding a new triplet (1,5,6) in Table 5.2. The gyrostats for $n = 5$ can be obtained from

those for $n = 6$ by deleting all the triplets containing the symbol $n = 6$. Thus, there is a slight asymmetry in going from n odd (=7) to n even (=6) and n even (=6) to n odd (=5).

3.4 CONCLUSION

From the development in Section 3.2, it follows that

$$\text{CVG}(n) \quad \subset \quad \text{SELOM}(n)\,. \tag{3.27}$$

The algorithm in Section 3.3 also guarantees the converse of (3.27). Thereby the equivalence

$$\text{CVG}(n) = \text{SELOM}(n) \tag{3.28}$$

is proved formally.

The earlier work of Obukhov (1973), Lorenz (1960) and Gluhovsky and his collaborators (1982), (1999), (2002) and (2006) using specific examples have explored the intrinsic relation between the two classes of energy conserving dynamical systems – LOM(n) arising from the application of Galerkin type projection technique arising in fluid mechanics and the system of coupled Volterra gyrostats arising from rigid body dynamics in mechanics. In this chapter, we have proved that a subclass of energy-conserving LOM(n) is indeed equivalent to systems of coupled Volterra gyrostats and it is a generalization of the results due to Lorenz (1960), Obukhov (1973) and Gluhovsky *et al*. This result verifies the importance of analyzing the LOM(n) arising in applications including fluid dynamics, turbulence and atmospheric sciences using modular system of coupled gyrostats. However, as we have studied in Chapter 2, SELOM(n) is just a special set of ELOM(n) (see Figure 2.1) and there are still systems of great interest in

geophysical fluid dynamics that are not in SELOM(n) (see Example 2.5). In Chapter 4, we generalize the results further by expanding the definition of the modular systems to include systems in ELOM(n).

Chapter 4
The Extended Definition of Gyrostats and Its Equivalence with Energy Conserving LOMs

4.1 INTRODUCTION

In Chapter 3, we have shown that the systems of coupled Volterra gyrostats is only equivalent to systems in SELOM(n) that is only a subset of the general energy conversing low-order models – ELOM(n). *i.e.*

$$\text{CVG}(n) \quad = \quad \text{SELOM}(n) \quad \subset \quad \text{ELOM}(n) \tag{4.1}$$

To further examine the relation between the general energy conserving model and the system of coupled gyrostats, it is necessary to expand on the notion of Volterra gyrostats. The coefficients of the linear terms on the right-hand side of the Volterra gyrostat in (3.1) admit two natural interpretations. First, as the (fixed) angular momenta caused by the relative motion of the rotor (Wittenberg (1977)). The second is the alternate interpretation following Leipnik and Newton (1981) as the coefficient of the state feed-back. In this Chapter, we extend the concept of Volterra gyrostats to **generalized Volterra gyrostats**, GVG(3), which includes nonlinear feedback. So that the set of all coupled generalized Volterra gyrostats of order n is denoted by CGVG(n). Using this class of gyrostats as the building block, we first prove the equivalence between CGVG(n) and ELOM(n). Then the algorithm for rewriting any system in ELOM(n) as a system in CGVG(n) is also provided. With this new development, the natural hierarchy of energy conserving low-order model mention in Chapter 3 is now linked with the hierarchy of coupled (generalized) Volterra gyrostats (see Figure 4.1).

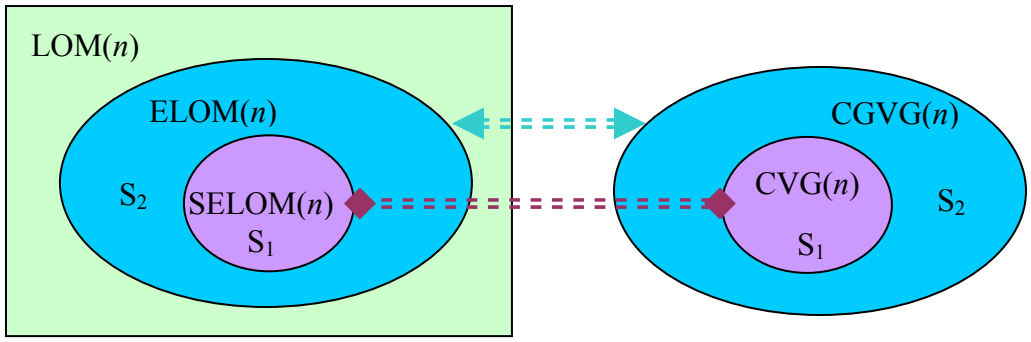

(a) (b)

Figure 4.1 Two classes of models: (a) low-order models arising from Galerkin projection (b) coupled gyrostats.

These results complete the journey, that began with the work of Lorenz (1960), Obukhov (1973) and was extensively studied and extended by Gluhovsky (1982), (2006) and Gluhovsky *et al*. (1999) and (2002), of exploring the intimate relation between the mechanical system of energy conserving coupled Euler gyroscopes and Volterra gyrostats on one hand and the energy conserving low-order models, LOM(n) derived by applying the Galerkin type projection methods to well known fluid dynamics models on the other. It further helps to focus attention on the important role played by the coupled gyrostats in the analysis of fluid dynamical system. This Chapter follows Lakshmivarahan and Wang (2007b) closely.

In Section 4.2, we define the generalized Volterra gyrostats with nonlinear feedback (GVG(3)) and provide examples for CGVG(n). The proof of the equivalence between CGVG(n) and ELOM(n) as well the algorithm for rewriting a system S_2 in

ELOM(n) to a system in CGVG(n) are contained in Section 4.3. At last, this Chapter is concluded in Section 4.4.

4.2 GENERALIZED VOLTERRA GYROSTATS WITH NONLINEAR FEEDBACK

Recall from the introduction that the constant coefficients h_{ij} on the right hand side of (3.1) can be considered as linear state feedback terms (Leipnik and Newton (1981)) that control the overall behaviour of the Volterra gyrostat VG(3). Let $h_{ij} : \Re^3 \to \Re$ for $1 \le i \ne j \le n$. By replacing the constant h_{ij} on the right hand side of (3.1) by a state dependent scalar valued function $h_{ij}(\mathbf{y})$, we obtain the following generalized Volterra gyrostat GVG(3) given by

$$\left.\begin{aligned} \dot{y}_1 &= \alpha y_2 y_3 + h_{12}(\mathbf{y}) y_2 + h_{13}(\mathbf{y}) y_3 \\ \dot{y}_2 &= \beta y_1 y_3 + h_{21}(\mathbf{y}) y_1 + h_{23}(\mathbf{y}) y_3 \\ \dot{y}_3 &= \gamma y_1 y_2 + h_{31}(\mathbf{y}) y_1 + h_{32}(\mathbf{y}) y_2 \end{aligned}\right\} \tag{4.2}$$

where α, β and γ are constants. It can be verified that (4.2) conserves energy $E_1(\mathbf{y})$ in (3.2) when

$$\begin{aligned} &\alpha + \beta + \gamma = 0 \\ &h_{ij}(\mathbf{y}) + h_{ji}(\mathbf{y}) = 0 \text{ for } 1 \le i \ne j \le 3. \end{aligned} \tag{4.3}$$

Analogous to the class of coupled Volterra gyrostats of order n, namely CVG(n), we can also combine generalized gyrostats of the type (4.2) and its special cases to define the new class of coupled generalized Volterra gyrostats of order n, denoted by CGVG(n).

Obviously, systems in CVG(n) are special cases of the generalized Volterra gyrostats in CGVG(n) when the functions $h_{ij}(\mathbf{y})$ are constants. Example 2.5 in Chapter 2

has shown that the Platzman's LOM for the Burgers equations does not belong to SELOM(n), hence it does not also belong to CVG(n). We now show that it is a member of GVG(3).

Example 4.1 Platzman's LOM for Burgers equation (Platzman (1964)).

Consider the third order LOM for the Burgers equation (Platzman (1964)) again given by

$$\left.\begin{aligned} \dot{u}_1 &= -\frac{1}{2}(u_1u_2 + u_2u_3) \\ \dot{u}_2 &= \frac{1}{2}u_1^2 - u_1u_3 \\ \dot{u}_3 &= \frac{3}{2}u_1u_2 \end{aligned}\right\}. \tag{4.4}$$

It is tempting to rewrite (4.4) as

$$\begin{array}{lll} \dot{u}_1 = & -\frac{1}{2}u_2u_3 & -\frac{1}{2}u_1u_2 \\ \dot{u}_2 = & -u_1u_3 & \frac{1}{2}u_1^2 \\ \dot{u}_3 = & \underbrace{\frac{3}{2}u_1u_2}_{\text{group I}} & \underbrace{\qquad\qquad}_{\text{group II}} \end{array} \tag{4.5}$$

and declare that (4.4) is equivalent to a system of coupled Volterra gyrostats. A closer examination, however, reveals that while the terms represented by the group I on the right hand side of (4.5) corresponds to the Euler gyroscope in (3.4), those given by the group II are not equivalent to the degenerate gyroscope in (3.5). Hence (4.4) does not belong to the class of coupled Volterra gyrostats but is a member of the class of the coupled generalized Volterra gyrostats, CGVG(3) as shown below.

Letting $\mathbf{u} = (u_1, u_2, u_3)^T$, we can rewrite (4.4) using matrix-vector notation of (2.2) as follows (with $B = 0$ and $\mathbf{c} = 0$)

$$\left.\begin{aligned} \dot{u}_1 &= \mathbf{u}^T A^{(1)} \mathbf{u} \\ \dot{u}_2 &= \mathbf{u}^T A^{(2)} \mathbf{u} \\ \dot{u}_3 &= \mathbf{u}^T A^{(3)} \mathbf{u} \end{aligned}\right\} \tag{4.6}$$

where

$$A^{(1)} = \begin{bmatrix} 0 & -0.5 & 0 \\ 0 & 0 & -0.5 \\ 0 & 0 & 0 \end{bmatrix}, \quad A^{(2)} = \begin{bmatrix} 0.5 & 0 & -1 \\ 0 & 0 & 0 \\ 0 & 0 & 0 \end{bmatrix}, \quad A^{(3)} = \begin{bmatrix} 0 & 1.5 & 0 \\ 0 & 0 & 0 \\ 0 & 0 & 0 \end{bmatrix}.$$

It can be verified that all of the energy conserving conditions in Theorem 2.1 hold. So the LOM(3) in (4.4) is a member of the class ELOM(3). The property of energy conserving of this system can also be verified using $\dot{\mathrm{E}}_1(\mathbf{u}) = (u_1\dot{u}_1 + u_2\dot{u}_2 + u_3\dot{u}_3) = 0$ directly. However, the additional condition for SELOM(n) in (2.37) does not hold because for $i = 1$ and $p = 2$, $a_{12}^{(1)} = -0.5 \neq 0 = a_{21}^{(1)}$, $a_{11}^{(2)} = 0.5$. Hence, the LOM(3) in (4.4) does not belong to SELOM(3).

By rewriting (4.4) as

$$\left.\begin{aligned} \dot{u}_1 &= -\tfrac{1}{2} u_2 u_3 - \left(\tfrac{1}{2} u_1\right) u_2 \\ \dot{u}_2 &= -u_1 u_3 + \left(\tfrac{1}{2} u_1\right) u_1 \\ \dot{u}_3 &= \tfrac{3}{2} u_1 u_2 \end{aligned}\right\} \tag{4.7}$$

and comparing it with (4.2), it follows that ELOM(3) in (4.7) is also a system in GVG(3) with $\alpha = -\tfrac{1}{2}$, $\beta = -1$, $\gamma = 1$, $h_{12}(u) = -\tfrac{1}{2} u_1$ and $h_{21}(u) = \tfrac{1}{2} u_1$, which in turn satisfies (4.3).

It can be verified readily that any system of order n with each equation satisfying (2.41) is a system in CGVG(n).

This example in addition to illustrating the need for the definition of the GVG(n), also brings out the following question to the lime light: what is the relation between ELOM(n) and the system of coupled generalized Volterra gyrostats, CGVG(n)?

We examine this question in the following section.

4.3 ON THE EQUIVALENCE BETWEEN ELOM(N) AND CGVG(N)

First, the inclusion of CGVG(n) in ELOM(n) is straight-forward as long as we apply the same arguments as those in Section 3.3 by induction. Again, the converse of the inclusion, *i.e.* $\text{ELOM}(n) \subset \text{CGVG}(n)$, is proved by an algorithm to rewrite any system in ELOM(n) as a system in CGVG(n). The algorithm is described in 4 stages.

Stage 1: In this stage we rewrite (2.1) in a form that is critical for our approach.

Taking the Conditions A1 and C of Theorem 2.1 into account, the ith component of (2.1) is given by

$$\dot{x}_i = \underbrace{\sum_{\substack{p=1 \\ p\neq i}}^{n} a_{pp}^{(i)} x_p^2}_{\text{Term I}} + \underbrace{\sum_{p=1}^{n}\sum_{\substack{q=1 \\ q\neq p}}^{n} a_{pq}^{(i)} x_p x_q}_{\text{Term II}} + \underbrace{\sum_{\substack{p=1 \\ p\neq i}}^{n} b_{ip} x_p}_{\text{Term III}} . \tag{4.8}$$

The sum in Term II can be further decomposed into three terms using the elements along the ith row, i^{th} column and the rest of the matrix $A^{(i)}$ as follows:

$$\text{Term II} = \sum_{p=1}^{n}\sum_{\substack{q=1\\q\neq p}}^{n} a_{pq}^{(i)} x_p x_q = \sum_{\substack{p=1\\p\neq i}}^{n} a_{pi}^{(i)} x_i x_p + \sum_{\substack{q=1\\q\neq i}}^{n} a_{iq}^{(i)} x_i x_q + \sum_{\substack{p=1\\p\neq i}}^{n}\sum_{\substack{q=1\\q\neq i\\q\neq p}}^{n} a_{pq}^{(i)} x_p x_q \,. \tag{4.9}$$

Substituting (4.9) into (4.8) and simplifying by collecting the like terms (since p and q are dummy indices), we obtain

$$\dot{x}_i = \sum_{\substack{p=1\\p\neq i}}^{n}\sum_{q>p}^{n} \left(a_{pq}^{(i)} + a_{qp}^{(i)}\right) x_p x_q + \sum_{\substack{p=1\\p\neq i}}^{n} \left[a_{pp}^{(i)} x_p + \left(a_{ip}^{(i)} + a_{pi}^{(i)}\right) x_i + b_{ip} \right] x_p \,. \tag{4.10}$$

By way of simplifying the notation, define

$$A_{pq}^{(i)} = \left(a_{pq}^{(i)} + a_{qp}^{(i)}\right) \tag{4.11}$$

$$d_{ip}(\mathbf{x}) = \left[a_{pp}^{(i)} x_p + \left(a_{ip}^{(i)} + a_{pi}^{(i)}\right) x_i + b_{ip} \right] \tag{4.12}$$

for $p \neq i$ and $q > p$. Substituting (4.11) – (4.12) into (4.10), we obtain a representation that is the basis for our approach, namely

$$\dot{x}_i = \sum_{\substack{p=1\\p\neq i}}^{n}\sum_{q>p}^{n} A_{pq}^{(i)} x_p x_q + \sum_{\substack{p=1\\p\neq i}}^{n} d_{ip}(\mathbf{x}) x_p \tag{4.13}$$

Recall that the collection of systems of the type (4.13) under the condition (A2) – (A3) and Condition B denotes the set ELOM(n).

Remark 4.1 For systems in SELOM(n), it can be verified that $d_{ip}(\mathbf{x}) = b_{ip}$, a constant.

Stage 2: In this stage we establish the relation between ELOM(3) of the type (4.13) and GVG(3) of the type in (4.2). It is useful to consider a third order (n = 3) system of the type (4.13) with three distinct indices $k < l < m$ as follows:

$$\left.\begin{aligned} \dot{x}_k &= A_{lm}^{(k)} x_l x_m + d_{kl}(\mathbf{x}) x_l + d_{km}(\mathbf{x}) x_m \\ \dot{x}_l &= A_{km}^{(l)} x_k x_m + d_{lk}(\mathbf{x}) x_k + d_{lm}(\mathbf{x}) x_m \\ \dot{x}_m &= A_{kl}^{(m)} x_k x_l + d_{mk}(\mathbf{x}) x_k + d_{ml}(\mathbf{x}) x_l \end{aligned}\right\}. \tag{4.14}$$

Define a linear transformation of the variables as follows:

$$\left.\begin{aligned} x_k &= \sqrt{K_l K_m}\, y_k \\ x_l &= \sqrt{K_k K_m}\, y_l \\ x_m &= \sqrt{K_k K_l}\, y_m \end{aligned}\right\} \tag{4.15}$$

where K_i (>0) are the elements of the diagonal elements of the matrix **K** appearing in the expression for energy E(**x**) in (2.4).

Substituting (4.15) into (4.14) and simplifying we get

$$\left.\begin{aligned} \dot{y}_k &= \overline{A}_{lm}^{(k)} y_l y_m + \overline{d}_{kl}(\mathbf{y}) y_l + \overline{d}_{km}(\mathbf{y}) y_m \\ \dot{y}_l &= \overline{A}_{km}^{(l)} y_k y_m + \overline{d}_{lk}(\mathbf{y}) y_k + \overline{d}_{lm}(\mathbf{y}) y_m \\ \dot{y}_m &= \overline{A}_{kl}^{(m)} y_k y_l + \overline{d}_{mk}(\mathbf{y}) y_k + \overline{d}_{ml}(\mathbf{y}) y_l \end{aligned}\right\} \tag{4.16}$$

where

$$\overline{A}_{pq}^{(r)} = K_r A_{pq}^{(r)} \tag{4.17}$$

$$\overline{d}_{pq} = \left(a_{pq}^{(p)} + a_{qp}^{(p)}\right)\sqrt{K_p K_r}\, y_p + a_{qq}^{(p)} K_p \sqrt{\frac{K_r}{K_q}}\, y_q + b_{pq}\sqrt{\frac{K_p}{K_q}} \tag{4.18}$$

for any (p, q, r) as a permutation of (k, l, m). Substituting (4.11) in (4.17) and combining it with the Condition (A3) of Theorem 2.1, we get

$$\overline{A}_{lm}^{(k)} + \overline{A}_{km}^{(l)} + \overline{A}_{kl}^{(m)} = K_k\left(a_{lm}^{(k)} + a_{ml}^{(k)}\right) + K_l\left(a_{km}^{(l)} + a_{mk}^{(l)}\right) + K_m\left(a_{kl}^{(m)} + a_{lk}^{(m)}\right) = 0\,. \tag{4.19}$$

Now, from Condition (A2) of Theorem 2.1, it follows that

$$K_k\left(a_{kl}^{(k)}+a_{lk}^{(k)}\right)=-K_l a_{kk}^{(l)}$$

and

$$K_l\left(a_{kl}^{(l)}+a_{lk}^{(l)}\right)=-K_k a_{ll}^{(k)}. \tag{4.20}$$

Substituting (4.20) into (4.18) for $p = k$ and $q = l$ after simplification, we get

$$\bar{d}_{kl}=a_{ll}^{(k)}K_k\sqrt{\frac{K_m}{K_l}}y_l-a_{kk}^{(l)}K_l\sqrt{\frac{K_m}{K_k}}y_k+b_{kl}\sqrt{\frac{K_k}{K_l}}$$

and

$$\bar{d}_{lk}=a_{kk}^{(l)}K_l\sqrt{\frac{K_m}{K_k}}y_k-a_{ll}^{(k)}K_k\sqrt{\frac{K_m}{K_l}}y_l+b_{lk}\sqrt{\frac{K_l}{K_k}}.$$

Combining these with Condition B of Theorem 2.1, namely $K_k b_{kl} = -K_l b_{lk}$, it can be verified that

$$\bar{d}_{kl}(\mathbf{y})+\bar{d}_{lk}(\mathbf{y})=0\,. \tag{4.21}$$

Since (4.19) and (4.21) are restatements of the conditions in (4.3), it follows immediately that ELOM(3) in (4.14) is indeed a generalized Volterra gyrostat GVG(3).

Table 4.1 Special cases of the GVG(3) corresponding to the triplet (k, l, m) in (4.14)

Case	Triplet (k, l, m)	Coefficients of the D-terms on the right hand side of *						Total number of non-zero D-terms in (4.14)
		$\dot{x}_k$ in (4.14)		$\dot{x}_l$ in (4.14)		$\dot{x}_m$ in (4.14)		
		d_{kl}	d_{km}	d_{lk}	d_{lm}	d_{mk}	d_{ml}	
Type A GVG(3)	(k, l, m)	1	1	1	1	1	1	6
Type B	(k, l, m)	0	1	0	1	1	1	4
Type C	(k, l, m)	0	0	0	1	0	1	2
Type D	(k, l, m)	0	0	0	0	0	0	0

* For simplicity in notation $d_{kl}(\mathbf{x})$ is denoted by d_{kl} and similarly for others. The entry 1 in the column for d_{kl} denotes $d_{kl}(\mathbf{x}) \neq 0$ and entry 0 denotes $d_{kl}(\mathbf{x}) = 0$ in (4.14).

Stage 3 The algorithm again uses only the gyrostat GVG(3) in (4.14) and three of its special cases. Just as in Section 3.3, we refer to the gyrostat of the type GVG(3) in

(4.14) involving the three state variables (x_k, x_l, x_m) by the triplet (k, l, m). The three nonlinear terms with $A_{lm}^{(k)}$, $A_{km}^{(l)}$ and $A_{kl}^{(m)}$ as coefficients in (4.14) are called the A-terms. Similarly, the six linear terms with $d_{kl}(\mathbf{x})$, $d_{lk}(\mathbf{x})$, $d_{km}(\mathbf{x})$, $d_{mk}(\mathbf{x})$, $d_{ml}(\mathbf{x})$ and $d_{lm}(\mathbf{x})$ as coefficients in (4.14) are called the D-terms.

The four types of GVG(3) to be used are listed in Table 4.1. It follows immediately that Table 4.1 is very similar to Table 3.1 except that the α-terms in Table 3.1 are replaced by A-terms and the h-terms are replace by D-terms in Table 4.1. Again, a generalized gyrostat (k, l, m) is said to be of **Type A**, if the right hand side of each of the three equations in (4.14) contains two non-zero D-terms. For simplicity in notation, in Table 4.1, we denote $d_{kl}(\mathbf{x})$ simply as d_{kl} and similarly for other coefficients of the D-terms. An entry 1 in the column for d_{kl} denotes that $d_{kl}(\mathbf{x}) \neq 0$ and an entry of 0 denotes $d_{kl}(\mathbf{x}) = 0$ in (4.14). Thus, referring to the Table 4.1, the generalized gyrostat (k, l, m) described in the first line has a total of six 1 entries corresponding to the six non-zero D-terms on the right hand side of (4.14) and hence it is of Type A. At the other extreme, a generalized gyrostat (k, l, m) is said to be of **Type D**, if there are no D-terms on the right hand side of (4.14). A generalized gyrostat of Type D corresponds to the well known **Euler gyroscope** with traditional definition and is represented by the fourth line with all six zero entries in Table 4.1. A triplet (k, l, m) is a generalized gyrostat of **Type B** (**Type C**) if two (four) of the symmetric D-terms on the right hand side of (4.14) are zeros. Thus, in the Type B triplet, the pair $d_{kl}(\mathbf{x}) = d_{lk}(\mathbf{x}) = 0$ and in the Type C triplet, $d_{kl}(\mathbf{x}) = d_{lk}(\mathbf{x}) = 0$ and $d_{km}(\mathbf{x}) = d_{mk}(\mathbf{x}) = 0$.

Stage 4 A framework for our algorithm is described here.

Again, the target of the algorithm is to determine the number of generalized gyrostats of each type to be used in the synthesis for an order n of the energy conserving LOM. We have *a priori* knowledge that only the four types of generalized gyrostats (Table 4.1) would be used in our construction. Take a close look at the system in (4.13), the following facts are revealed immediately just as those for system in SELOM(n). First, there are exactly $\frac{1}{2}(n-1)(n-2)$ A-terms and (n-1) D-terms in (4.13). Hence, in all of the n equations (i = 1, 2, …, n), there are a total of $\frac{1}{2}n(n-1)(n-2)$ A-terms and $n(n$-1) D-terms. In view of the identity $\frac{1}{2}n(n-1)(n-2)=3\binom{n}{3}$, the set of all A-terms could be divided into $\binom{n}{3}$ gyrostats. So the total number of generalized gyrostats to be decomposed is $\binom{n}{3}$. In distributing the D-terms across these gyrostats, let $W_j^{(n)}$ be the number of gyrostats that have j D-terms assigned to each of them, where j is confined to the set $\mathbf{I}=\{6,4,2,0\}$. As the number of gyrostats and the number of D-terms are fixed, a little reflection reveals that $W_j^{(n)}$ must satisfy the following two conditions:

$$\left.\begin{aligned} W_6^{(n)}+W_4^{(n)}+W_2^{(n)}+W_0^{(n)} &= \binom{n}{3} \\ 6W_6^{(n)}+4W_4^{(n)}+2W_2^{(n)} &= n(n-1) \end{aligned}\right\} \tag{4.22}$$

Clearly, the number of unknowns is greater than the number of available equations and there is no unique solution to (4.22). The purpose of our algorithm is to find at least one of the solutions, but not all of them.

Against this background, the algorithm would use the greedy strategy again just as it has been done in Section 3.3. Each step of the algorithm would be exactly the same as those described in Section 3.3.3 except that those mentions of *h*-terms should be replaced by "*D*-terms" here. To save space, we do not repeat those steps here again, but the general principle is described as following.

In applying the greedy strategy, we first create as many triplets of Type A as possible by assigning six *D*-terms to each. We then create as many triplets of Type B as possible by assigning four *D*-terms to each, followed by the creation of as many triplets of Type C as possible by assigning two *D*-terms to each. Once all the *D*-terms are assigned, the rest of the triplets are of Type D. These ideas apply to any system in ELOM(n).

4.4 CONCLUSION

In this Chapter, we first extend the definition of the classical Volterra gyrostat to include nonlinear feedback. The resulting new class of low-order models is called CGVG(n). Clearly, CGVG(n) is a superset of CVG(n) just as ELOM(n) is a superset of SELOM(n). By extending the equivalence between SELOM(n) and CVG(n), we have proved the equivalence between ELOM(n) and CGVG(n) formally. As a by-product, the algorithm described in Section 4.3 can be used to convert any energy conserving system into a system of coupled generalized Volterra gyrostats with nonlinear feedback. Based on this result, we can claim that the new class of generalized Volterra gyrostats with nonlinear feedback acts as a basic building block for a general class of energy conserving

low-order models that routinely arise in fluid dynamics, turbulence and atmospheric sciences.

This result brings out the importance of analyzing the LOM(n) arising in several application areas including fluid dynamics, turbulence and atmospheric sciences using the modular system of coupled (generalized) gyrostats. Motivated by the important role played by the gyrostats in the studies of energy conserving LOMs, the stability properties of the Volterra gyrostats and nine of its special cases (see Appendix B) is analyzed in much detail in the following Chapter 5.

Chapter 5

Analysis of Volterra Gyrostats: Stability of Equilibria

5.1 INTRODUCTION

A gyrostat by definition (Wittenberg (1977)) is a mechanical system consisting of one or more bodies that behaves like a rigid body with time invariant inertia components. Euler gyroscope is the special case of a gyrostat with a single rotating body or object. The equations describing the rotational motion of the gyroscope and gyrostat constitutes the prototype for the analysis of rigid body dynamics. Wittenberg (1977) provided an elegant derivation of the equations for the gyrostats. Refer to Arnol'd (1989), Landau and Lifschitz (1960) for a discussion of the gyroscope. Gyroscopes and gyrostats are routinely used in the attitude control of space crafts and refer to Hughs (1986) for details.

Mathematically, the Volterra gyrostat and its special cases including Euler gyroscope are described by a system of three coupled non-linear systems (with quadratic nonlinearity) of ordinary differential equations. It is the pioneering work of Lorenz (1960) that built the bridge between this mechanical system and the complex fluid dynamical systems of interest in turbulence and geophysical sciences. Lorenz in 1960 obtained a similar set of equations as Euler gyroscope as a result of the simplification of the spectral version of the vorticity equations (earlier studied by Saltzman (1959)), called "maximum simplification of the dynamical equations".

Obukhov *et al*. (1975) demonstrated the use of coupled Euler gyroscopes for modeling homogeneous flows. Recently, Gluhovsky and his collaborators (1982, 1997,

1999, and 2002) succeeded in showing that general lower order models of interest including the fluid motion within a rotating ellipsoid, connection with Shear, convection in an electrically conducting fluid and turbulence are equivalent to a system of coupled gyrostats which are special cases of a general Volterra gyrostat (with added friction and forcing). Those works have clearly demonstrated that complex dynamical systems can be modularly synthesized using a coupled system of basic building blocks which are special cases of the Volterra gyrostats. In previous chapters, we have gone further by proving formally the intrinsic relation between the two classes of energy conserving dynamical systems – LOM(n) arising from the application of Galerkin type projection technique arising in fluid mechanics and the system of coupled Volterra gyrostats arising from rigid body dynamics in mechanics.

Motivated by this important role played by the Volterra gyrostats in the study of energy conserving LOMs, our goal in this chapter is to analyze the stability of equilibria of the Volterra gyrostat and nine of its special cases. Actually, since the time of Euler, the system of gyroscopes has been the focus of many studies including Thompson (1957), Epstein (1969) and Lakshmivarahan *et al.* (2003). The study in this chapter is based on the earlier work by Lakshmivarahan *et al*. (2006), which is the stability analysis of Euler gyroscope that corresponds to Lorenz's maximum simplification equations.

It should be mentioned in passing that the interest in gyrostats is not confined to the dynamics of rigid bodies in mechanics and fluid mechanics. They arise naturally in a number of application domains — in the analysis of the mechanical models of DNA molecules (Starostin (1996)), open loop dynamic characteristics of smooth air gap brushless dc motors (Hemati (1994)), instabilities associated with the operation of lasers

(Haken (1975)), microscopic dynamics of deterministic chemical chaos (Li and Wang (1998)) and the dynamo effect that relates to the generation and reversal of magnetic fields in astronomical bodies resulting from the non-equilibrium phase transitions in electrically conducting convective fluid motions (Knobloch (1981) and Friedrich and Haken (1992)), to name a few.

Elipe *et al.* (1997) in an interesting paper convert the gyrostat dynamics into a two parameter Hamiltonian problem and analyze the bifurcation in a number of special cases. In a series of papers Tong et al. (1995, 1997) and Kuang et al. (2000, 2001, 2002) analyze the on set of chaos in the dynamics of the gyrostat with friction and external forcing. They rewrite the gyrostat dynamics using the canonical Deprit variables and use the Poincaré-Arnold-Melnikov method. In this chapter, we use the basic kinematics of the gyrostat and provide a comprehensive analysis of bifurcation in the general as well as the nine special cases.

A description of the Volterra gyrostat and nine of its special cases are provided in Section 5.2. Section 5.3 contains an analysis of bifurcation and stability of equilibria for all the cases. Concluding observations are given in Section 5.4.

5.2 THE FAMILY OF VOLTERRA GYROSTATS

A gyrostat consists of two bodies – a carrier and a (symmetric) rotor that rotates about an axis fixed on the carrier body. Let $\boldsymbol{\omega} = \left(\omega_1, \omega_2, \omega_3\right)^{\mathrm{T}} \in \Re^3$ be the vector of angular velocity of the carrier body, where T denotes the transpose of a vector and $\Re^3$ denotes the three dimensional space called the **state space**. Let $\mathbf{h} = (h_1, h_2, h_3)^{\mathrm{T}} \in \Re^3$ be the

vector of fixed angular momentum caused by the relative (gyrostatic) motion of the rotor. The mathematical model that describes the dynamics of this mechanical system is known as the Volterra gyrostat and is given by a set of three nonlinear coupled ordinary differential equations (ODE):

$$\begin{aligned} I_1\dot{\omega}_1 &= (I_2 - I_3)\omega_2\omega_3 + h_2\omega_3 - h_3\omega_2 \\ I_2\dot{\omega}_2 &= (I_3 - I_1)\omega_3\omega_1 + h_3\omega_1 - h_1\omega_3 \\ I_3\dot{\omega}_3 &= (I_1 - I_2)\omega_1\omega_2 + h_1\omega_2 - h_2\omega_1 \end{aligned} \tag{5.1}$$

where the components of the vector $\mathbf{I} = (I_1, I_2, I_3)^{\mathrm{T}}$ are the principal moment of inertia of the gyrostat where $I_i > 0, i = 1,2,3$. Let $(\Re^+)^3 = \{x \in \Re^3 \,|\, x_i > 0, i = 1,2,3\}$. Then $(\Re^+)^3 \times \Re^3$ denotes the **parameter space** where the vector of six parameter $\mathbf{p} = (\mathbf{I}^T, h^T) \in (\Re^+)^3 \times \Re^3$. Refer to Wittenberg (1977) for a derivation of this model dynamics. When $h_i = 0$ for $i = 1,2,3$, the resulting special case is wildly known as the Euler gyroscope (Arnol'd (1989), Landau et al. (1960)) in classical mechanics and as the Lorenz's maximum simplification equation in atmospheric sciences (Lorenz (1960)).

A fundamental property of the model (5.1) is that it conserves kinetic energy and the square of the angular momentum.

Property 5.1 Conservation of kinetic energy: The (rotational) kinetic energy in the system is given by

$$\mathrm{E}(t) = \frac{1}{2}\boldsymbol{\omega}^{\mathrm{T}}(t)\,\mathbf{K}\,\boldsymbol{\omega}(t) \tag{5.2}$$

where

$$\mathbf{K} = \begin{bmatrix} I_1 & 0 & 0 \\ 0 & I_2 & 0 \\ 0 & 0 & I_3 \end{bmatrix} = \text{diag}(I_1, I_2, I_3). \tag{5.3}$$

Note that the matrix **K** is associated with the principal moment of inertia I_i for i = 1, 2,3. It can be verified using conditions in Theorem 2.1 or by direct computation that $\dot{\text{E}}(t) \equiv 0$. Hence the trajectory of (5.1) lies on the surface of the three dimensional energy ellipsoid given by

$$f_E(\boldsymbol{\omega}) = \frac{\omega_1^2}{\left(\frac{2\,\text{E}(0)}{I_1}\right)} + \frac{\omega_2^2}{\left(\frac{2\,\text{E}(0)}{I_2}\right)} + \frac{\omega_3^2}{\left(\frac{2\,\text{E}(0)}{I_3}\right)} - 1 = 0 \tag{5.4}$$

where $\text{E}(0)$ is the initial kinetic energy computed from the initial condition $\boldsymbol{\omega}(0)$ for (5.1). Clearly, this ellipsoid is centered at the origin with its principal axes along the coordinate axes and $\left(\frac{2\,\text{E}(0)}{I_1}\right)^{1/2}$, $\left(\frac{2\,\text{E}(0)}{I_2}\right)^{1/2}$ and $\left(\frac{2\,\text{E}(0)}{I_3}\right)^{1/2}$ as the length of the three semi-axes.

Property 5.2 Conservation of square of the momentum: The square of the momentum is given by

$$\text{M}(t) = \boldsymbol{\omega}^{\text{T}} \mathbf{A} \boldsymbol{\omega} + 2\mathbf{d}^T \boldsymbol{\omega} + e \tag{5.5}$$

where $\mathbf{A} = \mathbf{K}^2, \mathbf{d} = (I_1 h_1, I_2 h_2, I_3 h_3)^{\text{T}}$ and

$$e = h_1^2 + h_2^2 + h_3^2.$$

Again, it can be verified by direct computation that $\dot{\text{M}}(t) \equiv 0$ and that the trajectory of (5.1) lies on the surface of the momentum ellipsoid given by

$$f_{\mathrm{M}}(\boldsymbol{\omega}) = \frac{\left(\omega_1 + h_1/I_1\right)^2}{\left(\dfrac{\mathrm{M}(0)}{I_1^2}\right)} + \frac{\left(\omega_2 + h_2/I_2\right)^2}{\left(\dfrac{\mathrm{M}(0)}{I_2^2}\right)} + \frac{\left(\omega_3 + h_3/I_3\right)^2}{\left(\dfrac{\mathrm{M}(0)}{I_3^2}\right)} - 1 = 0 \tag{5.6}$$

where $\mathrm{M}(0)$ is the initial value of the square of the momentum computed from the initial condition $\boldsymbol{\omega}(0)$ for (5.1). This ellipsoid is centered at $\left(\dfrac{h_1}{I_1}, \dfrac{h_2}{I_2}, \dfrac{h_3}{I_3}\right)^{\mathrm{T}}$ with its principal axes parallel to the coordinate axes and $\left(\dfrac{\mathrm{M}(0)}{I_1^2}\right)$, $\left(\dfrac{\mathrm{M}(0)}{I_2^2}\right)$ and $\left(\dfrac{\mathrm{M}(0)}{I_3^2}\right)$ as the length of the three semi-axes.

Combining these, it follows that the solution of (5.1) must lie on the set

$$S = \left\{ \boldsymbol{\omega} \in \Re^3 \,\middle|\, f_{\mathrm{E}}(\boldsymbol{\omega}) = 0 \text{ and } f_{\mathrm{M}}(\boldsymbol{\omega}) = 0 \right\} \tag{5.7}$$

which is the intersection of the two (not necessarily concentric) ellipsoids. That is this set *S* constitutes the **solution space** for (5.1).

An immediate consequence of (5.4) and (5.6) is that given **I**, **h** and **ω**(0), the trajectories of (5.1) remains bounded:

$$\left|\omega_i(t)\right| \le \min\left\{ \left(\frac{2\,\mathrm{E}(0)}{I_i}\right)^{1/2}, \left(\frac{\mathrm{M}^{1/2}(0)}{I_i} - \frac{h_i}{I_i}\right) \right\}. \tag{5.8}$$

In fluid dynamical applications, it is more convenient to rewrite (5.1) succinctly in the vector form as

$$\dot{\boldsymbol{\omega}} = f(\boldsymbol{\omega}) \tag{5.9}$$

where $\dot{\boldsymbol{\omega}} = (\dot{\omega}_1, \dot{\omega}_2, \dot{\omega}_3)^{\mathrm{T}}$ and $f : \Re^3 \to \Re^3$ is a mapping of the state space into itself (parameterized by the vector **p**) given by $f(\boldsymbol{\omega}) = \left(f_1(\boldsymbol{\omega}), f_2(\boldsymbol{\omega}), f_3(\boldsymbol{\omega})\right)^{\mathrm{T}}$ with

$$\begin{aligned} f_1(\boldsymbol{\omega}) &= a\omega_2\omega_3 + d_{21}\omega_3 - d_{31}\omega_2 \\ f_2(\boldsymbol{\omega}) &= b\omega_3\omega_1 + d_{32}\omega_1 - d_{12}\omega_3 \\ f_3(\boldsymbol{\omega}) &= c\omega_1\omega_2 + d_{13}\omega_2 - d_{23}\omega_1 \end{aligned} \tag{5.10}$$

where

$$\begin{aligned} &a = (I_2 - I_3)I_1^{-1}, \quad b = (I_3 - I_1)I_2^{-1}, \quad c = (I_1 - I_2)I_3^{-1} \\ &d_{ij} = h_i I_j^{-1} \quad i = 1,2,3, \quad j = 1,2,3 \quad \text{and} \quad j \neq i \end{aligned} \tag{5.11}$$

Notice that if $c = 0$, then $I_1 = I_2$ and $b = -a$.

Table 5.1 A listing of the special gyrostats and their number of equilibrium sets

Case No.	**Special Parameters**	**Pattern**		**Number of Equilibria**
		# of nonlinear terms	# of linear terms	
0	General form	3	6	One set
1 (Lorenz gyrostat)	$h_2 = h_3 = 0$ and $c = 0$	2	2	Two sets
2	$h_3 = 0$ and $c = 0$	2	4	Two sets
3	$h_2 = 0$ and $c = 0$	2	4	One sets
4	$c = 0$	2	6	One set
5 (Euler gyroscope)	$h_1 = h_2 = h_3 = 0$	3	0	Three sets
6	$h_2 = h_3 = 0$	3	2	Three sets
7	$h_3 = 0$	3	4	Two sets
8 (Degenerative gyroscope)	$h_1 = h_2 = h_3 = 0$ and $c = 0$	2	0	One set
9 (Degenerative gyrostat)	$h_1 = h_2 = 0$and $c = 0$	2	2	One set

The properties of this system critically depend on the values of six parameters – the values of three principal moments of inertia I_1, I_2, and I_3, and the values of the three angular momenta h_1, h_2, and h_3. When one or more of these six parameters are zero, it results a special case of the general gyrostat dynamics. Based on the definition in Gluhovsky (1999), there are total nine different particular cases of gyrostats (Table 5.1). Gyrostats are considered to be different if their dynamical equations cannot be converted into each other by a linear change of variables. Those nine special cases and the general form of gyrostats differ in the number of linear terms and the number of nonlinear terms. Since the sum of the coefficients for the nonlinear terms is zero, a gyrostat has at least two nonlinear terms. The number of linear (gyrostatic) terms, however, can be zero, two, four or six. The linear gyrostatic terms are usually occurred in LOMs due to various factors peculiar to geophysical fluid dynamics, such as stratification, rotation, and topography. A diagrammatic illustration of the simplification hierarchy with each special gyrostat is given in Figure 5.1. Note that in Figure 5.1, all gyrostats in the right-hand side contain three nonlinear terms and all other cases contains only two nonlinear cases. Based on study in previous chapters, it has been found that all cases (case 5, 6, 7 and the general Volterra gyrostat) on the right-hand side of Figure 5.1 play important roles in the analysis of energy conserving LOMs, and they are also critical cases in the analysis of the stability properties of gyrostats. Case 1 is also a special case with wide interest in atmospheric science because by adding dissipation and forcing, it can be converted to the celebrated Lorenz's system. So it is sometime referred as **Lorenz gyrostat**. We would explore its properties in much more details later.

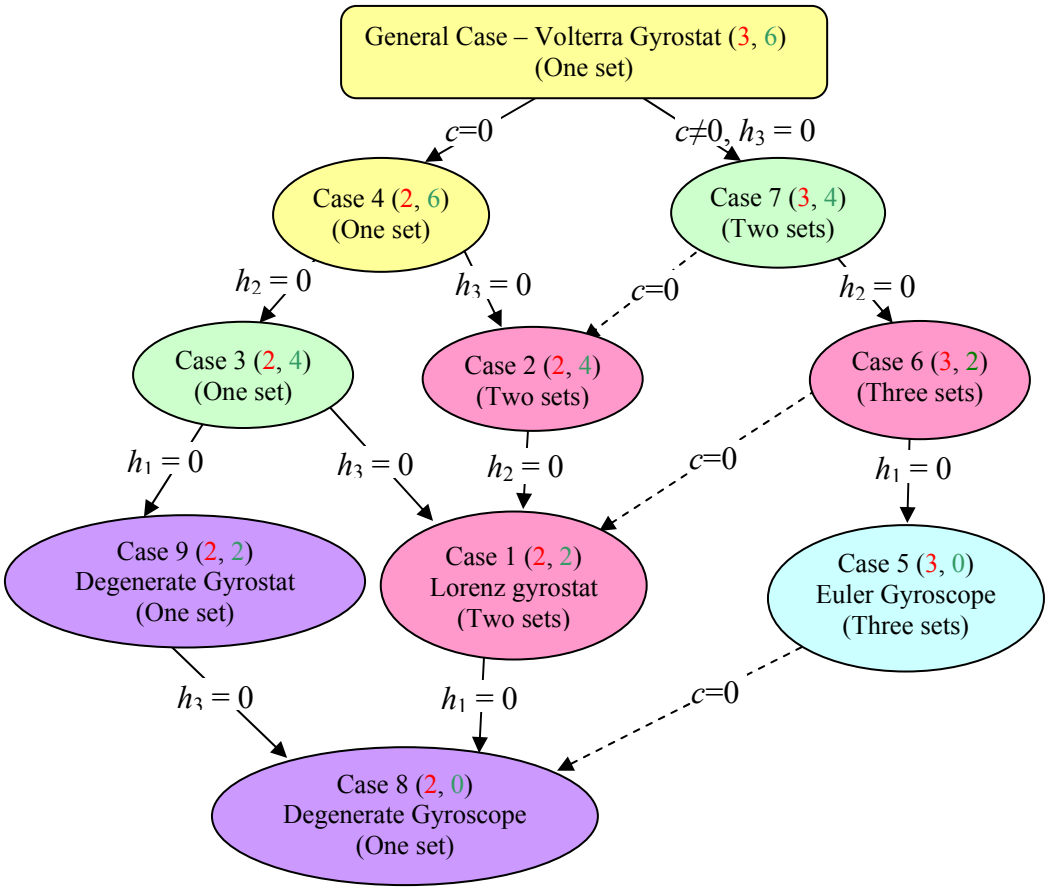

Figure 5.1 The relation between the various special cases of the Volterra Gyrostat. It is assumed that $a \neq 0$ and $b \neq 0$. Number of different sets of equilibria is given in brackets. Red numbers in parenthesis denote the number of nonlinear terms and green numbers for the number of linear terms. Background colors are used to distinguish the stability properties of the equilibria.

5.3 STABILITY ANALYSIS OF GYROSTATS

Referring to the gyrostat dynamics (5.9) or (5.10), the set of all equilibria is defined by the set (Hirsch and Smale (1974)):

$$\boldsymbol{\varepsilon} = \left\{ \boldsymbol{\omega} \in \Re^3 \,\middle|\, f(\boldsymbol{\omega}) = 0 \right\} \tag{5.12}$$

It is well known (Hirsch and Smale (1974), Devaney (1989)) that the stability properties of an equilibrium point $\boldsymbol{\omega}^* \in \boldsymbol{\varepsilon}$ is uniquely determined by the properties of the

eigenvalues of the Jacobian of the function evaluated at point $\boldsymbol{\omega}^*$**.** The Jacobian for any map function $f(\boldsymbol{\omega})$ is given by

$$D_f(\boldsymbol{\omega}) = \begin{bmatrix} \frac{\partial f_1}{\partial \omega_1} & \frac{\partial f_1}{\partial \omega_2} & \frac{\partial f_1}{\partial \omega_3} \\ \frac{\partial f_2}{\partial \omega_1} & \frac{\partial f_2}{\partial \omega_2} & \frac{\partial f_2}{\partial \omega_3} \\ \frac{\partial f_3}{\partial \omega_1} & \frac{\partial f_3}{\partial \omega_2} & \frac{\partial f_3}{\partial \omega_3} \end{bmatrix} \tag{5.13}$$

From the gyrostat dynamics (5.10), we get

$$D_f(\boldsymbol{\omega}) = \begin{bmatrix} 0 & a\omega_3 - d_{31} & a\omega_2 + d_{21} \\ b\omega_3 + d_{32} & 0 & b\omega_1 - d_{12} \\ c\omega_2 - d_{23} & c\omega_1 + d_{13} & 0 \end{bmatrix}. \tag{5.14}$$

Let λ_1, λ_2 and λ_3 be the eigenvalues of a matrix A. Then it is well known that

$$\sum_{i=1}^{n} \lambda_i = \mathrm{tr}(A)$$

where $tr(A)$ denotes the trace (which is the sum of the diagonal elements of) A. For the Jacobian matrix defined in (5.14), we get the following relation immediately,

$$\sum_{i=1}^{3} \lambda_i = tr(D_{\mathrm{f}}(\boldsymbol{\omega}^*) = 0\,.$$

Thus, the dynamics of gyrostat preserves the volume which is to be expected since it is a conservative system. An immediate consequence of this observation is that the equilibrium points for all gyrostats must be either a **center** or a **saddle** point (Guckenheimer and Holmes (1983)).

Based on the studies have been done in previous chapters, it has been found that Cases 5, 6, 7 and the general form in Table 5.1 play important roles in the synthesis process of the energy conserving LOMs. We have used these four cases exclusively in the algorithm for converting systems in ELOM(n) (systems in SELOM(n) are its special cases) into coupled (generalized) gyrostats (systems in CGVG(n) or its subclass CVG(n)). The properties for all other cases (Case 1, 2, 3, 4, 8, 9 in Table 5.1 or Figure 5.1) can be derived directly those four cases. So we identify Cases 5, 6, 7 and the general Volterra gyrostat as **critical cases** and their stability properties are studied in much detail below.

5.3.1 The degenerated gyrostats

We study the simple cases first. Both Case 8 and Case 9 are degenerated gyrostats and all their equilibria should be stable.

(**Case 8**) For Case 8, $h_1 = h_2 = h_3 = 0$ and $c = 0$ (*i.e.* $I_1 = I_2$). Then we obtain

$$\begin{aligned} f_1(\boldsymbol{\omega}) &= (a\omega_3)\omega_2 \\ f_2(\boldsymbol{\omega}) &= -(a\omega_3)\omega_1 \\ f_3(\boldsymbol{\omega}) &= 0 \cdot \end{aligned} \tag{5.15}$$

The parameter set affecting this case is $\mathbf{p} = \left(I_1, I_3\right)^{\mathrm{T}} \in (\Re^+)^2$. Since ω_3 is a constant, the solution reduces to a linear harmonic oscillator

$$\begin{pmatrix} \dot{\omega}_1 \\ \dot{\omega}_2 \end{pmatrix} = \begin{bmatrix} 0 & a\omega_3 \\ -a\omega_3 & 0 \end{bmatrix} \begin{pmatrix} \omega_1 \\ \omega_2 \end{pmatrix} \tag{5.16}$$

with $\boldsymbol{\omega}^* = (0,0,\omega_3)^{\mathrm{T}} \in \boldsymbol{\varepsilon}_3$ as its only equilibrium point. The eigenvalues of the Jacobian $D_f(\boldsymbol{\omega}^*)$ which is the 2×2 matrix on the right-hand side of (5.16) are given by

$$\lambda = \pm i|a|\omega_3 . \tag{5.17}$$

Hence, the equilibrium is a **center** and the solution of (5.16) is periodic (Hirsch and Smale (1974)).

(**Case 9**) Similarly, consider the parameters for Case 9, $h_1 = h_2 = 0$ and $c = 0$. Then (5.10) reduces to

$$\begin{aligned} f_1(\boldsymbol{\omega}) &= \quad (a\omega_3 - d_{31})\omega_2 \\ f_2(\boldsymbol{\omega}) &= -(a\omega_3 - d_{32})\omega_1 \\ f_3(\boldsymbol{\omega}) &= 0. \end{aligned} \tag{5.18}$$

Note that $d_{31} = d_{32}$ for this case and let $d_3 = d_{31} = d_{32}$. The parameter set affecting this case is $\mathbf{p} = (I_1, I_3, h_3)^{\mathrm{T}} \in (\Re^+)^2 \times \overline{\Re}$. Again, since ω_3 is a constant, assuming $a\omega_3 \neq d_3$, (5.9) becomes a linear harmonic oscillator

$$\begin{pmatrix} \dot{\omega}_1 \\ \dot{\omega}_2 \end{pmatrix} = \begin{bmatrix} 0 & (a\omega_3 - d_3) \\ -(a\omega_3 - d_3) & 0 \end{bmatrix} \begin{pmatrix} \omega_1 \\ \omega_2 \end{pmatrix} \tag{5.19}$$

with $\boldsymbol{\omega}^* = (0,0,\omega_3)^{\mathrm{T}} \in \boldsymbol{\varepsilon}_3$ as its only equilibrium as in case 8. The eigenvalues of the Jacobian $D_f(\boldsymbol{\omega}^*)$ which is the 2×2 matrix on the right-hand side of (5.19) are given by

$$\lambda = \pm i|a\omega_3 - d_3| . \tag{5.20}$$

Thus, the equilibrium is a **center** and the solution of (5.19) is periodic.

5.3.2 Gyrostats with uniform properties for the equilibria

(**Case 5**) Case 5 in Table 5.1 is the well known Euler gyroscope and has been the subject of analysis by various authors including Arnol'd (1989), Epstein (1969), Hughs (1986), Lakshmivarahan et al. (2003, 2006), Landau and Lifschitz (1960), Lorenz (1960), Thompson (1957) and Wittenburg (1977). From Table 5.1, the choice of parameters are $h_1 = h_2 = h_3 = 0$. Then the corresponding parameter vector for this case becomes $\mathbf{p} = (I_1, I_2, I_3)^{\mathrm{T}} \in (\Re^+)^3$, and the dynamical system (5.10) reduces to

$$\begin{aligned} f_1(\boldsymbol{\omega}) &= a\omega_2\omega_3 \\ f_2(\boldsymbol{\omega}) &= b\omega_3\omega_1 \\ f_3(\boldsymbol{\omega}) &= c\omega_1\omega_2 \cdot \end{aligned} \tag{5.21}$$

Since Lakshmivarahan *et al.* (2006) have provided a comprehensive analysis of the stability of this case, to save space, we only provide a summary of these results. There are three sets of equilibrium given by

$$\begin{aligned} \boldsymbol{\varepsilon}_1 &= \left\{\boldsymbol{\omega} \in \mathrm{R}^3 \,\middle|\, \omega_1 \text{ is free, } \omega_2 = \omega_3 = 0\right\} = \text{the } \omega_1 \text{ axis} \\ \boldsymbol{\varepsilon}_2 &= \left\{\boldsymbol{\omega} \in \mathrm{R}^3 \,\middle|\, \omega_2 \text{ is free, } \omega_3 = \omega_1 = 0\right\} = \text{the } \omega_2 \text{ axis} \\ \boldsymbol{\varepsilon}_3 &= \left\{\boldsymbol{\omega} \in \mathrm{R}^3 \,\middle|\, \omega_3 \text{ is free, } \omega_1 = \omega_2 = 0\right\} = \text{the } \omega_3 \text{ axis} \cdot \end{aligned} \tag{5.22}$$

The Jacobian of $f(\boldsymbol{\omega})$ in (5.21) is given by

$$D_f(\boldsymbol{\omega}) = \begin{bmatrix} 0 & a\omega_3 & a\omega_2 \\ b\omega_3 & 0 & b\omega_1 \\ c\omega_2 & c\omega_1 & 0 \end{bmatrix}. \tag{5.23}$$

The characteristic properties of the equilibria are listed in Table 5.2. A distinguishing feature of this case is that depending only on the components of **I**, every point $\boldsymbol{\omega}^* \in \boldsymbol{\varepsilon}_i, i = 1,2,3$ is uniformly a saddle point or a center. From Table 5.2, it is clear that

one of the eigenvalues of $D_f(\boldsymbol{\omega}^*)$ is always zero. For definiteness, consider $\boldsymbol{\omega}^* \in \boldsymbol{\varepsilon}_1$. Then, for $bc > 0$, that is, when $I_3 > I_1 > I_2$ or $I_3 < I_1 < I_2$, the non-zero eigenvalues λ_2 and λ_3 are real, equal in magnitude but opposite in sign. For these values of the parameters, $\boldsymbol{\omega}^*$ is an unstable **saddle point**. In this case, the solution of (5.21) forms a **heteroclinic orbit** (Sparrow (1982)) that connects the pair of unstable equilibria $\boldsymbol{\omega}^* = (\omega_1, 0, 0)^{\mathrm{T}}$ and $-\boldsymbol{\omega}^* = (-\omega_1, 0, 0)^{\mathrm{T}}$ for every $\omega_1 \neq 0$. Refer to Figure 5.2 for an example of this orbit.

For all other values of parameters I_1, I_2, I_3 not satisfying $I_3 > I_1 > I_2$ or $I_3 < I_1 < I_2$, the eigenvalues λ_2 and λ_3 are purely imaginary and conjugates of each other. In this case, $\boldsymbol{\omega}^*$ is called a **center**. The solution of (5.21) in this case exhibits oscillatory behavior. Refer to Figure 5.3 for an illustration. Similar behavior of the orbits can be observed starting from points close to the equilibrium points in $\boldsymbol{\varepsilon}_2$ and $\boldsymbol{\varepsilon}_3$.

Table 5.2 Properties of equilibria – Case 5

Equilibria	Jacobian	Eigenvalues	Characteristics of Equilibria
$\boldsymbol{\omega}^* \in \boldsymbol{\varepsilon}_1$	$\begin{bmatrix} 0 & 0 & 0 \\ 0 & 0 & b\omega_1 \\ 0 & c\omega_1 & 0 \end{bmatrix}$	$\lambda_1 = 0$ $\lambda_{2,3} = \pm\omega_1\sqrt{bc}$	For $bc > 0$, that is, $I_3 > I_1 > I_2$ or $I_3 < I_1 < I_2$, $\boldsymbol{\omega}^*$ is an unstable **saddle point**. Otherwise, $\boldsymbol{\omega}^*$ is a **center**.
$\boldsymbol{\omega}^* \in \boldsymbol{\varepsilon}_2$	$\begin{bmatrix} 0 & 0 & a\omega_2 \\ 0 & 0 & 0 \\ c\omega_2 & 0 & 0 \end{bmatrix}$	$\lambda_1 = 0$ $\lambda_{2,3} = \pm\omega_2\sqrt{ac}$	For $ac > 0$, that is, $I_1 > I_2 > I_3$ or $I_1 < I_2 < I_3$, $\boldsymbol{\omega}^*$ is an unstable **saddle point**. Otherwise, $\boldsymbol{\omega}^*$ is a **center**.
$\boldsymbol{\omega}^* \in \boldsymbol{\varepsilon}_3$	$\begin{bmatrix} 0 & a\omega_3 & 0 \\ b\omega_3 & 0 & 0 \\ 0 & 0 & 0 \end{bmatrix}$	$\lambda_1 = 0$ $\lambda_{2,3} = \pm\omega_3\sqrt{ab}$	For $ab > 0$, that is, $I_2 > I_3 > I_1$ or $I_2 < I_3 < I_1$, $\boldsymbol{\omega}^*$ is an unstable **saddle point**. Otherwise, $\boldsymbol{\omega}^*$ is a **center**.

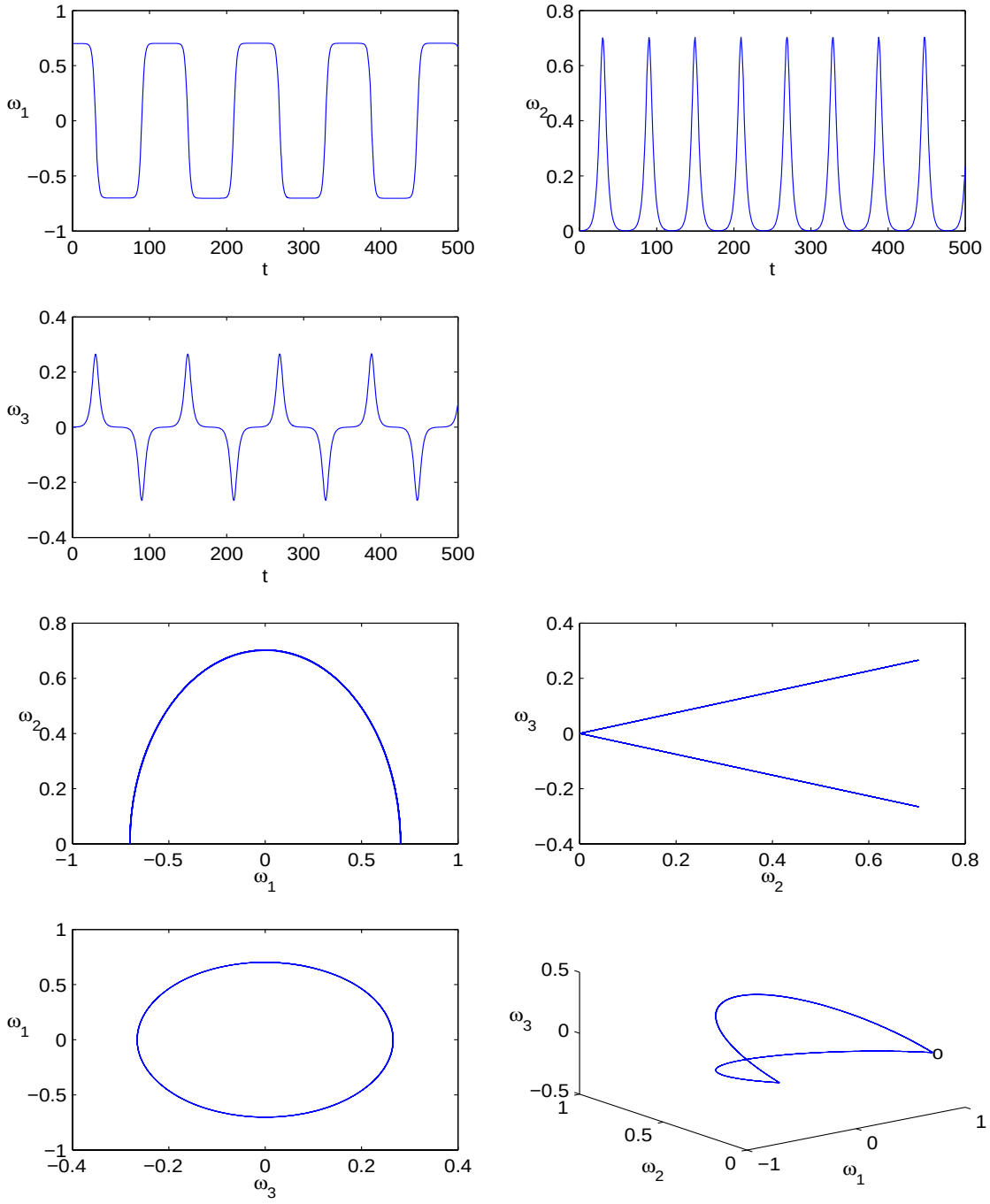

Figure 5.2 An illustration of the heteroclinic orbit starting from $\boldsymbol{\omega}(0) = \boldsymbol{\omega}^* + \boldsymbol{\delta}$, $\boldsymbol{\omega}^* = (0.7, 0, 0)^{\mathrm{T}}$, $\boldsymbol{\delta} = (0, 0.001, 0)^{\mathrm{T}}$, $\mathbf{I} = (4, 3, 7)^{\mathrm{T}}$ and $\mathbf{h} = (0, 0, 0)^{\mathrm{T}}$ for Case 5. $\boldsymbol{\omega}^* \in \boldsymbol{\varepsilon}_1$ is a saddle point.

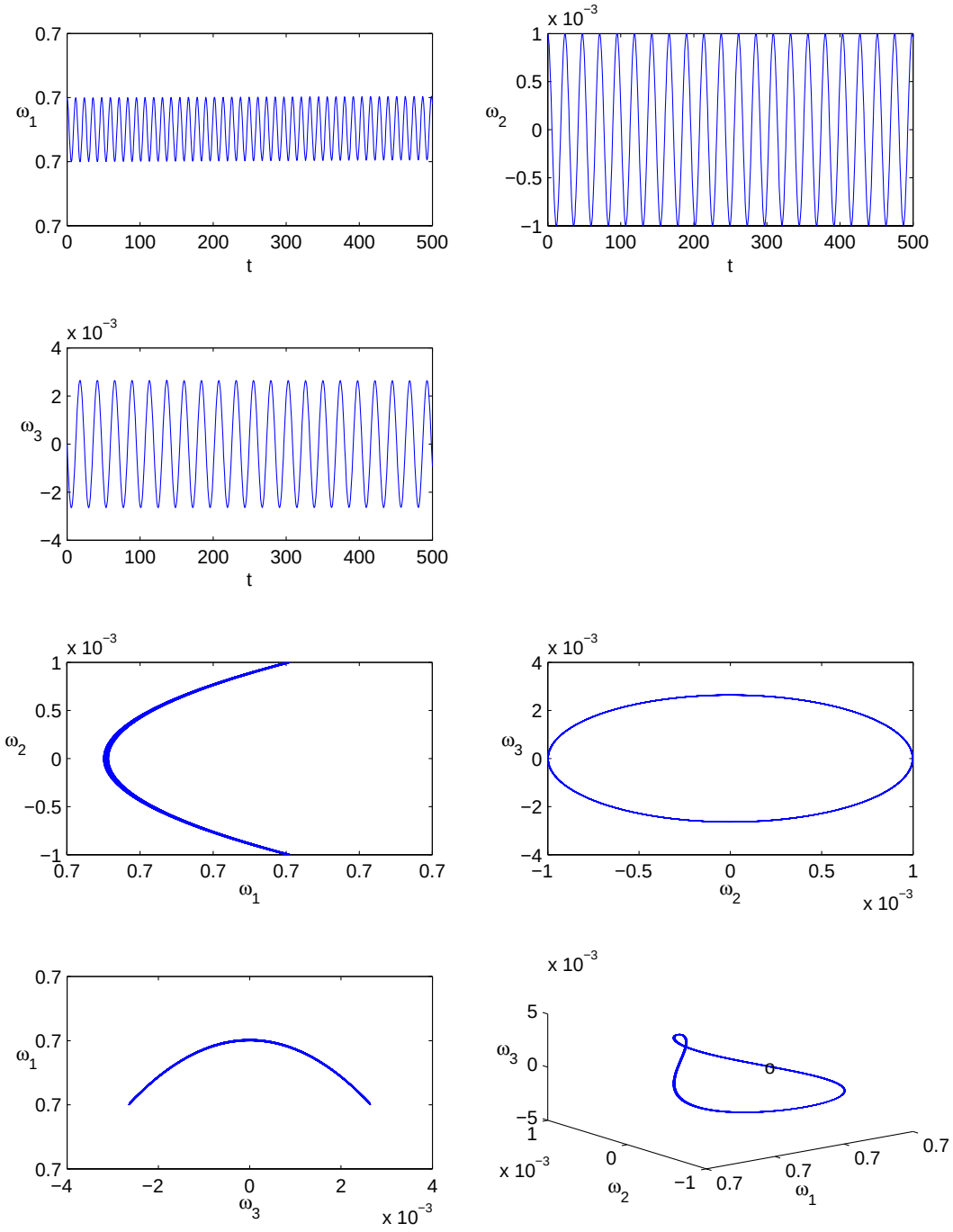

Figure 5.3 An illustration of the orbit starting from $\boldsymbol{\omega}(0) = \boldsymbol{\omega}^* + \boldsymbol{\delta}$, $\boldsymbol{\omega}^* = (0.7, 0, 0)^{\mathrm{T}}$, $\boldsymbol{\delta} = (0, 0.001, 0)^{\mathrm{T}}$, $\mathbf{I} = (3, 7, 4)^{\mathrm{T}}$ and $\mathbf{h} = (0, 0, 0)^{\mathrm{T}}$ for Case 5. $\boldsymbol{\omega}^* \in \boldsymbol{\varepsilon}_1$ is a center.

5.3.3 Gyrostats with linear equilibria but the stability is not uniform

Cases 1, 2 and 6 in Table 5.1 have all equilibria as straight lines in the state space just as those for Case 5. However, those straight lines are not strictly the axes any more, and they are also not uniformly saddle or uniformly center.

(**Case 6**) We study Case 6 first. The special parameters are $h_2 = h_3 = 0$. Then the parameter space is $\mathbf{p} = (I_1, I_2, I_3, h_1)^{\mathrm{T}} \in (\Re^+)^3 \times \overline{\Re}$ where $\overline{\Re} = \{x \in \Re \,|\, x \neq 0\}$ and the dynamical equations are

$$\begin{aligned} f_1(\boldsymbol{\omega}) &= a\omega_2\omega_3 \\ f_2(\boldsymbol{\omega}) &= b\omega_3\omega_1 - d_{12}\omega_3 \\ f_3(\boldsymbol{\omega}) &= c\omega_1\omega_2 + d_{13}\omega_2 \,. \end{aligned} \tag{5.24}$$

There are three sets of equilibria given by

$$\begin{aligned} \boldsymbol{\varepsilon}_1 &= \{\boldsymbol{\omega} \in \mathrm{R}^3 \,|\, \omega_1 \text{ is free, } \omega_2 = \omega_3 = 0\} = \text{the } \omega_1 \text{ axis} \\ \boldsymbol{\varepsilon}_2 &= \left\{\boldsymbol{\omega} \in \mathrm{R}^3 \,\middle|\, \omega_1 = -\frac{d_{13}}{c}, \omega_2 \text{ is free, } \omega_3 = 0\right\} \\ &= \text{a straight line parallel to the } \omega_2 \text{ axis in the } (\omega_1, \omega_2)\text{-plane} \end{aligned} \tag{5.25}$$

and

$$\begin{aligned} \boldsymbol{\varepsilon}_3 &= \left\{\boldsymbol{\omega} \in \mathrm{R}^3 \,\middle|\, \omega_1 = \frac{d_{12}}{b}, \omega_2 = 0, \omega_3 \text{ is free}\right\} \\ &= \text{a straight line parallel to the } \omega_3 \text{ axis in the } (\omega_1, \omega_3)\text{-plane.} \end{aligned}$$

The relative disposition of these three equilibria is shown in Figure 5.4. The Jacobian of (5.24) is given by

$$D_{\mathrm{f}}(\boldsymbol{\omega}) = \begin{bmatrix} 0 & a\omega_3 & a\omega_2 \\ b\omega_3 & 0 & b\omega_1 - d_{12} \\ c\omega_2 & c\omega_1 + d_{13} & 0 \end{bmatrix}. \tag{5.26}$$

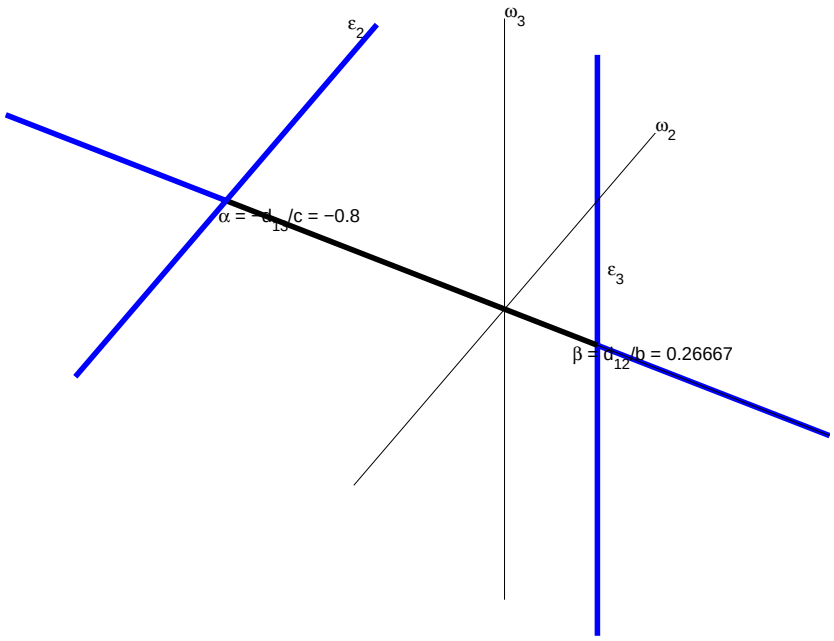

Figure 5.4 Relative disposition of the three equilibria for Case 6. $\boldsymbol{\varepsilon}_1 = (\omega_1, 0, 0)^{\mathrm{T}}$, $\boldsymbol{\varepsilon}_2 = (-\frac{d_{13}}{c}, \omega_2, 0)^{\mathrm{T}}$ and $\boldsymbol{\varepsilon}_3 = (\frac{d_{12}}{b}, 0, \omega_3)^{\mathrm{T}}$. $\mathbf{I} = (4,3,7)^{\mathrm{T}}$, $\mathbf{h} = (0.8,0,0)^{\mathrm{T}}$, a = -1, b = 1, c = 0.14286, d_{12} = 0.2667, d_{13} =0.1143. Every point along the ω_1–axis that are in the interval (α, β) is a center. Points along the ω_1-axis outside of the interval (α, β) are saddle points.

Since the equilibria $\boldsymbol{\varepsilon}_2$ and $\boldsymbol{\varepsilon}_3$ are straight line parallel to the axes, they have similar properties just as those equilibria for Case 5. The points in either $\boldsymbol{\varepsilon}_2$ or $\boldsymbol{\varepsilon}_3$ are all uniformly a saddle point or a center depending only on the values of the parameters I_i, i = 1,2,3. Hence, as in case 5, orbits starting from points $\boldsymbol{\omega}(0)$ close to $\boldsymbol{\omega}^* \in \boldsymbol{\varepsilon}_2$ or $\boldsymbol{\omega}^* \in \boldsymbol{\varepsilon}_3$ in (5.25) are heteroclinic or periodic orbits depending on whether the equilibrium point $\boldsymbol{\omega}^*$ is a saddle point or a center. This property can also be verified by calculating the eigenvalues of (5.26) at equilibrium $\boldsymbol{\varepsilon}_2$ or $\boldsymbol{\varepsilon}_3$ and it has exactly the same eigenvalues as Case 5 at equilibrium $\boldsymbol{\varepsilon}_2$ and $\boldsymbol{\varepsilon}_3$.

It turns out however that the coefficient h_1 for the two linear terms plays an critical role in separating equilibrium $\boldsymbol{\varepsilon}_2$ and equilibrium $\boldsymbol{\varepsilon}_3$, hence, changing the properties of equilibrium $\boldsymbol{\varepsilon}_1$. In equilibrium $\boldsymbol{\varepsilon}_1$, the Jacobian $D_f(\boldsymbol{\omega}^*)$ becomes

$$D_f(\boldsymbol{\omega}^*)\Big|_{\boldsymbol{\omega}^* \in \boldsymbol{\varepsilon}_1} = \begin{bmatrix} 0 & 0 & 0 \\ 0 & 0 & b\omega_1 - d_{12} \\ 0 & c\omega_1 + d_{13} & 0 \end{bmatrix}$$

with eigenvalues as

$$\lambda_1 = 0$$
$$\lambda_{2,3} = \pm\sqrt{\mathrm{P}(\omega_1)}$$

where
$$\mathrm{P}(\omega_1) = (b\omega_1 - d_{12})(c\omega_1 + d_{13})\,. \tag{5.27}$$

The properties of the equilibrium $\boldsymbol{\varepsilon}_1$ depends on the sign of the quadratic function $\mathrm{P}(\omega_1)$ in (5.27). It can be verified that $\mathrm{P}(0) < 0$ and the two real roots of $\mathrm{P}(\omega_1) = 0$ are given by

$$\omega_1^{(1)} = \frac{d_{12}}{b} = \frac{h_1}{I_3 - I_1}$$

and
$$\omega_1^{(2)} = -\frac{d_{13}}{c} = -\frac{h_1}{I_1 - I_2}\,. \tag{5.28}$$

Referring to the Figure 5.4, it can be verified that these two roots correspond to the two points of intersection of ε_1 with ε_2 and ε_3 respectively. Further, $\omega_1^{(1)} = \omega_1^{(2)} = 0$ when $h_1 = 0$ (Case 5) and $\omega_1^{(1)} = \omega_1^{(2)} \neq 0$ when $h_1 \neq 0$. Recall from assumption in earlier sections that $a \neq 0$ and $b \neq 0$ is a common requirement and also $h_1 \neq 0$ for this case (Case 6), it follows that the two roots of $\mathrm{P}(\omega_1)$ are non-zero, real and unequal. Let

$$\alpha = \min\{\omega_1^{(1)}, \omega_1^{(2)}\} \text{ and } \beta = \max\{\omega_1^{(1)}, \omega_1^{(2)}\}$$

where $\alpha < \beta$.

Two cases arise depending on the sign of *bc* (see (5.27)).

Case A: when $bc > 0$ (that is, when $I_3 > I_2 > I_1$ or $I_3 < I_2 < I_1$ in (5.1)), $P(\omega_1)$ is convex (exhibits a minimum) with $\alpha < 0 < \beta$ and $P(\omega_1) < 0$ for $\omega_1 \in (\alpha, \beta)$ and $P(\omega_1) > 0$ for $\omega_1 \in (-\infty, \alpha)$ or (β, ∞). Thus, $\omega^* = (\omega_1, 0, 0)^T \in \boldsymbol{\varepsilon}_1$ in (5.25) is a (stable) **center** when $\omega_1 \in (\alpha, \beta)$ and it is an (unstable) **saddle** point otherwise.

Case B: when $bc < 0$, $P(\omega_1)$ is concave (exhibits a maximum) with $0 < \alpha < \beta$ or $\alpha < \beta < 0$ and $P(\omega_1) > 0$ for $\omega_1 \in (\alpha, \beta)$ and $P(\omega_1) < 0$ for $\omega_1 \notin (\alpha, \beta)$. Thus, $\omega^* = (\omega_1, 0, 0)^T \in \boldsymbol{\varepsilon}_1$ is an (unstable) **Saddle point** when $\omega_1 \in (\alpha, \beta)$ and it is a (stable) **center** otherwise.

Combining these, we see that every point $\mathbf{p} = (I_1, I_2, I_3, h_1)^T$ in the parameter space $(\Re^+)^3 \times \overline{\Re}$ is a bifurcation point. **Bifurcation points** by definition are those points that a small perturbations in the parameter space of a dynamical system could lead to drastic changes in the behavior of the states. The unique pair of points $(\alpha,0,0)^T$ and $(\beta,0,0)^T$ with $\boldsymbol{\varepsilon}_1$ in the state space defines the boundary between the (stable) center and the (unstable) saddle point. Also recall that these two points correspond to the two points of intersection of $\boldsymbol{\varepsilon}_1$ with $\boldsymbol{\varepsilon}_2$ and $\boldsymbol{\varepsilon}_3$.

Another property about the orbits starting from a point near to equilibrium $\boldsymbol{\varepsilon}_1$ is that they are not heteroclinic any more, but homoclinic. Consider case A above when $bc > 0$. Considering the orbit starting from $\boldsymbol{\omega}(0) = \boldsymbol{\omega}^* + \delta$ with $\omega^* = (\omega_1, 0, 0)^T \in \boldsymbol{\varepsilon}_1$,

$\omega_1 \notin (\alpha, \beta)$ and δ is a small perturbation in the state space. It turns out that the distortion of the vector field due to the presence of the linear terms (with $h_1 \neq 0$) on the right-hand side of (5.24) does not permit the orbits starting close to $\boldsymbol{\omega}^* = (\omega_1,0,0)^T$ with $\omega_1 > \beta$ approach any point $(\omega_1,0,0)^T$ with $\omega_1 < \alpha$. The resulting closed orbit approaches $\boldsymbol{\omega}^*$ along the stable direction and moves away from it along the unstable direction and does not get close to any equilibrium points. That is, the orbits are homoclinic (Sparrow 1987) but not heteroclinic orbits.

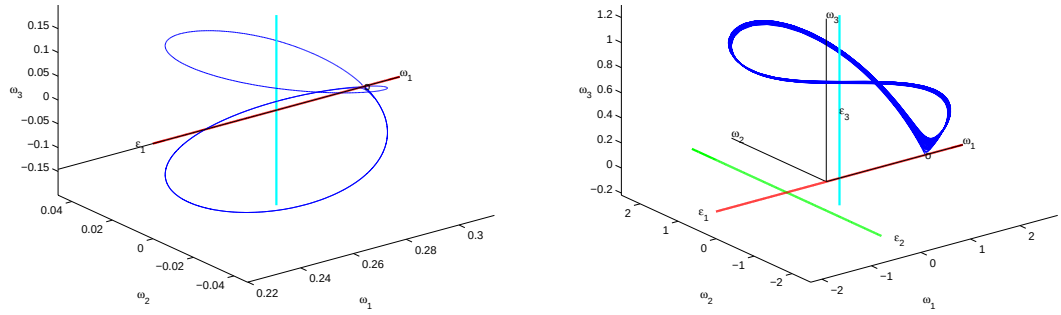

Figure 5.5 An illustration of the homoclinic orbits for Case 6 with equilibria affixed. The parameters are $\mathbf{I} = (4,3,7)^T$ and $\mathbf{h} = (0.8,0,0)^T$. Both orbits starts from $\boldsymbol{\omega}(0) = \boldsymbol{\omega}^* + \boldsymbol{\delta}$ with $\boldsymbol{\delta} = (0,0.001,0)^T$ and $\boldsymbol{\omega}^* \in \boldsymbol{\varepsilon}_1$ is a saddle point. (a) $\boldsymbol{\omega}^* = (0.7,0,0)^T$ (b) $\boldsymbol{\omega}^* = (2,0,0)^T$.

A **heteroclinic orbit** (sometimes called a heteroclinic connection) is a path in phase space which joins two different equilibrium points. A **homoclinic orbit**, however, means the trajectory of a flow of a dynamical system which joins a saddle equilibrium point to itself. More precisely, a homoclinic orbit lies in the intersection of the stable manifold and the unstable manifold of the equilibrium. Figure 5.5 contains two illustrations of the homoclinic orbits in the 3-D state space. In other words, as h_1 changes

from being zero to non-zero, the orbits in 3-D state space have also a transition from being heteroclinic (Case 5) to being homoclinic (Case 6).

(**Case 1**) Case 1 is a special case of Case 6 with additional condition $c = 0$, *i.e.* ($I_1 = I_2$) in (5.1). Its parameter vector takes the form $\mathbf{p} = (I_1, I_3, h_1)^{\mathrm{T}} \in (\Re^+)^2 \times \overline{\Re}$ and dynamic model is

$$\begin{aligned} f_1(\boldsymbol{\omega}) &= a\omega_2\omega_3 \\ f_2(\boldsymbol{\omega}) &= -a\omega_3\omega_1 - d_{12}\omega_3 \\ f_3(\boldsymbol{\omega}) &= d_{13}\omega_2 \,. \end{aligned} \tag{5.29}$$

This gyrostat is sometime called the **Lorenz gyrostat** because it can be transformed to the well know Lorenz system when adding dissipation and forcing. By adding dissipation and external forcing to the dynamics, we get from (5.1)

$$\begin{aligned} I_1\dot{\omega}_1 &= (I_1 - I_3)\omega_2\omega_3 - \alpha_1\omega_1 + N_1 \\ I_1\dot{\omega}_2 &= (I_3 - I_1)\omega_3\omega_1 - h_1\omega_3 - \alpha_2\omega_2 \\ I_3\dot{\omega}_3 &= + h_1\omega_2 - \alpha_3\omega_3 \end{aligned} \tag{5.30}$$

where α_i's are the non-negative dissipation coefficients and N_1 is the external forcing term. Gluhovsky and Tong (1999) have shown that using the following (affine) transformation of variables

$$X = \frac{(I_3 - I_1)}{\alpha_2}\omega_3$$

$$Y = \frac{(I_3 - I_1)h_1}{\alpha_2\alpha_3}\omega_2$$

$$Z = \frac{(I_3 - I_1)h_1}{\alpha_2\alpha_3}\left[\frac{N_1}{\alpha_1} - \omega_1\right]$$

and

$$\tau = \frac{\alpha_2 t}{I_1}$$

indeed (5.30) reduces to

$$\begin{aligned} \dot{X} &= \sigma(Y - X) \\ \dot{Y} &= -XZ + rX - Y \\ \dot{Z} &= XY - bZ \end{aligned} \tag{5.31}$$

where $\sigma = \dfrac{\alpha_3 I_1}{\alpha_2 I_3}$, $r = \dfrac{h_1}{\alpha_2 \alpha_3}\left[(I_3 - I_1)\dfrac{N_1}{\alpha_1} - h_1 \right]$ and $b = \dfrac{\alpha_1}{\alpha_2}$. Equation (5.31) is exactly the celebrated chaos system initially studied by Lorenz (1963).

It can be verified that there are just two sets of equilibria because of the effect of $c = 0$. The two equilibria are given by

$$\begin{aligned} \boldsymbol{\varepsilon}_1 &= \left\{ \boldsymbol{\omega} \in \mathrm{R}^3 \,\middle|\, \omega_1 \text{ is free, } \omega_2 = \omega_3 = 0 \right\} = \text{the } \omega_1 \text{ axis} \\ \text{and} \qquad \boldsymbol{\varepsilon}_3 &= \left\{ \boldsymbol{\omega} \in \mathrm{R}^3 \,\middle|\, \omega_1 = -\frac{d_{12}}{a}, \omega_2 = 0, \omega_3 \text{ is free} \right\} \\ &= \text{a straight line parallel to the } \omega_3 \text{ axis in the } (\omega_1, \omega_3)\text{-plane.} \end{aligned} \tag{5.32}$$

The relative disposition of the equilibria is given in Figure 5.6.

The Jacobian of $f(\boldsymbol{\omega})$ for (5.29) is given by

$$D_{\mathrm{f}}(\boldsymbol{\omega}) = \begin{bmatrix} 0 & a\omega_3 & a\omega_2 \\ -a\omega_3 & 0 & -(a\omega_1 + d_{12}) \\ 0 & d_{13} & 0 \end{bmatrix}. \tag{5.33}$$

From (5.33), we get immediately that $\lambda_1 = 0, \lambda_{2,3} = \pm i|a|\omega_3$ for $\boldsymbol{\omega}^* \in \boldsymbol{\varepsilon}_3$. So the properties of the equilibrium points $\boldsymbol{\omega}^*$ along $\boldsymbol{\varepsilon}_3$ depends only on $\mathbf{I}$ and not on h_1 and every point $\boldsymbol{\omega}^* \in \boldsymbol{\varepsilon}_3$ is uniformly a center for all $\mathbf{I} = (I_1, I_1, I_3) \in (\Re^+)^3$.

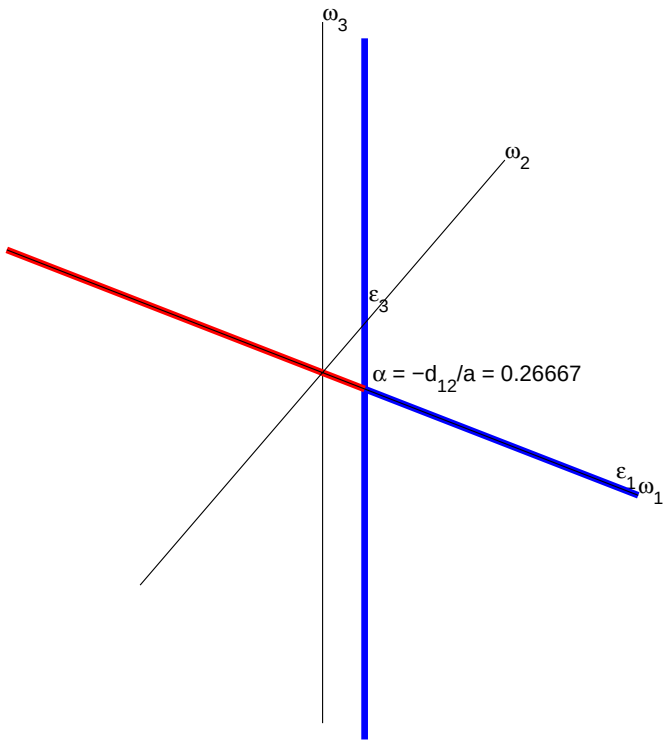

Figure 5.6 Relative disposition of the two equilibria for the Lorenz gyrostat. $\boldsymbol{\varepsilon}_1 = \{(\omega_1, 0, 0)^{\mathrm{T}}, \omega_1 \in \mathrm{R}\}$ and $\boldsymbol{\varepsilon}_3 = \{(\omega_1 = -\frac{d_{12}}{a}, 0, \omega_3)^{\mathrm{T}}, \omega_3 \in \mathrm{R}\}$. The parameters are $\mathbf{I} = (4, 4, 7)^{\mathrm{T}}$, $\mathbf{h} = (0.8, 0, 0)^{\mathrm{T}}$, a = -0.75, c = 0, d_{12} = 0.2, d_{13} = 0.1143 and α = 0.2667.

The eigenvalues for $\boldsymbol{\omega}^* \in \boldsymbol{\varepsilon}_1$, however, is quiet different, $\lambda_1 = 0, \lambda_{2,3} = \pm\sqrt{\mathrm{P}(\omega_1)}$ where $\mathrm{P}(\omega_1) = -(a\omega_1 + d_{12})d_{13}$. The properties of the equilibrium points $\omega^* \in \boldsymbol{\varepsilon}_1$ in (5.32) depends on the sign of the linear function

$$\begin{aligned} P(\omega_1) &= -(a\omega_1 + d_{12})d_{13} \\ &= \frac{h_1}{I_1 I_3}\left[(I_3 - I_1)\omega_1 - h_1\right]. \end{aligned} \tag{5.34}$$

It can be verified that $\mathrm{P}(\omega_1) = 0$ when

$$\omega_1^{(1)} = -\frac{d_{12}}{a} = \frac{h_1}{I_3 - I_1} = \alpha\,.$$

From Figure 5.6, we readily see point $(\alpha,0,0)^{\mathrm{T}}$ in the state space is exactly the point where the two equilibria $\boldsymbol{\varepsilon}_1$ and $\boldsymbol{\varepsilon}_3$ meet. So the point $(\alpha,0,0)^{\mathrm{T}}$ is a critical point in the state space. Following the same arguments as those for Case 5, we claim that every point of the form $\mathbf{p} = (I_1, I_1, I_3, h)^{\mathrm{T}}$ in the parameter space $(\Re^+)^3 \times \overline{\Re}$ uniquely defines an equilibrium point $\boldsymbol{\omega}^* = (\alpha, 0, 0)^{\mathrm{T}} \in \boldsymbol{\varepsilon}_1$ (which is also the point of intersection between $\boldsymbol{\varepsilon}_1$ and $\boldsymbol{\varepsilon}_2$) defines the boundary between the (unstable) saddle point and the center. Just as in Case 5, every orbit in the state space with respect to the saddle point in $\boldsymbol{\varepsilon}_1$ is a homoclinic orbit.

(**Case 2**) Case 2 is the special case of Case 4 or Case 7. However, since its equilibria are two straight lines in the state space, we exhibit its stability properties here together with Case 6 and Case 1. Taking into consider the parameters $h_3 = 0$ and $c = 0$ ($I_1 = I_2$). Then (5.10) reduces to

$$\begin{aligned} f_1(\boldsymbol{\omega}) &= \quad a\omega_2\omega_3 + d_{21}\omega_3 \\ f_2(\boldsymbol{\omega}) &= -a\omega_3\omega_1 - d_{12}\omega_3 \\ f_3(\boldsymbol{\omega}) &= \qquad\quad d_{13}\omega_2 - d_{23}\omega_1\,. \end{aligned} \tag{5.35}$$

The parameter vector for this case is $\mathbf{p} = (I_1, I_3, h_1, h_2)^{\mathrm{T}} \in (\Re^+)^2 \times \overline{\Re}^2$. It can be verified that there are only two sets of equilibria given by

$$\boldsymbol{\varepsilon}_1 = \left\{ \boldsymbol{\omega} \in \mathrm{R}^3 \,\middle|\, \omega_1 \text{ is free, } \omega_2 = \frac{d_{21}}{d_{12}}\omega_1 = \frac{h_2}{h_1}\omega_1, \omega_3 = 0 \right\}$$

$$= \text{a straight line through the origin in the } (\omega_1, \omega_2)\text{-plane with a slope } \frac{h_2}{h_1} \qquad (5.36)$$

and $$\boldsymbol{\varepsilon}_3 = \left\{ \boldsymbol{\omega} \in \mathrm{R}^3 \,\middle|\, \omega_1 = -\frac{d_{12}}{a}, \omega_2 = -\frac{d_{21}}{a}, \omega_3 \text{ is free} \right\}$$

$$= \text{a straight line parallel to the } \omega_3 \text{ axis.}$$

The relative disposition of the two sets of equilibria is given in Figure 5.7. It can be seen that this is the first gyrostat with one equilibrium that is not going along the axes. It is because it has 4 linear terms, *i.e.* two linear coefficients are not zero. It can be verified that the two equilibria meet at the point $\left(-\frac{d_{12}}{a}, -\frac{d_{21}}{a}, 0\right)^{\mathrm{T}} = \left(\frac{h_1}{I_3 - I_1}, \frac{h_2}{I_3 - I_1}, 0\right)^{\mathrm{T}}$.

From the Jacobian for (5.35)

$$D_f(\boldsymbol{\omega}) = \begin{bmatrix} 0 & a\omega_3 & a\omega_2 + d_{21} \\ -a\omega_3 & 0 & -(a\omega_1 + d_{12}) \\ d_{23} & d_{13} & 0 \end{bmatrix} \qquad (5.37)$$

We summarize the properties of the equilibria as following.

Again it turns out, as in case 6, that the properties of $\boldsymbol{\omega}^*$ in $\boldsymbol{\varepsilon}_3$ do not depend on h_1 and h_2, but depend on **I** only. It follows that every point $\boldsymbol{\omega}^* \in \boldsymbol{\varepsilon}_3$ is uniformly a center for all $\mathbf{I} \in (\Re^+)^3$. Equilibrium $\boldsymbol{\varepsilon}_1$, however, exhibits bifurcation feature again and all orbits starting near a saddle point of the equilibrium $\boldsymbol{\varepsilon}_1$, however, are homoclinic orbits. The critical point that separates the unstable saddle points and the sable center on equilibrium $\boldsymbol{\varepsilon}_1$ is given by (α, α, 0), which is also the point of intersection between the equilibria ε_1 and ε_3.

The critical point is calculated as following. From

$$D_f(\boldsymbol{\omega}^*)\Big|_{\boldsymbol{\omega}^*\in\varepsilon_1} = \begin{bmatrix} 0 & 0 & d_{21}\left(\dfrac{a\omega_1}{d_{12}}+1\right) \\ 0 & 0 & -(a\omega_1+d_{12}) \\ -d_{23} & d_{13} & 0 \end{bmatrix},$$

we compute the eigenvalues as $\lambda_1 = 0, \lambda_{2,3} = \pm\sqrt{\mathrm{P}(\omega_1)}$ where

$$\begin{aligned} \mathrm{P}(\omega_1) &= -(a\omega_1 + d_{12})\frac{\left(d_{13}^2 + d_{23}^2\right)}{d_{13}} \\ &= \left(\frac{I_3}{I_1}\right)\frac{1}{h_1}\left[(I_3 - I_1)\omega_1 - h_1\right]\left(d_{12}^2 + d_{23}^2\right). \end{aligned} \tag{5.38}$$

It can be verified that $\mathrm{P}(\omega_1) = 0$ exactly when

$$\omega_1^{(1)} = -\frac{d_{12}}{a} = \frac{h_1}{I_3 - I_1} = \alpha$$

which is the same as in (5.34). Since $\left(d_{13}^2 + d_{23}^2\right)$ is always positive, comparing (5.38) with (5.34), it follows that $\mathrm{P}(\omega_1)$ in (5.38) is positive or negative exactly when $\mathrm{P}(\omega_1)$ in (5.34) is positive or negative. Thus the critical point is given by (since $I_1 = I_2$ for this case)

$$\left(\frac{h_1}{I_3 - I_1}, \frac{h_2}{I_3 - I_1}, 0\right).$$

It is exactly the meet point between equilibrium ε_1 and ε_3 mentioned before.

Thus, every point $\mathbf{p} = (I_1, I_1, I_3, h_1, h_2)^{\mathrm{T}} \in (\Re^+)^3 \times \overline{\Re}^2$ also gives rise to a bifurcation point in the parameter space.

5.3.4 Gyrostats with equilibrium as a 2-D curve line

Both gyrostat 7 and gyrostat 3 contain four linear terms and one of its equilibrium is not a straight line, but a 2-D curve with discontinuous point.

(**Case 7**) Taking into consider the special parameter $h_3 = 0$, the equation for Case 7 is

$$\begin{aligned} f_1(\boldsymbol{\omega}) &= a\omega_2\omega_3 + d_{21}\omega_3 \\ f_2(\boldsymbol{\omega}) &= b\omega_3\omega_1 - d_{12}\omega_3 \\ f_3(\boldsymbol{\omega}) &= c\omega_1\omega_2 - d_{23}\omega_1 + d_{13}\omega_2 \cdot \end{aligned} \tag{5.39}$$

The vector p of parameters for this case is given by $\mathbf{p} = (I_1, I_2, I_3, h_1, h_2)^{\mathrm{T}} \in (\Re^+)^3 \times \overline{\Re}^2$.

There are two sets of equilibria and they are given by

$$\begin{aligned} \boldsymbol{\varepsilon}_1 &= \left\{ \boldsymbol{\omega} \in \mathrm{R}^3 \,\middle|\, \omega_1 \text{ is free, } \omega_2 = \frac{d_{23}\omega_1}{c\omega_1 + d_{13}}, \omega_3 = 0 \right\} \\ \text{and} \qquad \boldsymbol{\varepsilon}_3 &= \left\{ \boldsymbol{\omega} \in \mathrm{R}^3 \,\middle|\, \omega_1 = \frac{d_{12}}{b}, \omega_2 = -\frac{d_{21}}{a}, \omega_3 \text{ is free} \right\} \end{aligned} \tag{5.40}$$

The first equilibrium has an equivalent expression with ω_2 as free variable

$$\boldsymbol{\varepsilon}_1 = \boldsymbol{\varepsilon}_2 = \left\{ \boldsymbol{\omega} \in \mathrm{R}^3 \,\middle|\, \omega_1 = \frac{d_{13}\omega_2}{d_{23} - c\omega_2}, \ \omega_2 \text{ is free variable}, \omega_3 = 0 \right\}.$$

An example of the plot of this first equilibrium ε_1 is given in Figure 5.7. So the equilibrium ε_1 is a 2-D curve on the $\omega_3 = 0$ plane. The second equilibrium $\boldsymbol{\varepsilon}_3$ is a straight line parallel to the ω_3 axis, refer to Figure 5.7.

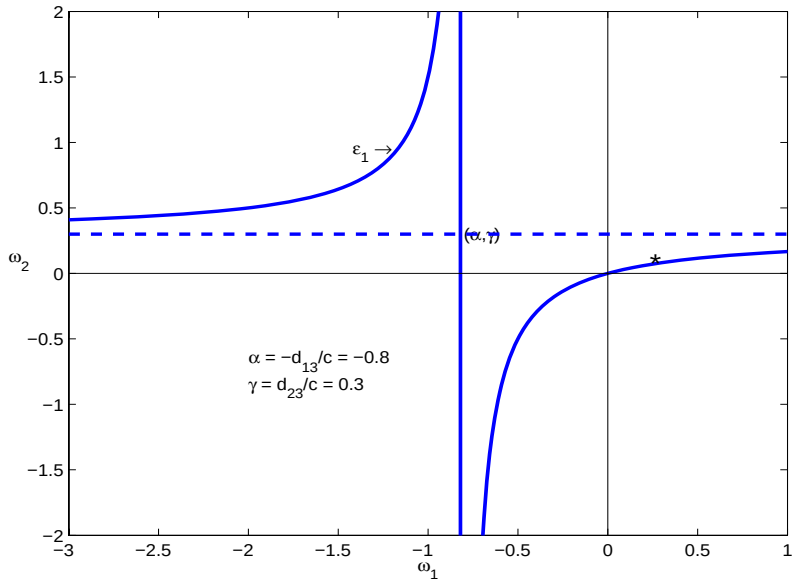

(a). A plot of the equilibrium curve ε_1: $\omega_2 = \dfrac{d_{23}\omega_1}{c\omega_1 + d_{13}} = \dfrac{h_2\omega_1}{h_1 + (I_1 - I_2)\omega_1}$ in the $\omega_3 = 0$ plane. The point * denotes the intersection of ε_3 with the plane $\omega_3 = 0$.

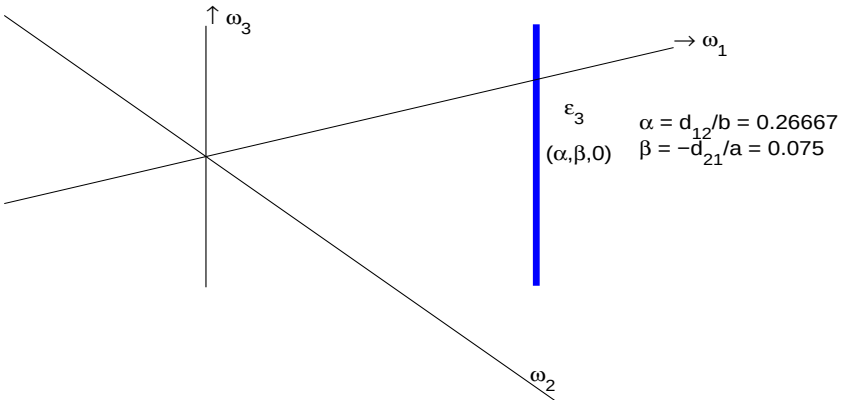

(b). A plot of the equilibrium ε_3 which is a straight line parallel to the ω_3-axis that intersects the $\omega_3 = 0$ plane at $\omega_1 = \dfrac{d_{12}}{b} = \dfrac{h_1}{(I_3 - I_1)}$ and $\omega_2 = -\dfrac{d_{21}}{a} = \dfrac{h_2}{(I_3 - I_2)}$.

Figure 5.7 A relative disposition of the two equilibria in case 7. The parameters used are $\mathbf{I} = (4,3,7)^T$ and $h = (0.8,0.3,0)^T$.

In examining the intersection between ε_1 and ε_3, since ω_1 is free in ε_1, set $\omega_1 = \frac{d_{12}}{b}$. Substituting this in the expression for ω_2 in ε_1, after simplification we get

$$\omega_2 = \left.\frac{d_{23}\omega_1}{c\omega_1 + d_{13}}\right|_{\omega_1 = \frac{d_{12}}{b}} = -\frac{d_{21}}{a}$$

Hence, ε_1 and ε_3 intersect at the point $\left(\frac{d_{12}}{b}, -\frac{d_{21}}{a}, 0\right)^{\mathrm{T}} = \left(\frac{h_1}{I_3 - I_1}, \frac{h_2}{I_3 - I_2}, 0\right)^{\mathrm{T}}$. It is noticeable that the curve for equilibrium ε_1 is not a continuous curve and its single points lie at either line $\omega_1 = -\frac{d_{13}}{c}$ or line $\omega_2 = \frac{d_{23}}{c}$ on the 2-D place (ω_1, ω_2) as it has been shown in Figure 5.7 (a).

The Jacobian of (5.39) is given by

$$D_f(\boldsymbol{\omega}) = \begin{bmatrix} 0 & a\omega_3 & a\omega_2 + d_{21} \\ b\omega_3 & 0 & b\omega_1 - d_{12} \\ c\omega_2 - d_{23} & c\omega_1 + d_{13} & 0 \end{bmatrix}. \tag{5.41}$$

For the points $\boldsymbol{\omega}^* \in \boldsymbol{\varepsilon}_3$, $D_f(\boldsymbol{\omega}^*)$ reduces to

$$D_f(\boldsymbol{\omega}^*) = \begin{bmatrix} 0 & a\omega_3 & 0 \\ b\omega_3 & 0 & 0 \\ \frac{I_3 - I_1}{I_2 - I_3} d_{23} & \frac{I_3 - I_2}{I_3 - I_1} d_{13} & 0 \end{bmatrix}$$

and the eigenvalues are $\lambda_1 = 0, \lambda_{2,3} = \pm\omega_3\sqrt{ab}$, which are independent of h_1 and h_2 and depends only on **I**. It follows that $\boldsymbol{\omega}^* \in \boldsymbol{\varepsilon}_3$ is a saddle point if $I_2 > I_3 > I_1$ or $I_2 < I_3 < I_1$. Otherwise $\boldsymbol{\omega}^* \in \boldsymbol{\varepsilon}_3$ is a center.

For the points $\boldsymbol{\omega}^* \in \boldsymbol{\varepsilon}_1$, it can be verified that the eigenvalues of the Jacobian matrix (5.41) is $\lambda_1 = 0$ and $\lambda_{2,3} = \pm\sqrt{\mathrm{P}(\omega_1)}$ where

$$\mathrm{P}(\omega_1) = \frac{(b\omega_1 - d_{12})(d_{13} + c\omega_1)^3 - d_{21}d_{13}d_{23}(d_{13} + c\omega_1) - d_{13}d_{23}^2 a\omega_1}{(d_{13} + c\omega_1)^2}. \qquad (5.42)$$

The properties of points in ε_1 depends on the sign of $P(\omega_1)$. Since the denominator of (5.42) is positive, the sign of $P(\omega_1)$ depends entirely on the fourth degree polynomial on the numerator of the right-hand side of (5.42). Using results from the book by Uspensky (1948) one can get general conditions on the roots of a fourth degree polynomial. Instead we resort to the simple graphical approach. An example of the plot of the numerator of $P(\omega_1)$ in (5.42) is given in Figure 5.8. Usually, a fourth order polynomial has two critical points at which it intersects with the abscissa. Clearly every point in ε_1 for which $P(\omega_1)$ is positive is an unstable saddle point, otherwise it is a center. Thus every point $\mathbf{p} = (I_1, I_2, I_3, h_1, h_2)^{\mathrm{T}} \in (\Re^+)^3 \times \bar{\Re}^2$ defines a unique bifurcation point in the state space and all orbits starting close to an unstable saddle point are homoclinic orbits. One typical homoclinic trajectory is demonstrated in Figure 5.9 for Case 7.

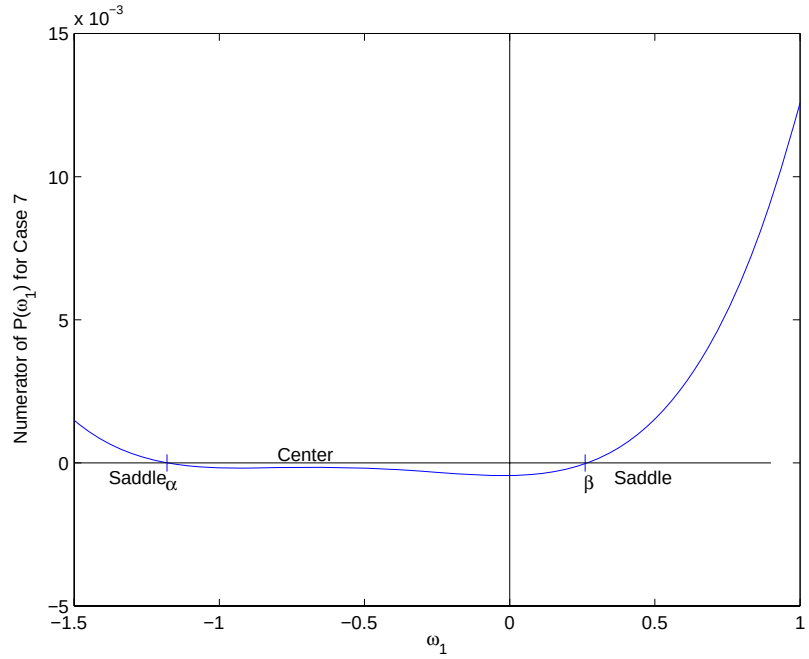

Figure 5.8 A plot of the numerator of P(ω_1) for Case 7.

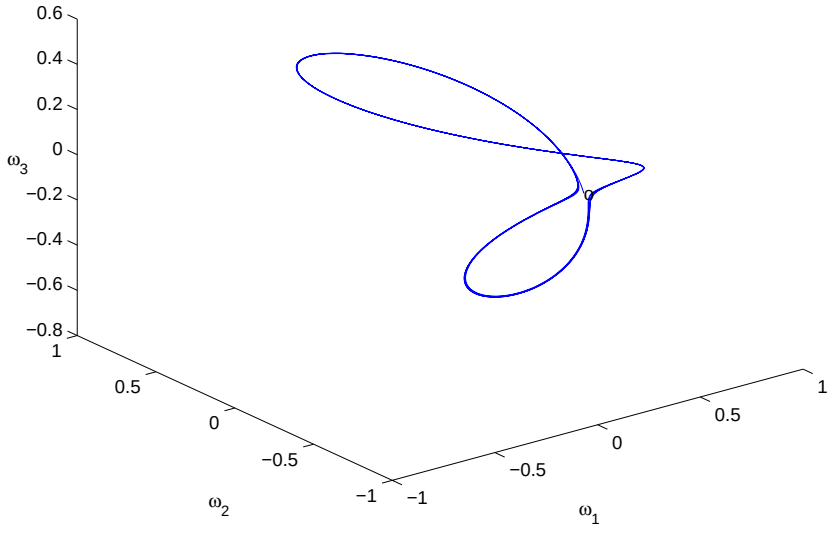

Figure 5.9 An illustration of the closed orbit that is homoclinic for Case 7. The orbit starting from $\boldsymbol{\omega}(0) = \boldsymbol{\omega}^* + \boldsymbol{\delta}$ with $\boldsymbol{\omega}^* = (0.7, 0.140, 0)^T$ and $\boldsymbol{\delta} = (0, 0.001, 0)^T$. The parameters used are $\mathbf{I} = (4,3,7)^T$, $h = (0.8,0.3,0)^T$.

(**Case 3**) The equations for Case 3 are

$$\begin{aligned} f_1(\boldsymbol{\omega}) &= \quad a\omega_2\omega_3 + d_{31}\omega_2 \\ f_2(\boldsymbol{\omega}) &= -a\omega_3\omega_1 + d_{32}\omega_1 - d_{12}\omega_3 \\ f_3(\boldsymbol{\omega}) &= \qquad\qquad d_{13}\omega_2 . \end{aligned} \tag{5.43}$$

Since $h_2 = 0$ and $c = 0$ (*i.e.* $I_1 = I_2$ in (5.1)), The vector of parameters for this case is $\mathbf{p} = (I_1, I_3, h_1, h_3)^{\mathrm{T}} \in (\Re^+)^2 \times \bar{\Re}^2$. Note that $d_{31} = d_{32} = d_3$. It can be verified that there is only one set of equilibrium given by

$$\boldsymbol{\varepsilon} = \boldsymbol{\varepsilon}_1 = \left\{ \boldsymbol{\omega} \in \mathrm{R}^3 \,\middle|\, \omega_1 \text{ is free, } \omega_2 = 0, \omega_3 = \frac{d_{32}\omega_1}{d_{12} + a\omega_1} \right\}. \tag{5.44}$$

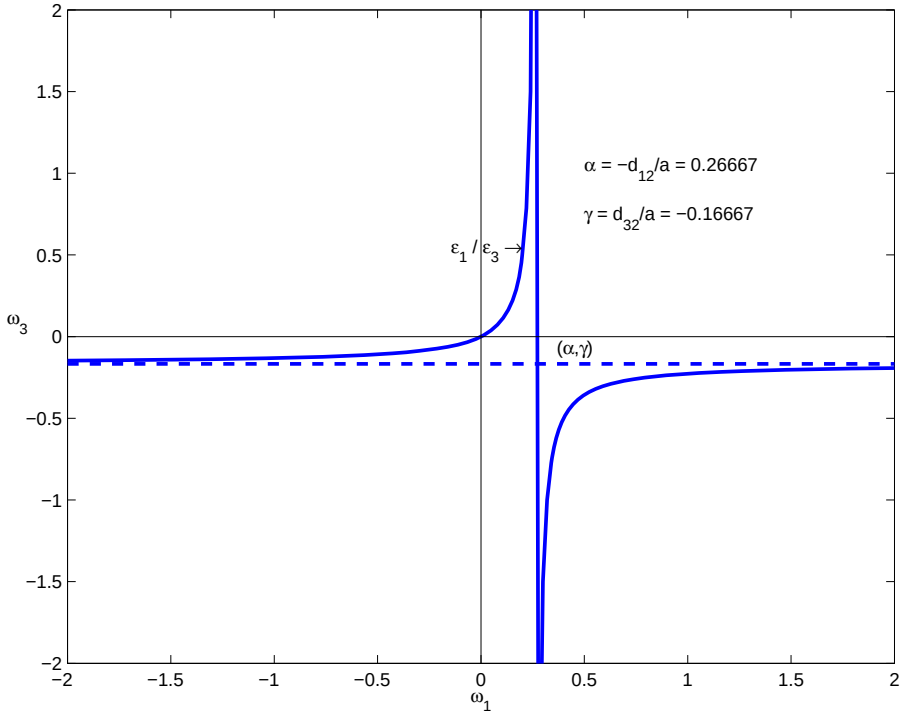

Figure 5.10 A plot of the equilibrium curve in the (ω_1, ω_3)-plane ($\omega_2 = 0$) for Case 3.

Or equivalently

$$\boldsymbol{\varepsilon} = \boldsymbol{\varepsilon}_3 = \left\{ \boldsymbol{\omega} \in \mathrm{R}^3 \,\middle|\, \omega_1 = \frac{d_{12}\omega_3}{d_{32} - a\omega_3}, \omega_2 = 0, \omega_3 \text{ is free} \right\}.$$

This equilibrium set is a curve that lies in the (ω_1,ω_3)-plane and passes through the origin. An example of this equilibrium curve is given in Figure 5.10.

The Jacobian of (5.43) is given by

$$D_{\mathrm{f}}(\boldsymbol{\omega}) = \begin{bmatrix} 0 & a\omega_3 - d_{31} & a\omega_2 \\ -a\omega_3 + d_{32} & 0 & -(a\omega_1 + d_{12}) \\ 0 & d_{13} & 0 \end{bmatrix}. \tag{5.45}$$

On the equilibrium curve $\boldsymbol{\omega}^* \in \boldsymbol{\varepsilon}$,

$$D_f(\boldsymbol{\omega}^*) = \begin{bmatrix} 0 & -\dfrac{d_{12}d_{31}}{d_{12} + a\omega_1} & 0 \\ \dfrac{d_{12}d_{32}}{d_{12} + a\omega_1} & 0 & -(a\omega_1 + d_{12}) \\ 0 & d_{13} & 0 \end{bmatrix}$$

Then the eigenvalues are $\lambda_1 = 0, \lambda_{2,3} = \pm\sqrt{\mathrm{P}(\omega_1)}$, where

$$\mathrm{P}(\omega_1) = \frac{-d_{13}(d_{12} + a\omega_1)^3 - d_{31}^2 d_{12}^2}{(d_{12} + a\omega_1)^2}. \tag{5.46}$$

So the properties of the equilibrium points in $\boldsymbol{\varepsilon}_1$ depends on the sign of $P(\omega_1)$ only. It can be verified that $P(\omega_1) = 0$ when

$$\omega_1 = \frac{1}{a}\left(d_{12} - \beta\right) = \alpha \quad \text{where} \qquad \beta^3 = \left|\frac{d_{12}^2 d_{31}^2}{d_{13}}\right| = \left|\frac{h_1 h_3 I_3}{I_1^4}\right| \tag{5.47}$$

A graph of the numerator of $P(\omega_1)$ is given in Figure 5.11. Thus. $\boldsymbol{\omega}^* = \left(\omega_1, 0, \frac{d_{32}\omega_1}{d_{12} + a\omega_1} \right)^{\mathrm{T}} \in \boldsymbol{\varepsilon}_1$ with $\omega_1 > \alpha$ in (5.47) is a saddle point and otherwise it is a center. Hence every point $\mathbf{p} = (I_1, I_1, I_3, h_1, h_3)^{\mathrm{T}} \in (\Re^+)^3 \times \overline{\Re}^2$ uniquely defines a bifurcation point in the state space. With respect to the unstable saddle points, any orbit starting near them are homoclinic orbits, which is similar as that shown in Figure 5.9.

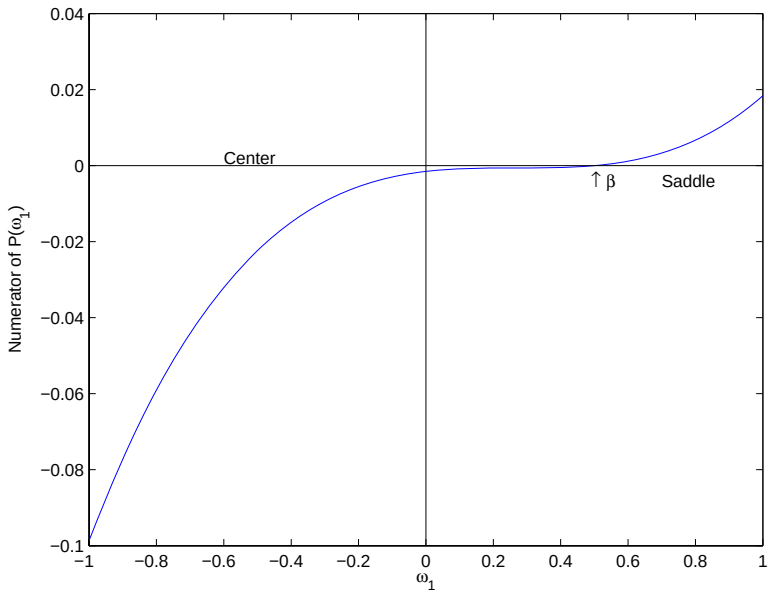

Figure 5.11 A plot of the numerator of $P(\omega_1)$ for Case 3.

Consider gyrostats for Case 2 and Case 3. Although both types have 2 nonlinear terms and 4 liner terms, their equilibria, however, take different appearances. The equilibria for Case 2 are two straight lines in the 3-D state space. The equilibrium for Case 3 is just a 2-D curve in the state space. Take a close look at equations (5.35) and (5.43), we found that the three equation set for Case 3 contains one equation in *full*. That

is it contains one nonlinear term and two nonlinear terms. Checking back with all the gyrostats that have been analyzed, it comes out immediately that all systems with equilibria as straight lines do not have any equation in full. So the property of the equilibria for a gyrostatic system does not only depend on the number of linear terms, but also depends on the disposition of those linear terms.

5.3.5 Stability of equilibrium for gyrostat in general form

Since both the equilibria of the general Volterra gyrostat and Case 9 are 3-D curve in the state space, we study their properties together. Both gyrostats in general form and Case 9 contain 6 linear terms. The Volterra gyrostat in general as shown in (5.10) is

$$\begin{aligned} f_1(\boldsymbol{\omega}) &= a\omega_2\omega_3 + d_{21}\omega_3 - d_{31}\omega_2 \\ f_2(\boldsymbol{\omega}) &= b\omega_3\omega_1 + d_{32}\omega_1 - d_{12}\omega_3 \\ f_3(\boldsymbol{\omega}) &= c\omega_1\omega_2 + d_{13}\omega_2 - d_{23}\omega_1 \end{aligned} \tag{5.48}$$

and the equations for Case 4 reduces to

$$\begin{aligned} f_1(\boldsymbol{\omega}) &= \quad a\omega_2\omega_3 + d_{21}\omega_3 - d_{31}\omega_2 \\ f_2(\boldsymbol{\omega}) &= -a\omega_3\omega_1 + d_{32}\omega_1 - d_{12}\omega_3 \\ f_3(\boldsymbol{\omega}) &= \qquad\qquad d_{13}\omega_2 - d_{23}\omega_1 \end{aligned} \tag{5.49}$$

since $c = 0$, The parameters vector for Case 4 is $\mathbf{p} = (I_1, I_3, h_1, h_2, h_3)^{\mathrm{T}} \in (\Re^+)^2 \times \bar{\Re}^3$.

Setting the right-hand side of (5.48) to zero and solving, we get a set of three relations defining the equilibria:

$$\omega_3 = \frac{d_{31}\omega_2}{a\omega_2 + d_{21}}$$
$$\omega_1 = \frac{d_{12}\omega_3}{b\omega_3 + d_{32}} \qquad (5.50)$$
$$\omega_2 = \frac{d_{23}\omega_1}{c\omega_1 + d_{13}}.$$

We can break this circular dependence by declaring one of the three variables as an independent variable. Accordingly we obtain three sets of relations defining equilibria given in Table 5.3.

Table 5.3 Specification of Equilibria – General gyrostat

$\boldsymbol{\varepsilon}_1$: ω_1 is free	$\boldsymbol{\varepsilon}_2$: ω_2 is free	$\boldsymbol{\varepsilon}_3$: ω_3 is free
$\omega_2 = \frac{d_{23}\omega_1}{c\omega_1 + d_{13}}$	$\omega_3 = \frac{d_{31}\omega_2}{a\omega_2 + d_{21}}$	$\omega_1 = \frac{d_{12}\omega_3}{b\omega_3 + d_{32}}$
$\omega_3 = \frac{d_{32}\omega_1}{-b\omega_1 + d_{12}}$	$\omega_1 = \frac{d_{13}\omega_2}{-c\omega_2 + d_{23}}$	$\omega_2 = \frac{d_{21}\omega_3}{-a\omega_3 + d_{31}}$

It turns out that these seemingly different equilibria are actually equivalent in mathematics and they refer to the same set of points. Consider the first column of Table 5.3. Rewriting $\omega_2 = \frac{d_{23}\omega_1}{c\omega_1 + d_{13}}$ as $\omega_1 = \frac{d_{13}\omega_2}{-c\omega_2 + d_{23}}$ and substituting the latter on the right-hand side of ω_3 we obtain, after simplification $\omega_3 = \frac{d_{31}\omega_2}{a\omega_2 + d_{21}}$. That is, the second column of Table 5.3 is equivalent to the expressing in the first column. Similarly, it can be verified the third column is equivalent to the second column also and the first column is equivalent to the third column. In view of this equivalence, in the following without loss of generality, we describe the properties of the equilibrium using $\boldsymbol{\varepsilon}_1$ (Column one in

Table 5.3) where ω_1 is a free variable. An example of this equilibrium curve is given with Figure 5.12.

Since gyrostats for Case 4 have a reduced parameter space, the expressions for the equilibria are just a little simpler,

$$\begin{aligned}
\boldsymbol{\varepsilon}_1 &= \left\{ \boldsymbol{\omega} \in \mathrm{R}^3 \,\middle|\, \omega_1 \text{ is free, } \omega_2 = \frac{d_{23}\omega_1}{d_{13}}, \omega_3 = \frac{d_{32}\omega_1}{d_{12} + a\omega_1} \right\} \text{ or} \\
\boldsymbol{\varepsilon}_2 &= \left\{ \boldsymbol{\omega} \in \mathrm{R}^3 \,\middle|\, \omega_1 = \frac{h_1}{h_2}\omega_2 = \frac{d_{12}}{d_{21}}\omega_2, \omega_2 \text{ is free}, \omega_3 = \frac{d_{31}\omega_2}{d_{21} + a\omega_2} \right\} \text{ or} \\
\boldsymbol{\varepsilon}_3 &= \left\{ \boldsymbol{\omega} \in \mathrm{R}^3 \,\middle|\, \omega_1 = \frac{d_{12}\omega_3}{d_{32} - a\omega_3}, \omega_2 = \frac{d_{21}\omega_3}{d_{31} - a\omega_3}, \omega_3 \text{ is free} \right\}.
\end{aligned} \tag{5.51}$$

Evaluating the Jacobian of (5.48) along the equilibrium ε_1, we get

$$D_f(\omega_1) = \begin{bmatrix} 0 & A & B \\ C & 0 & D \\ E & F & 0 \end{bmatrix} \tag{5.52}$$

where

$$\begin{aligned}
A &= A(\omega_1) = a\omega_3 - d_{31} \\
B &= B(\omega_1) = a\omega_2 + d_{21} \\
C &= C(\omega_1) = b\omega_3 + d_{32} \\
D &= D(\omega_1) = b\omega_1 - d_{12} \\
E &= E(\omega_1) = c\omega_2 - d_{23} \\
F &= F(\omega_1) = c\omega_1 + d_{13}
\end{aligned} \tag{5.53}$$

and from the expression in Column one of Table 5.3, we have

$$\omega_2 = \frac{d_{23}\omega_1}{c\omega_1 + d_{13}} \text{ and } \omega_3 = \frac{d_{32}\omega_1}{-b\omega_1 + d_{12}}.$$

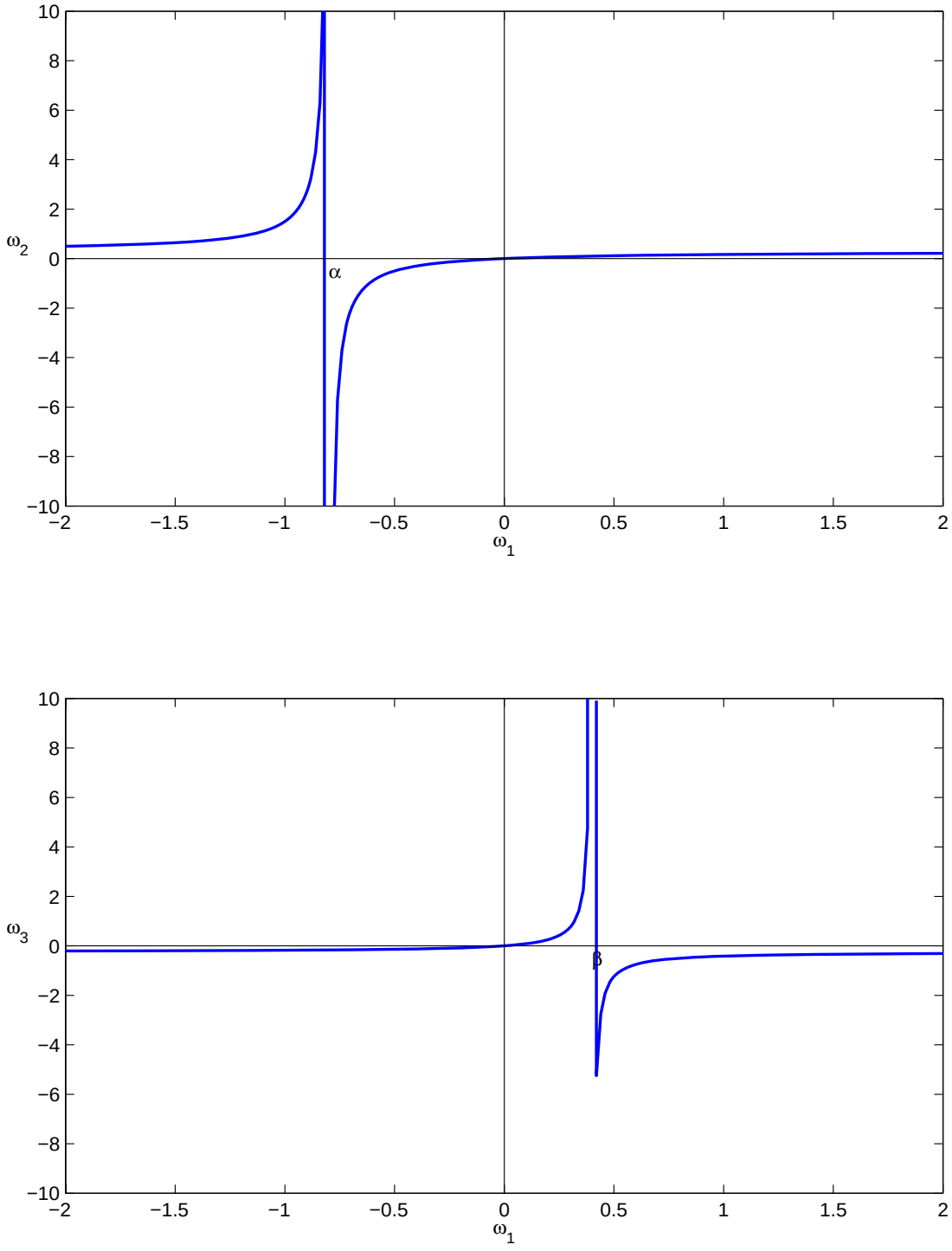

Figure 5.12 A plot of the projection of the equilibrium curve $\boldsymbol{\varepsilon}_1$ on plane (ω_1, ω_2) and plane (ω_1, ω_3) respectively for the general Volterra gyrostat.

The characteristic polynomial of $D_{\mathrm{f}}(\omega_1)$ in (5.52) - (5.53) takes the form

$$-\mathrm{g}(\lambda,\omega_1)=\lambda^3+p\lambda+q=0 \tag{5.54}$$

where

$$\begin{aligned} p&=\mathrm{p}(\omega_1)=-(FD+AC+BE)\\ q&=\mathrm{q}(\omega_1)=-(ADE+BCF). \end{aligned} \tag{5.55}$$

Based on the derivation in Appendix C, it follows that the properties of the eigenvalues of $D_f(\omega_1)$ in (5.52) critically depend on the value of the discriminant

$$\begin{aligned} \Delta=\Delta(\omega_1)&=4p^3+27q^2\\ &=-4(FD+AC+BE)^3+27(ADE+BCF)^2. \end{aligned} \tag{5.56}$$

Referring to the Appendix C, we conclude that the three eigenvalues of $D_f(\omega_1)$ in (5.52) are real when $\Delta = 0$ or $\Delta < 0$ and one of the eigenvalues is real and the other two are complex conjugates when $\Delta > 0$.

An example of the plot of $\Delta(\omega_1)$ is given in Figure 5.13, where we have denoted the regions where the equilibrium $\omega^* \in \boldsymbol{\varepsilon}_1$ is a saddle point and where it is a center. Thus, the full parameter space $\mathbf{p}=(I_1,I_2,I_3,h_1,h_2,h_3)^{\mathrm{T}} \in (\Re^+)^3 \times \overline{\Re}^3$ defines a bifurcation point also. Note that the gyrostats for Case 4 have a similar discriminant function $\Delta(\omega_1)$ and it is shown in Figure 5.14. Again, since the reduced parameter space, it has one critical point only in the plot.

An example of the homoclinic orbit for the general gyrostat and its projections on the 2-D planes as well as the time series for each state variable are shown in Figure 5.15.

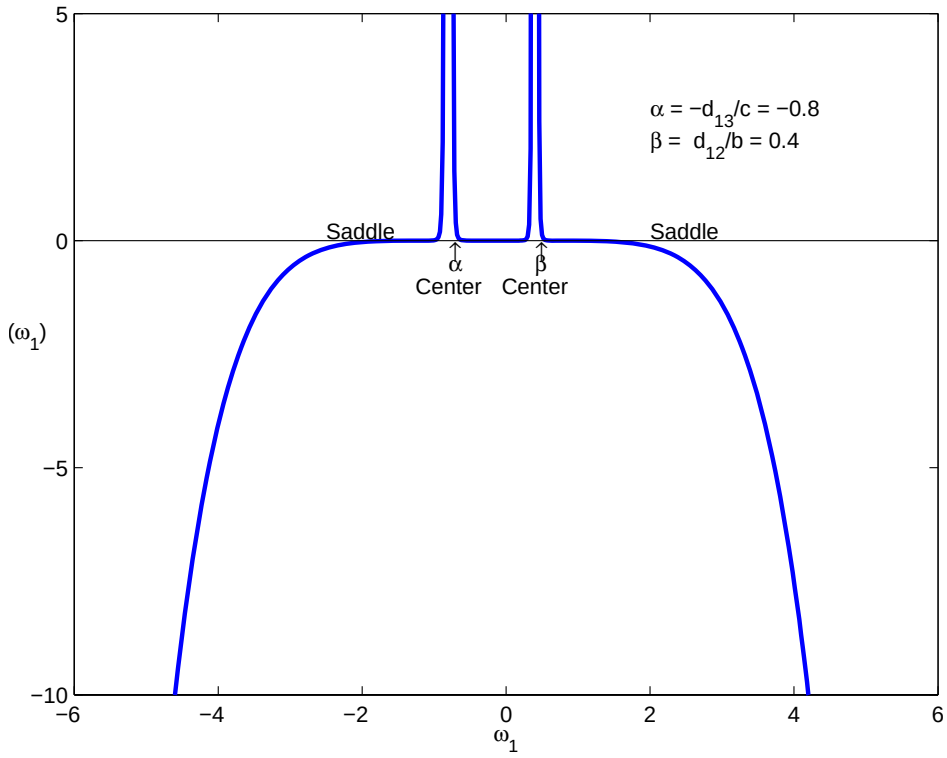

Figure 5.13 A plot of the discriminant $\Delta(\omega_1)$ for the Volterra gyrostat

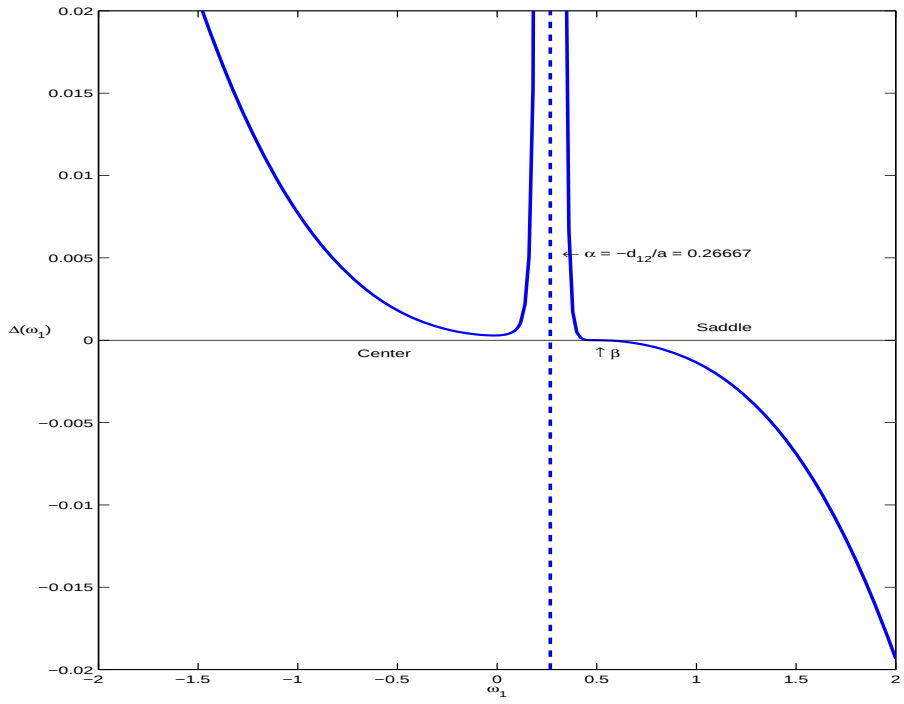

Figure 5.14 A plot of the discriminant $\Delta(\omega_1)$ for Case 4.

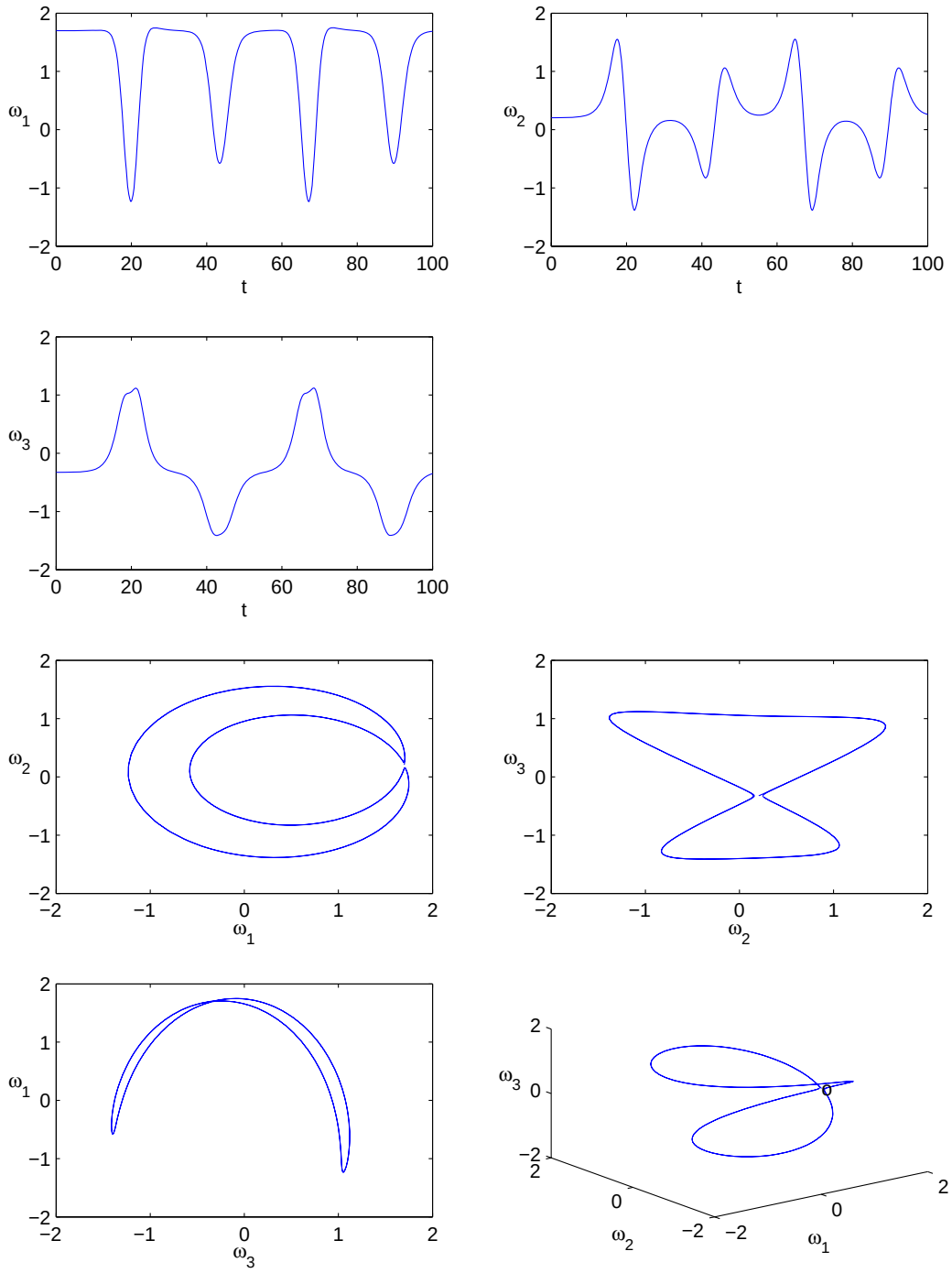

Figure 5.15 An illustration of the homoclinic orbit starting from $\boldsymbol{\omega}(0) = \boldsymbol{\omega}^* + \boldsymbol{\varepsilon}$ with $\boldsymbol{\omega}^* = (1.7, 0.204, -0.32692)^T$ and $\boldsymbol{\varepsilon} = (0, 0.001, 0)^T$. Parameters used are $\mathbf{I} = (5,4,7)^T$ and $h = (0.8, 0.3, 0.5)^T$.

5.4 CONCLUSION

Based on the classification in Gluhovsky and Tong (1999), this Chapter has provided a comprehensive analysis of bifurcation and the stability of equilibria for all nine special gyrostats and its general form in the Volterra gyrostat. Since the dynamics is conservative, the equilibria for each of the ten cases are either an (unstable) saddle or a (stable) center. The conservative property further restricts the solution to lie at the intersection of the energy and momentum ellipsoids.

Table 5.4 The shapes of the equilibria in the state space for each case

Case No.	Parameter Space	Number of Equil.	Shape	Stability
0	$(\Re^+)^3 \times \overline{\Re}^3$	1	3-D curve	Saddle & Center
4	$(\Re^+)^2 \times \overline{\Re}^3$	1	3-D curve	Saddle & Center
7	$(\Re^+)^3 \times \overline{\Re}^2$	2	2-D curve on plane (ω_1, ω_2) Straight line parallel ω_3-axis	Saddle & Center Uniform Saddle/Center
3	$(\Re^+)^2 \times \overline{\Re}^2$	1	2-D curve on plane (ω_1, ω_3)	Saddle & Center
2	$(\Re^+)^2 \times \overline{\Re}^2$	2	Straight line parallel ω_3-axis Straight line on plane (ω_1, ω_2)	Uniform Center Saddle & Center
6	$(\Re^+)^3 \times \overline{\Re}$	3	ω_1-axis Straight line parallel ω_2-axis Straight line parallel ω_3-axis	Saddle & Center Uniform Saddle/Center Uniform Saddle/Center
1	$(\Re^+)^2 \times \overline{\Re}$	2	ω_1-axis Straight line parallel ω_3-axis	Saddle & Center Uniform Center
9	$(\Re^+)^2 \times \overline{\Re}$	1	ω_3-axis	Uniform Center
5	$(\Re^+)^3$	3	ω_1-axis ω_2-axis ω_3-axis	Uniform Saddle/Center
8	$(\Re^+)^2$	1	ω_3-axis	Uniform Center

In the 3-D state space, the appearances of the equilibria for each gyrostat take three shapes, straight line, 2-D curve or 3-D curve. A summary of the parameter space and its corresponding equilibria shapes are summarized in Table 5.4. Note that one linear

parameter corresponding to two linear terms in set of equations for gyrostats. From the table, we found that the number of linear terms plays an important role in determining the shape of the equilibrium curves. If there is no linear term, all equilibria of gyrostats are the axes in the state space. When there is two linear terms (one more parameter of $\overline{\Re}$ in the parameter space), one or more equilibria lines are pushed away from the state origin except for Case 9. If there are 4 linear terms (two parameters of $\overline{\Re}^2$ in the parameter space except for Case 2, two or all three of the equilibria are transformed into a 2-D curve. Similarly, all three equilibria are transformed into a 3-D curve in the state space with 6 linear terms in the set of equations for gyrostats. Considering the special Case 2 and Case 9, it seems that not only the number of linear coefficients, but the disposition of those linear terms also plays role in determining the appearances of the equilibria.

About the stability of the equilibrium sets, it is clear from Table 5.4 that if there is no linear term, all of the equilibria are uniformly a saddle or uniformly a center. The introducing of linear terms has changed at least one of the equilibrium into partially a saddle and partially a center except for the degenerated Case 9. If the gyrostat has more than two equilibrium sets, it is usually the intersections of those equilibria that separate the regions between saddle points and center points (for example, Case 1, 2 and 6). In general, the system orbits with respect to the saddle in an equilibrium are homoclinic in nature if the equilibrium set is only partial saddle. Otherwise, if the equilibrium set is uniformly a saddle, then the orbits are heteroclinic (Case 5, 6 and 7).

Chapter 6
The Hamiltonian Structure of Energy Conserving LOMs

6.1 INTRODUCTION

Thus far we have analyzed the structure of the energy conserving LOM and their relation to the system of coupled gyrostats. In classical physics another class of energy conserving systems called Hamiltonian systems has been the basis for analysis of a wide class of systems. In this chapter, we examine the relation between the energy conserving LOM and the Hamiltonian systems (HS).

In Section 6.2, we review the basic principles of the canonical HS and their properties. Structure of the non-canonical HS of which the gyrostat is a special case is described in Section 6.3. Section 6.4 examines the relation between energy conserving LOM and HS. The Hamiltonian structures of LOMs for the Burger's equation are stated in Section 6.5. Finally, this chapter is summarized in Section 6.6.

6.2 THE CANONICAL HAMILTONIAN SYSTEM AND THE POISSON BRACKET

Consider the phase space $\mathbf{z} \in \Re^{2n}$ where $\mathbf{z} = (\mathbf{q}^T, \mathbf{p}^T)$ with $\mathbf{p} \in \Re^n$, $\mathbf{q} \in \Re^n$. Let $\mathrm{H} : \Re^n \to \Re$ be a Hamiltonian (function). If the dynamics can be written as

$$\dot{\mathbf{z}} = \mathbf{J} \nabla_{\mathbf{z}} \mathrm{H} \tag{6.1}$$

where **J** is the **structure matrix** and it satisfies the following condition

$$\mathbf{J} = \begin{bmatrix} \mathbf{0} & \mathbf{I} \\ -\mathbf{I} & \mathbf{0} \end{bmatrix} \tag{6.2}$$

where **I** is a $n \times n$ identity matrix. Then the system (6.1) is called the **canonical system**. The dynamics can also be expressed as

$$\left.\begin{aligned} q_i &= \frac{\partial H}{\partial p_i} \\ p_i &= -\frac{\partial H}{\partial q_i} \end{aligned}\right\} \quad i = 1, 2, \cdots, n \tag{6.3}$$

$\mathbf{p}_i$ is called generalized momentum, and $\mathbf{q}_i$ is called generalized position. It is obviously that the structure matrix **J** also satisfies the orthogonal condition for canonical systems

$$\mathbf{J}^T = \mathbf{J}^{-1}$$

First integrals / **constants of notion** / **conserved quantity**: Let $\mathrm{G} : \Re^{2n} \to \Re$. G when evaluated along $\mathbf{z}(t)$, the trajectory of (6.1) defines the variation of G along the solution. We now examine the condition when $\mathrm{G}(\cdot)$ is a constant along the solution. To this end, compute

$$\begin{aligned} \dot{\mathrm{G}} &= \frac{d}{dt}\mathrm{G}(\mathbf{z}(t)) \\ &= \sum_{i=1}^{2n} \frac{\partial G}{\partial z_i}\frac{\partial z_i}{\partial t} \\ &= \left[\nabla_{\mathbf{z}} \mathrm{G}(\mathbf{z}(t))\right]^T \dot{\mathbf{z}}(t) \end{aligned} \tag{6.4}$$

Substituting (6.1) into (6.4), we get

$$
\begin{aligned}
\dot{\mathrm{G}} &= \left[\nabla_{\mathbf{z}} G\right]^T \dot{\mathbf{z}}(t) \\
&= \left[\nabla_{\mathbf{z}} G\right]^T \mathbf{J} \left[\nabla_{\mathbf{z}} H\right] \\
&= \left(\left[\nabla_{\mathbf{q}} G\right]^T, \left[\nabla_{\mathbf{p}} G\right]^T\right) \begin{pmatrix} \mathbf{0} & \mathbf{I} \\ -\mathbf{I} & \mathbf{0} \end{pmatrix} \begin{pmatrix} \nabla_{\mathbf{q}} H \\ \nabla_{\mathbf{p}} H \end{pmatrix} \\
&= \left(\left[\nabla_{\mathbf{q}} G\right]^T, \left[\nabla_{\mathbf{p}} G\right]^T\right) \begin{pmatrix} \nabla_{\mathbf{p}} H \\ -\nabla_{\mathbf{q}} H \end{pmatrix} \\
&= \left[\nabla_{\mathbf{q}} G\right]^T \nabla_{\mathbf{p}} H - \left[\nabla_{\mathbf{p}} G\right]^T \nabla_{\mathbf{q}} H \\
&= \sum_{i=1}^{n} \frac{\partial G}{\partial q_i} \frac{\partial H}{\partial p_i} - \sum_{i=1}^{n} \frac{\partial G}{\partial p_i} \frac{\partial H}{\partial q_i} \\
&= \sum_{i=1}^{n} \left(\frac{\partial G}{\partial q_i} \frac{\partial H}{\partial p_i} - \frac{\partial G}{\partial p_i} \frac{\partial H}{\partial q_i} \right) \\
&\triangleq \left[G, H\right]
\end{aligned}
\qquad . \tag{6.5}
$$

The definition in (6.5) is called the **Poisson bracket**. That is the rate of change of a scalar function on $\Re^{2n}$ along the trajectory of (6.1) is given by the Poisson bracket as

$$\dot{G} = \left[G, H\right]. \tag{6.6}$$

Thus, a necessary and a sufficient condition for the Hamiltonian system (6.1) to conserve G(**z**) is that the Poisson bracket for G(**z**) and the Hamiltonian H(**z**) must be zero, *i.e.* $\left[G, H\right] = 0$.

For convenience, we quote without proof several properties of the Poisson brackets. Let F, G, H be function from $\Re^{2n}$ to $\Re$. Then

$\left[F, G\right] = -\left[G, F\right]$ – skew symmetry
$\left[F, \alpha G + \beta H\right] = \alpha\left[F, G\right] + \beta\left[F, H\right]$ – bilinear
$\left[\left[F, G\right], H\right] + \left[\left[H, F\right], G\right] + \left[\left[G, H\right], F\right] = 0$ – Jacobi identity

6.3 NON-CANONICAL HAMILTONIAN SYSTEM AND THE CASIMIR INVARIANT

Let $x_i, i = 1, 2, \cdots, n$ be a system of dynamical variables and let $\mathrm{H} : \Re^n \to \Re$ be a Hamiltonian (function). A finite-dimensional Hamiltonian dynamics system is given by

$$\dot{\mathbf{x}} = \mathbf{J}(\mathbf{x}) \nabla_{\mathbf{x}} \mathrm{H} \tag{6.7}$$

where **J**(**x**) is the structure matrix (function). The structure matrix **J** must be a skew symmetric matrix and satisfies the following conditions

$$\mathbf{J} = -\mathbf{J}^T \quad \mathbf{J} \text{ is skew-symmetric and}$$

$$\sum_{k=1}^{n} \sum_{j=1}^{n} \sum_{i=1}^{n} \sum_{m=1}^{n} \sigma_{ijk} J_{im} \frac{\partial J_{jk}}{\partial x_m} = 0 \tag{6.8}$$

with $\sigma_{ijk} = \begin{cases} 0 & \text{if } i = j, \text{ or } j = k, \text{ or } i = k \\ 1 & \text{if } (i, j, k) \text{ is an even permutation} \\ -1 & \text{if } (i, j, k) \text{ is an odd permutation} \end{cases}$ for any $(i, j, k) \in \{1, 2, \cdots, n\}$.

Condition (6.8) is called the **Jacobi identity**. The dynamical system (6.7) is called the **non-canonical Hamiltonian system**.

Remark 6.1 The order of the Hamiltonian system (6.7), *n*, can be odd or even, and the canonical system is just a special case of the non-canonical system with a special constant structure matrix **J**.

Remark 6.2 The Jacobi identity is automatically satisfied for all constant structure matrix **J** that is skew symmetric.

Remark 6.3 The Hamiltonian is conserved along the trajectory. Consider the rate of change of H(t) along the dynamics (6.7),

$$\begin{aligned}\frac{dH}{dt} &= \sum_{i=1}^{n} \frac{\partial H}{\partial x_i} \frac{\partial x_i}{\partial t} \\ &= \sum_{i=1}^{n} \frac{\partial H}{\partial x_i} \left(\sum_{j=1}^{n} J_{ij} \frac{\partial H}{\partial x_j} \right). \\ &= \sum_{i=1}^{n} \sum_{j=1}^{n} \frac{\partial H}{\partial x_i} J_{ij} \frac{\partial H}{\partial x_j} \\ &= 0 \quad \text{since } J_{ij} = -J_{ji}\end{aligned} \tag{6.9}$$

Example 6.1 Consider $\mathbf{x} = (m_1, m_2, m_3)^T$, $H(\mathbf{x}) = \frac{1}{2}\left(\frac{m_1^2}{I_1}, \frac{m_2^2}{I_2}, \frac{m_3^2}{I_3} \right)$ and write the structure matrix **J** as

$$\mathbf{J} = \begin{pmatrix} 0 & -m_3 & m_2 \\ m_3 & 0 & -m_1 \\ -m_2 & m_1 & 0 \end{pmatrix},$$

Then

$$\nabla_{\mathbf{x}} H = \begin{pmatrix} \frac{\partial H}{\partial m_1} \\ \frac{\partial H}{\partial m_2} \\ \frac{\partial H}{\partial m_3} \end{pmatrix} = \begin{pmatrix} \frac{m_1}{I_1} \\ \frac{m_2}{I_2} \\ \frac{m_3}{I_3} \end{pmatrix}$$

and the Hamiltonian system is

$$\begin{pmatrix} \dot{m}_1 \\ \dot{m}_2 \\ \dot{m}_2 \end{pmatrix} = \mathbf{J} \nabla_{\mathbf{x}} H$$

$$= \begin{pmatrix} 0 & -m_3 & m_2 \\ m_3 & 0 & -m_1 \\ -m_2 & m_1 & 0 \end{pmatrix} \begin{pmatrix} \frac{m_1}{I_1} \\ \frac{m_2}{I_2} \\ \frac{m_3}{I_3} \end{pmatrix}$$

$$= \begin{pmatrix} m_2 m_3 (-\frac{1}{I_2} + \frac{1}{I_3}) \\ m_1 m_3 (\frac{1}{I_1} - \frac{1}{I_3}) \\ m_1 m_2 (-\frac{1}{I_1} + \frac{1}{I_2}) \end{pmatrix} . \tag{6.10}$$

Define $m_i = I_i \omega_i$ for i = 1, 2, 3 and substitute them into (6.10), we get

$$\left.\begin{aligned} I_1 \dot{\omega}_1 &= \omega_2 \omega_3 (I_2 - I_3) \\ I_2 \dot{\omega}_2 &= \omega_1 \omega_3 (I_3 - I_1) \\ I_3 \dot{\omega}_3 &= \omega_1 \omega_2 (I_1 - I_2) \end{aligned}\right\} \tag{6.11}$$

Compare with equation (B.1), we find immediately that (6.11) is a special case of the general Volterra gyrostats. Actually, it is the well-known Euler gyroscope, *i.e.* equation (6.10) is the Hamiltonian version of the Euler gyrostat and the Hamiltonian H is just the kinetic energy in (B.2).

Since the structure matrix **J** for a Hamiltonian system is skew symmetric, if the order n is odd, then its determinant must be zero. Hence, the matrix **J** is singular. It can be seen that the homogeneous system

$$\mathbf{J} \nabla_{\mathbf{x}} C = \sum_{i=1}^{n} J_{ij} \frac{\partial C}{\partial x_j} = 0 \tag{6.12}$$

for $i = 1, 2, \ldots, n$ has a non-trivial solution. It implies that there exists a function $C : \Re^n \to \Re$ such that $\nabla_{\mathbf{x}} C$ is a solution of the homogenous system (6.12).

We now verify that the function C that arises out of (6.12) is invariant.

$$\begin{aligned}
\frac{dC}{dt} &= \sum_{i=1}^{n} \frac{\partial C}{\partial x_i} \frac{\partial x_i}{\partial t} \\
&= \sum_{i=1}^{n} \frac{\partial C}{\partial x_i} \left(\sum_{j=1}^{n} J_{ij} \frac{\partial C}{\partial x_j} \right) \\
&= \sum_{i=1}^{n} \sum_{j=1}^{n} \left(\frac{\partial H}{\partial x_i} J_{ij} \frac{\partial H}{\partial x_j} \right) \\
&= 0 \quad \text{since } J_{ij} = -J_{ji}
\end{aligned}$$

The invariant functions $C(\mathbf{x})$ so obtained from (6.12) are called **Casimir invariants**. Obviously, the odd order Hamiltonian system may have zero or more Casimir invariants.

Remark 6.4 For canonical systems or even order non-canonical systems, since the structure matrix **J** is non-singular, the only solution of (6.12) is $\nabla_{\mathbf{x}} C = 0$, *i.e.* C must be constants.

Example 6.2 For the matrix **J** in example 6.1, we can verify that $C = \mathbf{m}^2 = \sum_{i=1}^{3} m_i^2$ is a Casimir invariant. Substitute $m_i = I_i \omega_i$ into C and it is found that this Casimir invariant is exactly the square of the angular momentum defined in (B.3). Hence the sum of the square of the angular momentum is one Casimir invariant for the Euler gyroscope.

6.4 STUDY OF COUPLED GYROSTATS AS HAMILTONIAN LOMS

All gyrostatic LOMs conserve the phase-space volume and the definition of kinetic energy

$$H = \sum_{i=1}^{n} \frac{x_i^2}{2} \tag{6.13}$$

is a good candidate for the Hamiltonian function. With (6.13), any system of coupled gyrostats can be written readily in form (6.7) with easily determined skew symmetric matrix **J**. Thus, the search for Hamiltonian structure with gyrostatic LOMs is left to check the Jacobi conditions with the structure matrix **J**.

Since the equivalence of SELOM(n) and CVG(n) has been proved in Chapter 3, we start by considering systems in SELOM(n) first.

$$\dot{\mathbf{x}} = \mathbf{A}(\mathbf{x}, \mathbf{x}) + B\mathbf{x} \tag{6.14}$$

where the parameter matrices $A^{(i)} \in \Re^{n\times n}, B \in \Re^{n\times n}$ satisfy the energy conserving conditions A1-A3 and condition B in Theorem 2.1 as well as the additional condition in (2.37).

In (6.13), we have assumed that **K** = **I** for equation (1.22). It is because any system with **K** ≠ **I** can be converted to a system with **K** = **I** with proper linear transformation. Then

$$\nabla_{\mathbf{x}} H = \frac{\partial H}{\partial \mathbf{x}} = \begin{pmatrix} x_1 \\ x_2 \\ \vdots \\ x_n \end{pmatrix}$$

The purpose is to rewrite the LOM of type (6.14) as

$$\dot{\mathbf{x}} = \mathbf{J}(\mathbf{x})\nabla_{\mathbf{x}} H \tag{6.15}$$

where the structure matrix **J** must be skew symmetric (also anti-symmetric in some references) and it should also satisfies the Jacobi condition for a Hamiltonian structure.

6.4.1 Variants of the skew symmetric matrix J for SELOM(*n*)

The matrix **J** must be a *n* x *n* matrix with zero diagonal elements and let it be

$$\mathbf{J} = \begin{pmatrix} 0 & J_{12} & J_{13} & \cdots & J_{1n} \\ J_{21} & 0 & J_{23} & \cdots & J_{2n} \\ \vdots & \vdots & \vdots & \vdots & \vdots \\ J_{n1} & J_{n2} & J_{n3} & \cdots & 0 \end{pmatrix}. \tag{6.16}$$

where J_{ij} depends on the structure parameters $a_{ij}^{(k)}$ and b_{ij} of (6.14) and the state variables x_i. Note that given a system of order *n*, there are many ways to write the matrix **J** so that it is skew symmetric. It is because any nonlinear term $a_{jk}^{(i)} x_j x_k$ in (6.14) has many ways to be written as $\left(a_{jk}^{(i)} x_j x_k + a_{kj}^{(i)} x_k x_j\right)$. So that it can contribute to either element J_{ik} or element J_{ij}. We can again use the greedy strategy used before. However, the matrix **J** so obtained does not guarantee the Jacobi conditions (see examples below). Here, we state the general rules for the skew symmetric matrix **J**.

General cases Since the matrix **J** is skew symmetric, we consider element J_{ij} only, where $i < j$ and write it as

$$J_{ij} = \left(a_{ij}^{(i)} + a_{ji}^{(i)}\right) x_i + \sum_{\substack{p=1 \\ p \neq i}}^{j-1} \left(a_{pj}^{(i)} + a_{jp}^{(i)}\right) x_p + a_{jj}^{(i)} x_j + b_{ij}. \tag{6.17}$$

The matrix **J** so obtained is a skew symmetric matrix and it satisfies all the requisites for a Hamiltonian structure except for the Jacobi identity. The following observations are in order.

1. J_{ij} is a linear expression with respect to the state variables x_i, which contains j linear terms and one constant.

2. In order for the matrix **J** to be skew symmetric, when writing J_{ji}, we have used the following energy conserving conditions:

   a. Condition A2: $a_{ii}^{(j)} = -\left(a_{ij}^{(i)} + a_{ji}^{(i)}\right)$.

   b. Condition A3: $\left(a_{pi}^{(j)} + a_{ip}^{(j)}\right) = -\left(a_{pj}^{(i)} + a_{jp}^{(i)}\right) - \left(a_{ij}^{(p)} + a_{ji}^{(p)}\right)$ with $p < j$, $i < j$ and $p \neq i$, $p \neq j$. That is the coefficient for any term of $x_i x_p$ should be divided into two coefficients as $-\left(a_{pj}^{(i)} + a_{jp}^{(i)}\right)$ and $-\left(a_{ij}^{(p)} + a_{ji}^{(p)}\right)$ respectively, and they contribute to two elements (J_{jp} and J_{ji}) of **J**.

   c. Condition B: $b_{ji} = -b_{ij}$.

Special cases for gyrostats with two nonlinear terms only If any gyrostat (x_i, x_j, x_k) according to our decomposing algorithm in Chapter 3 contains two quadratic terms only, the structure matrix **J** can be written in an alternative way. Suppose that the quadratic term for equation $\dot{x}_k$ is not available, then according to (6.17) we have to add virtual terms to ensure that the matrix **J** is skew symmetric as

$$\dot{x}_k = \left(a_{ik}^{(j)} + a_{ki}^{(j)}\right) x_i x_j + \left(a_{jk}^{(i)} + a_{kj}^{(i)}\right) x_j x_i + \cdots .$$

It is based on the energy conservation condition A3, $\left(a_{ik}^{(j)}+a_{ki}^{(j)}\right)+\left(a_{ik}^{(j)}+a_{ki}^{(j)}\right)=0$.

In order to avoid adding virtual terms, we introduce a variant matrix **J** as following:

For any triplet (x_i, x_j, x_k), if $\left(a_{ij}^{(k)}+a_{ji}^{(k)}\right)=0$, we write

$$\begin{aligned} J_{ij} &= \left(a_{ij}^{(i)}+a_{ji}^{(i)}\right)x_i+\sum_{\substack{p=1\\p\neq i\\p\neq k}}^{j-1}\left(a_{pj}^{(i)}+a_{jp}^{(i)}\right)x_p+a_{jj}^{(i)}x_j+\left(a_{kj}^{(i)}+a_{jk}^{(i)}\right)x_k+b_{ij} \quad \text{for } i<j \\ J_{ji} &= a_{ii}^{(j)}x_i+\sum_{\substack{p=1\\p\neq j\\p\neq k}}^{j-1}\left[-\left(a_{pj}^{(i)}+a_{jp}^{(i)}\right)x_p-\left(a_{ji}^{(p)}+a_{ij}^{(p)}\right)x_i\right]+\left(a_{ij}^{(j)}+a_{ji}^{(j)}\right)x_j+\left(a_{ki}^{(j)}+a_{ik}^{(j)}\right)x_k+b_{ij} \end{aligned} \tag{6.18}$$

The matrix **J** so obtained satisfies the algebraic properties of a Hamiltonian system also except for the Jacobi identity.

6.4.2 Verification of Jacobin identity

Given the definition of the Hamiltonian (6.13) and the structure matrix **J** obtained from either (6.17) or (6.18), the last task left is to verify the Jacobi condition for matrix **J** in order to claim that the system (6.14) is a Hamiltonian.

For any indices (i, j, k), the Jacobi condition (6.8) can be written as

$$\sum_{p=1}^{n}J_{ip}\frac{\partial J_{jk}}{\partial x_p}+\sum_{p=1}^{n}J_{jp}\frac{\partial J_{ki}}{\partial x_p}+\sum_{p=1}^{n}J_{kp}\frac{\partial J_{ij}}{\partial x_p}=0. \tag{6.19}$$

Since we have shown that the matrix **J** is skew-symmetric, the order of (i, j, k) is not significant. Then for any number n (order), we have to verify $\binom{n}{3}$ linear equations. It

needs totally $3\times 2\times(n-1)$ computations for each equation. So the complexity for the verification of the Jacobi identity is $O(n^3)$.

We start with the simplest case when n = 3, *i.e.* systems in ELOM(3). For simplicity, we use notation $a_{ij}^{(p)} = (a_{ij}^{(p)} + a_{ji}^{(p)})$ for $i < j$ and $i \neq j$. Then the general form of systems in ELOM(3) is

$$\begin{aligned}
\dot{x}_1 &= a_{12}^{(1)}x_1x_2 + a_{13}^{(1)}x_1x_3 + a_{23}^{(1)}x_2x_3 + a_{22}^{(1)}x_2^2 + a_{33}^{(1)}x_3^2 + b_{12}x_2 + b_{13}x_3 \\
\dot{x}_2 &= a_{12}^{(2)}x_1x_2 + a_{13}^{(2)}x_1x_3 + a_{23}^{(2)}x_2x_3 + a_{11}^{(2)}x_1^2 + a_{33}^{(2)}x_3^2 + b_{21}x_1 + b_{23}x_3 \\
\dot{x}_3 &= a_{12}^{(3)}x_1x_2 + a_{13}^{(3)}x_1x_3 + a_{23}^{(3)}x_2x_3 + a_{22}^{(3)}x_2^2 + a_{11}^{(3)}x_1^2 + b_{32}x_2 + b_{31}x_1
\end{aligned} \tag{6.20}$$

Note that $a_{ij}^{(i)} = -a_{ii}^{(j)}$, $a_{ij}^{(j)} = -a_{jj}^{(i)}$ $(j > i)$ from Condition A2 and $a_{ij}^{(k)} + a_{ik}^{(j)} + a_{jk}^{(i)} = 0$ for $i < j < k$ from Condition A3. The matrix **J** obtained from (6.17) is

$$\mathbf{J} = \begin{pmatrix}
0 & -a_{11}^{(2)}x_1 + a_{22}^{(1)}x_2 + b_{12} & -a_{11}^{(3)}x_1 + a_{23}^{(1)}x_2 + a_{33}^{(1)}x_3 + b_{13} \\
a_{11}^{(2)}x_1 - a_{22}^{(1)}x_2 + b_{21} & 0 & a_{13}^{(2)}x_1 - a_{22}^{(3)}x_2 + a_{33}^{(2)}x_3 + b_{23} \\
a_{11}^{(3)}x_1 - a_{23}^{(1)}x_2 - a_{33}^{(1)}x_3 + b_{31} & -a_{13}^{(2)}x_1 + a_{22}^{(3)}x_2 - a_{33}^{(2)}x_3 + b_{32} & 0
\end{pmatrix}$$

The Jacobi condition for n = 3 becomes

$$\left(J_{12}\frac{\partial J_{23}}{\partial x_2} + J_{13}\frac{\partial J_{23}}{\partial x_3}\right) + \left(J_{21}\frac{\partial J_{31}}{\partial x_1} + J_{23}\frac{\partial J_{31}}{\partial x_3}\right) + \left(J_{31}\frac{\partial J_{12}}{\partial x_1} + J_{32}\frac{\partial J_{12}}{\partial x_2}\right) = 0$$

Rearrange the above based on the skew symmetric property of matrix **J** ($J_{ij} = -J_{ji}$), we get

$$J_{12}\left(\frac{\partial J_{23}}{\partial x_2} - \frac{\partial J_{31}}{\partial x_1}\right) + J_{23}\left(\frac{\partial J_{31}}{\partial x_3} - \frac{\partial J_{12}}{\partial x_2}\right) + J_{31}\left(\frac{\partial J_{12}}{\partial x_1} - \frac{\partial J_{23}}{\partial x_3}\right) = 0$$

Since J_{ij} are linear functions of x_1, x_2, x_3 and $\left(\frac{\partial J_{23}}{\partial x_2} - \frac{\partial J_{31}}{\partial x_1}\right), \left(\frac{\partial J_{31}}{\partial x_3} - \frac{\partial J_{12}}{\partial x_2}\right), \left(\frac{\partial J_{12}}{\partial x_1} - \frac{\partial J_{23}}{\partial x_3}\right)$ are scalar coefficients. The above equation holds for any (x_1, x_2, x_3) only when all those scalar coefficients in the parenthesis are zeros. That is

$$\begin{aligned} \left(\frac{\partial J_{23}}{\partial x_2} - \frac{\partial J_{31}}{\partial x_1}\right) &= -a_{22}^{(3)} + a_{11}^{(3)} = 0 \\ \left(\frac{\partial J_{31}}{\partial x_3} - \frac{\partial J_{12}}{\partial x_2}\right) &= -a_{33}^{(1)} + a_{22}^{(1)} = 0 \ . \\ \left(\frac{\partial J_{12}}{\partial x_1} - \frac{\partial J_{23}}{\partial x_3}\right) &= a_{11}^{(2)} - a_{33}^{(2)} = 0 \end{aligned} \tag{6.21}$$

So any system in ELOM(3) that satisfies the above conditions is a Hamiltonian system. The above conditions imply that the traces of matrices $A^{(1)}$, $A^{(2)}$, $A^{(3)}$ in (6.14) are all zeros.

Theorem 6.1 Any system in ELOM(3) is a Hamiltonian system as long as the traces for all matrices $A^{(i)}$ for i = 1, 2, 3 are zeros.

Note that the Euler gyroscope, the Lorenz gyrostat and the general Volterra gyrostat are all special cases of ELOM(3) with zero-trace matrices $A^{(i)}$ for i = 1, 2, 3 . So they are all Hamiltonian systems.

Example 6.3 Consider the Volterra gyrostat in (B.5). If we write the matrix **J** according to (6.17)

$$\mathbf{J} = \begin{bmatrix} 0 & -c & px_2 + b \\ c & 0 & qx_1 - a \\ -px_2 - b & -qx_1 + a & 0 \end{bmatrix},$$

then it can be verified that the matrix **J** so obtained obeys the Jacobi conditions. So VG(3) is a Hamiltonian system. It can be further verified that the square of the angular momentum is one Casimir invariant of the Hamiltonian system.

If we drop the linear terms in (B.5), it becomes the Euler gyroscope. Compare the matrix **J** obtained above with that in Example 6.1. We should find that they are in different forms. These two examples demonstrate the fact that even for a Hamiltonian system, there may be many different ways to obtain the structure matrix **J** so that it satisfies all the algebraic requisites for a Hamiltonian system.

For the systems with order $n > 3$ (systems in ELOM(n) or SELOM(n)), however, we do not find a general condition for it to be a Hamiltonian system in this study. Actually, it has been found that it is practically impossible to develop a Hamiltonian LOM with more than 3-modes (see Zeitlin (1991)). In the following subsection, we provide several special examples of systems in CVG(n) that are Hamiltonian.

6.4.3 Examples of the coupled gyrostats as Hamiltonian systems

Since it is hard to develop general conditions for Hamiltonian systems with order greater than 3, in this Section we study several special LOMs that keep the Hamiltonian structure.

Example 6.4 According to Gluhovsky (2006), the following LOM(8) is Hamiltonian with the Hamiltonian function defined in (6.13).

$$\begin{cases} \dot{x}_1 = a_{23}^{(1)} x_2 x_3 + a_{45}^{(1)} x_4 x_5 \\ \dot{x}_2 = a_{13}^{(2)} x_1 x_3 + a_{57}^{(2)} x_5 x_7 + b_{23} x_3 \\ \dot{x}_3 = b_{32} x_2 \\ \dot{x}_4 = a_{15}^{(4)} x_1 x_5 + a_{37}^{(4)} x_3 x_7 + b_{45} x_5 \\ \dot{x}_5 = b_{54} x_4 \\ \dot{x}_6 = a_{78}^{(6)} x_7 x_8 \\ \dot{x}_7 = a_{25}^{(7)} x_2 x_5 + a_{34}^{(7)} x_3 x_4 + a_{68}^{(7)} x_6 x_8 + b_{78} x_8 \\ \dot{x}_8 = b_{87} x_7 \end{cases} \tag{6.22}$$

where

$$\begin{cases} a_{23}^{(1)} = -1, & a_{45}^{(1)} = -1 & & \\ \mathrm{a}_{13}^{(2)} = 1, & a_{57}^{(2)} = -\tfrac{1}{2}, & & b_{23} = -1 \\ & & & b_{32} = 1 \\ a_{15}^{(4)} = 1, & a_{37}^{(4)} = -\tfrac{1}{2}, & & b_{45} = -1 \\ & & & b_{54} = 1 \\ a_{78}^{(6)} = -2\beta & & & \\ a_{25}^{(7)} = \tfrac{1}{2}, & a_{34}^{(7)} = \tfrac{1}{2}, & a_{68}^{(7)} = 2\beta, & b_{78} = -\beta \\ & & & b_{87} = \beta \end{cases}$$

Note that $a_{ij}^{(p)}$ here is actually $\left(a_{ij}^{(p)} + a_{ji}^{(p)}\right)$ in Chapter 3.

If we derive the skew symmetric matrix $\mathbf{J_1}$ from (6.17)

$$\mathbf{J}_1 = \begin{pmatrix} 0 & 0 & -x_2 & 0 & -x_4 & 0 & 0 & 0 \\ 0 & 0 & x_1 - 1 & 0 & 0 & 0 & -\tfrac{1}{2} x_5 & 0 \\ x_2 & -x_1 + 1 & 0 & 0 & 0 & 0 & 0 & 0 \\ 0 & 0 & 0 & 0 & x_1 - 1 & 0 & -\tfrac{1}{2} x_3 & 0 \\ x_4 & 0 & 0 & -x_1 + 1 & 0 & 0 & 0 & 0 \\ 0 & 0 & 0 & 0 & 0 & 0 & 0 & -2\beta x_7 \\ 0 & \tfrac{1}{2} x_5 & 0 & \tfrac{1}{2} x_3 & 0 & 0 & 0 & 2\beta x_6 - \beta \\ 0 & 0 & 0 & 0 & 0 & 2\beta x_7 & -2\beta x_6 + \beta & 0 \end{pmatrix}.$$

Since the order $n = 8$, we have to verify $\binom{8}{3} = 56$ triplets of (i, j, k) for the Jacobi condition. With the help of Mathematica, we find that the matrix $\mathbf{J_1}$ does not satisfy the Jacobi condition for several triplets (i, j, k). For example, (1, 2, 7) is one of such triplets.

However, the matrix $\mathbf{J_2}$ derived according to (6.18) is

$$\mathbf{J}_2 = \begin{pmatrix} 0 & -x_3 & 0 & -x_5 & 0 & 0 & 0 & 0 \\ x_3 & 0 & -1 & 0 & 0 & 0 & -\tfrac{1}{2}x_5 & 0 \\ 0 & 1 & 0 & 0 & 0 & 0 & 0 & 0 \\ x_5 & 0 & 0 & 0 & -1 & 0 & -\tfrac{1}{2}x_3 & 0 \\ 0 & 0 & 0 & 1 & 0 & 0 & 0 & 0 \\ 0 & 0 & 0 & 0 & 0 & 0 & -2\beta x_8 & 0 \\ 0 & \tfrac{1}{2}x_5 & 0 & \tfrac{1}{2}x_3 & 0 & 2\beta x_8 & 0 & -\beta \\ 0 & 0 & 0 & 0 & 0 & 0 & \beta & 0 \end{pmatrix}$$

It can be verified (with the help of Mathematica) that matrix $\mathbf{J_2}$ satisfies the Jacobi condition. It is just the matrix given in Gluhovsky (2006).

Remark 6.5 This example demonstrate the fact that a system in CVG(n) has many different ways to obtain skew symmetric matrices **J**. However, some of them may satisfy the Jacobi condition and some of them may not.

Example 6.5 A system in CVG(5) for 3D Rayleigh-Bénard convection (the 3D analog of the Lorenz model without friction and forcing) is given by

$$\begin{cases} \dot{x}_1 = -x_2x_3 - x_4x_5 \\ \dot{x}_2 = x_1x_3 - x_3 \\ \dot{x}_3 = x_2 \\ \dot{x}_4 = x_1x_5 - x_5 \\ \dot{x}_5 = x_4 \end{cases} . \tag{6.23}$$

It can be verified that this system is Hamiltonian because the matrix **J** derived according to (6.18) is

$$\mathbf{J}_2 = \begin{pmatrix} 0 & -x_3 & 0 & -x_5 & 0 \\ x_3 & 0 & -1 & 0 & 0 \\ 0 & 1 & 0 & 0 & 0 \\ x_5 & 0 & 0 & 0 & -1 \\ 0 & 0 & 0 & 1 & 0 \end{pmatrix},$$

which obeys the Jacobi conditions. The matrix obtained from (6.17), however, does not satisfy the Jacobi conditions.

Example 6.6 A system in CVG(7) for 2D Rayleigh-Bénard convection with small aspect ratio (Gluhovsky 2006) is also Hamiltonian.

$$\begin{cases} \dot{x}_1 = -d_1 x_2 x_3 & -d_2 x_4 x_5 & -d_3 x_6 x_7 \\ \dot{x}_2 = d_1 x_1 x_3 - d_1 x_3 & & \\ \dot{x}_3 = d_1 x_2 & & \\ \dot{x}_4 = d_2 x_1 x_5 - d_2 x_5 & & \\ \dot{x}_5 = d_2 x_4 & & \\ \dot{x}_6 = & d_3 x_1 x_7 - d_3 x_7 & \\ \dot{x}_7 = & d_3 x_6 & \end{cases} \tag{6.24}$$

Again, the structure matrix should be derived from (6.18) instead of (6.17).

From Examples 4-6, we have observed the following facts.

1. All of the coupled gyrostats are either Lorenz gyrostats (Case 1 in Appendix B) or degenerated Euler gyroscopes. Both gyrostats contain two nonlinear terms only.

2. The coupled triplets are (1,2,3), (1,4,5), (2,5,7), (3,4,7), (6,7,8) for Example 6.4, (1,2,3), (1,4,5) for Example 6.5 and (1,2,3), (1,4,5), (1,6,7) for Example 6.6, *i.e.* no any two triples have more than 1 common indices.

Example 6.7 To examine our observations, we make a system with an extra Lorenz gyrostat (triplet (6, 7, 8)) added to Example 6.4 and get

$$\begin{cases} \dot{x}_1 = a_{23}^{(1)} x_2 x_3 + a_{45}^{(1)} x_4 x_5 - d_3 x_6 x_7 \\ \dot{x}_2 = a_{13}^{(2)} x_1 x_3 + a_{57}^{(2)} x_5 x_7 + b_{23} x_3 \\ \dot{x}_3 = b_{32} x_2 \\ \dot{x}_4 = a_{15}^{(4)} x_1 x_5 + a_{37}^{(4)} x_3 x_7 + b_{45} x_5 \\ \dot{x}_5 = b_{54} x_4 \\ \dot{x}_6 = a_{78}^{(6)} x_7 x_8 - d_3 x_7 x_1 - d_3 x_7 \\ \dot{x}_7 = a_{25}^{(7)} x_2 x_5 + a_{34}^{(7)} x_3 x_4 + a_{68}^{(7)} x_6 x_8 + b_{78} x_8 + d_3 x_6 \\ \dot{x}_8 = b_{87} x_7 \end{cases} \tag{6.25}$$

The matrix **J** according (6.18) is

$$\mathbf{J} = \begin{pmatrix} 0 & -x_3 & 0 & -x_5 & 0 & -d_3 x_7 & 0 & 0 \\ x_3 & 0 & -1 & 0 & 0 & 0 & -\tfrac{1}{2} x_5 & 0 \\ 0 & 1 & 0 & 0 & 0 & 0 & 0 & 0 \\ x_5 & 0 & 0 & 0 & -1 & 0 & -\tfrac{1}{2} x_3 & 0 \\ 0 & 0 & 0 & 1 & 0 & 0 & 0 & 0 \\ d_3 x_7 & 0 & 0 & 0 & 0 & 0 & -2\beta x_8 - d_3 & 0 \\ 0 & \tfrac{1}{2} x_5 & 0 & \tfrac{1}{2} x_3 & 0 & 2\beta x_8 + d_3 & 0 & -\beta \\ 0 & 0 & 0 & 0 & 0 & 0 & \beta & 0 \end{pmatrix}$$

It can be verified (with the help of Mathematica) that this matrix does not satisfy the Jacobi conditions. It has been noticed that system (6.25) contains a couple of triplets of (1,6,7) and (6,7,8), which have two common indices. However, even the triple (6,7,8) is removed from the system, the matrix **J** still does not satisfy the Jacobi conditions. It

seems that the triplet (1,6,7) still conflicts with triplets (2,5,7) and (3,4,7). So our observations above do not guarantee a system is Hamiltonian.

6.5 LOMS FOR BURGER'S EQUATION AS HAMILTONIAN SYSTEMS

6.5.4 Kinetic energy as Hamiltonian

The LOM(3) for Burger's equation in Example 2.5 is

$$\begin{cases} \dot{u}_1 = -\frac{1}{2}u_2u_3 - \frac{1}{2}u_1u_2 \\ \dot{u}_2 = -u_1u_3 + \frac{1}{2}u_1^2 \\ \dot{u}_3 = \frac{3}{2}u_1u_2 \end{cases} \tag{6.26}$$

It can be verified that it is a Hamiltonian system with the Hamiltonian defined as $H = \frac{1}{2}(u_1^2 + u_2^2 + u_3^2)$. And one of the structure matrix **J** can be written as

$$\mathbf{J} = \begin{pmatrix} 0 & -\frac{1}{2}u_1 - \frac{1}{2}u_3 & 0 \\ \frac{1}{2}u_1 + \frac{1}{2}u_3 & 0 & -\frac{3}{2}u_1 \\ 0 & \frac{3}{2}u_1 & 0 \end{pmatrix}.$$

Note that equation (6.26) is a system in ELOM(3). However, it does not satisfy the condition summarized in Theorem 6.1. The parameter matrices for (6.26) is

$$A^{(1)} = \begin{bmatrix} 0 & -\frac{1}{2} & 0 \\ 0 & 0 & -\frac{1}{2} \\ 0 & 0 & 0 \end{bmatrix}, A^{(2)} = \begin{bmatrix} \frac{1}{2} & 0 & -1 \\ 0 & 0 & 0 \\ 0 & 0 & 0 \end{bmatrix}, A^{(3)} = \begin{bmatrix} 0 & \frac{2}{3} & 0 \\ 0 & 0 & 0 \\ 0 & 0 & 0 \end{bmatrix}.$$

Obviously, the trace of $A^{(2)}$ is not zero. So Theorem 6.1 is just a sufficient condition for a system in ELOM(3) to be Hamiltonian.

Again, we did not find the Hamiltonian structure for LOM(n) (n > 3) of the Burger's equation. It is because the number of possible forms for matrix **J** is too large and there is no practical way to verify the Jacobi identity for all of them.

6.5.5 Cubic Hamiltonian function

Gardner (1971) has shown that the LOMs for the Burger's equation are canonical Hamiltonian systems for any order. The Burger's equation without diffusion is

$$u_t = uu_x . \tag{6.27}$$

Consider the Fourier expansion

$$u(x) = \sum_{n=-\infty}^{\infty} u_n e^{inx} \tag{6.28}$$

and define

$$F(u) = \frac{1}{6}\int_0^{2\pi} u^3 dx . \tag{6.29}$$

Then it can be verified that equation (6.27) becomes

$$u_t = \frac{\partial}{\partial x}\left(\frac{\delta F(u)}{\delta u}\right) \tag{6.30}$$

where $\frac{\delta F(u)}{\delta u}$ means the functional derivative of F with respect to u.

Substitute (6.28) into (6.29) and (6.30), we get

$$\frac{du_n}{dt} = \frac{i}{2\pi} n \frac{\partial F}{\partial u_{-n}} . \tag{6.31}$$

Equation (6.31) is a Hamiltonian system. If one defines (for n > 0)

$$q_n \equiv u_n / n, \quad p_n \equiv u_{-n}, \quad H \equiv (i/2\pi)F, \tag{6.32}$$

it can be verified that the system (6.31) is a canonical Hamiltonian system with respect to the Hamiltonian function H.

The Hamiltonian function H can be derived as following

$$\begin{aligned} H &= \frac{i}{2\pi}F = \frac{i}{2\pi}\frac{1}{6}\int_0^{2\pi}\sum_{n=-\infty}^{\infty} u_n e^{inx}dx \\ &= \frac{i}{2\pi}\frac{1}{6}\left(u_0^3 + 6u_0\sum_{n=1}^{\infty}u_n u_{-n} + 3\sum_{i=1}^{\infty}\sum_{j=1}^{\infty}u_i u_j u_{-(i+j)} + 3\sum_{i=1}^{\infty}\sum_{j=1}^{\infty}u_{-i}u_{-j}u_{(i+j)}\right). \end{aligned}$$

So the Hamiltonian function is a cubic polynomial with respect to the state variable u_n and u_{-n}. Since the Hamiltonian H does not relate to any form of energy, it is not the topic of this study.

6.6 CONCLUSIONS

We have found a sufficient condition for systems in ELOM(3) to be Hamiltonian and it is summarized in Theorem 6.1. For systems with order $n > 3$, however, it is hard to find a general condition for them to be Hamiltonian. Based on the study in Section 6.4.2 and the examples in Section 6.4.3, we draw the following conclusions.

1. System in ELOM(3) is always Hamiltonian as long as all the traces of matrices $A^{(i)}$ for i =1,2,3 are zeros.
2. It is hard to find general conditions for a system in either ELOM(n) or SELOM(n) for n >= 4 to be Hamiltonian.
3. We know several systems in CVG(n) n >= 4 that are Hamiltonian. All these systems satisfy some conditions as observed in Section 6.4.3. However, these conditions are neither sufficient nor necessary for a system to be Hamiltonian.

4. If a system is Hamiltonian, finding the right form of matrix **J** to be skew symmetric is always tricky. Even with the same definition of Hamiltonian function, many forms of the matrix **J** exist that are skew symmetric. However, only one (or some) of them satisfies the Jacobi conditions.

5. From all of the known Hamiltonian systems and their matrices **J**, we found special conditions for the Jacobi identity, for any triplet (i, j, k):

    a. either $J_{il} = 0$;

    b. or $\frac{\partial J_{jk}}{\partial x_l} = 0$ for all $l = 1, 2, \ldots, n$.

    c. If both J_{il} and $\frac{\partial J_{jk}}{\partial x_l}$ are not zero for any $l = 1, 2, \ldots, n$, then the term $J_{il}\frac{\partial J_{jk}}{\partial x_l} \neq 0$ for any $l = 1, 2, \cdots, n$ must be canceled later by a term either in $J_{jl}\frac{\partial J_{ik}}{\partial x_l} \neq 0$ for any $l = 1, 2, \cdots, n$ or in $J_{kl}\frac{\partial J_{ij}}{\partial x_l} \neq 0$ for any $l = 1, 2, \cdots, n$.

Chapter 7
CONCLUSION

LOMs are commonly obtained by applying a spectral Galerkin approximation to partial differential equations of interest in several applications such as the quasi geostrophic vorticity equation, Rayleigh-Bérnard convection equation, Burgers' equation to mention a few. LOMs contribute to the understanding of basic mechanisms and are successful in proving insights for hydrodynamic problems. Although its great success in simplifying the original PDEs of interest in geophysical applications, the Galerkin method does not provide criteria for selecting modes. The modes retained in the truncations are often chosen in *ad hoc* way, resulting in LOMs with unphysical behaviors because the fundamental conservation properties of the fluid dynamical equations may be violated.

To avoid unphysical behaviors in LOMs, it is undoubtedly clear that a LOM must at least retain the energy conservation property of the original dynamic system (Lorenz 1960, Obukhov 1969, Thiffeault and Horton 1996). However, there is still no systematic method for testing if a given LOM conserves energy. It turns out that most of all the LOMs that aris in atmospheric dynamics and turbulence are special cases of the nth order (nonlinear) ordinary differential equation

$$\dot{x}_i = \mathbf{x}^T A^{(i)} \mathbf{x} + B_i \mathbf{x} + c_i, \quad i = 1, 2, \cdots, n$$

where $A^{(i)}$ are matrices, B_i is a row vector, c_i is a scalar. With this study, we first derived a set of sufficient conditions for this general class of LOM to conserve the energy. The conditions are summarized as the following:

Condition A: The matrices $A^{(i)}$, $i = 1, 2 \ldots, n$ are such that

Condition A1: $a_{ii}^{(i)} = 0$ for $i = 1, 2, \cdots, n$

Condition A2: $K_i \left(a_{ip}^{(i)} + a_{pi}^{(i)} \right) = -K_p a_{ii}^{(p)}$ for all $i = 1, 2, \ldots, n$ and $p \neq i$

Condition A3: For $i < p < q$,

$$K_i \left(a_{pq}^{(i)} + a_{qp}^{(i)} \right) + K_p \left(a_{iq}^{(p)} + a_{qi}^{(p)} \right) + K_q \left(a_{ip}^{(q)} + a_{pi}^{(q)} \right) = 0$$

Condition B: The matrix ***B*** is such that

$$b_{ii} = 0 \quad 1 \leq i \leq n$$
$$\operatorname{sgn}(b_{ij}) \operatorname{sgn}(b_{ji}) = -1 \text{ for } i \neq j$$

and every 3×3 principal submatrix $B(1,i,j)$ formed by the elements at the intersection of the rows and columns at positions 1, i and j for $2 \leq i \leq n$ and $j > i$ is singular, and

Condition C: The vector $\boldsymbol{c} = 0$.

The matrix satisfying the condition B is called a generalized skew symmetric matrix. In particular, when $K = \mathbf{I}$, the identity matrix, the condition B implies that B must be a skew symmetric matrix.

In general, systems of order n satisfying these energy conserving conditions consist a subset of LOMs, called ELOM(n) in the dissertation. With additional conditions $a_{pp}^{(i)} = 0$ and $a_{ip}^{(i)} = a_{pi}^{(i)} = 0$ for all matrices $A^{(i)}$, $i = 1, 2, \ldots, n$, that is the elements along the principal diagonal and those along the ith row and i^{th} column of $A^{(i)}$ are zero for $i = 1, 2, \ldots, n$, an interesting subset of ELOM(n) is identified and denoted as SELOM(n).

It is well known that the Volterra gyrostat and many of its special cases including the Euler gyroscope represent a prototype of energy conserving dynamical systems.

Using these gyrostats as the basic building blocks, Obukhov (1973) and Gluhovsky et. al (1997), (1999), (2000), (2002) and (2006) have shown that many of the low-order models (LOM) of interest in geophysical fluid dynamics can be expressed as a system of coupled gyrostats. In the second part of this study, we prove the formal relation between systems in SELOM(n) and systems of coupled gyrostats. This formal connection generalizes the results of Obukhov and Gluhovsky *et al*. mentioned above. However, we also found that there is no unique decomposition from a system in SELOM(n) to the systems of coupled gyrostats. One algorithm with greedy strategy as basis is provided in the study for the synthesis purpose.

This study extended the modular approach for studying energy conserving LOMs proposed by works of Gluhovsky (1982) and Gluhovsky and his collaborator (1997, 1999, 2002 and 2006) to include the general energy conserving systems in ELOM(n). For this purpose, the generalized Volterra gyrostat is defined to includes nonlinear feedback, which is used as the elementary building block for systems not in SELOM(n), but inside of ELOM(n). Again, an algorithm similar the one proposed above is provided in the dissertation for converting any system in ELOM(n) into coupled generalized gyrostats.

As the basic building modular for LOMs studied in the geophysical fluid dynamics systems, the Volterra gyrostat and all of its special cases should be well understood. To this purpose, a comprehensive analysis of the stability of equilibria with the Volterra gyrostat and nine of its special cases was provided. The Volterra gyrostat is a three mode nonlinear systems and it has two quadratic invariants: the kinetic energy and the square of the angular momentum. The invariants further restrict the solution to lie at the intersection of the energy and the momentum ellipsoids. So the phase volume of the

system is also conserved. Thus, the equilibria in the general Volterra gyrostat and all of its special case are either stable centers or unstable saddles. Table 5.4 summarizes all of the equilibrium stability and bifurcated characteristics. It is found that the equilibrium set for all gyrostat cases can be either uniformly a saddle or uniformly a center or parts of it being a saddle and the rest are center. When the equilibrium set is uniformly a saddle, the orbits are heteroclinic with respect to the saddle. Otherwise, when the given equilibrium set is partly saddle and partly center, the orbits with respect to the saddle point is always a homoclinic in nature.

All the energy conserving LOMs are studied in the absence of forcing and dissipation. It is shown (Gluhovsky 1999) that one special case of the Volterra gyrostat, case 1 of Table 5.1 in a forced dissipative regime, can be converted to the widely known Lorenz model (Lorenz 1963) after a linear transformation of variables. The study of LOMs (Leipnik and Newton, 1981) also shows that the stability and transient behavior of ODEs exhibits strange attractors for particular parameter ranges, while for other parameter ranges the flow is periodic or even steady. As the elementary modules for constructing LOMs of nonlinear fluid dynamic, the Volterra gyrostats including the systems with terms describing forcing and friction should be studied thorough to understand the basic dynamic behavior. So it is meaningful to extend the stability study in Chapter 5 to include the forcing terms and dissipative terms. A generalization about the parameter ranges when the strange attractor appears and when it vanishes will also be useful.

While we have a good knowledge about the bifurcation and stability properties of individual gyrostat, the properties of coupled gyrostats is virtually unknown. Another

interesting area of study is to analyze the effect of coupling gyrostats in order to understand the behavior of the overall system. Furthermore, stability properties for the generalized gyrostats (GVG(3)) are also desired for better understandings about the systems not in SELOM(n).

Another interesting class of energy conserving systems includes both the canonical and non-canonical Hamiltonian systems of order n denoted by HS(n). It is well known that the Euler gyroscope is a prototype of the non-canonical HS(3) (Marsden and Ratiu (1999)). Gluhovsky (2006) has a number of interesting results relating coupled Volterra gyrostats and HS(n). A comprehensive study of the relation between energy conserving LOM(n), CGVG(n) and the HS(n) constitutes an important open problem.

BIBLIOGRAPHY

Abramowitz, M. and I. A. Stegun, 1965: *Handbook of Mathematical Functions*. Dover Publications, Inc., New York, 1046 pp.

Achatz, V., G. Schmitz and K. M. Greisinger, 1995: "Principal interaction patterns in baroclinic wave life cycles". *Journal of Atmospheric Sciences*, **52**, 3201-3213.

Arnol'd, V. I., 1989: *Mathematical Methods of Classical Mechanics*. Springer-Verlag, 462 pp.

Bellman, R., 1995: *Introduction to Matrix Analysis*, Classics in Applied Mathematics Series, **12,** SIAM, PA, U.S.A. 328 pages.

Bohr, T., M. H. Jensen, G. Paladin and A. Vulpiani, 1998: *Dynamical systems approach to turbulence*. Cambridge University Press, 350 pages.

Brown, R. and L. O. Chua, 1992: "Chaos or turbulence?", *Int. J. Bifurcation Chaos Appl. Sci. Eng.* **2**, 1005.

Canuto, C., M. Y. Hussaini, A. Quarteroni and T. A. Zang, 2006: *Spectral Methods*: *Fundamentals in Single Domain*, Springer Verlag, 563 pages.

Charney, J. G. and J. G. De Vore, 1979: "Multiple Flow Equilibria in the atmosphere and Blocking". *Journal of Atmospheric Sciences*, **36,** 1205-1216.

Cormen, T. H., C. E. Leiserson, R. L. Rivest and C. Stein, 2004: *Introduction to Algorithms*, The MIT Press, Cambridge, MA. 1180 pages.

Crommelin, D. T. and A. J. Majda, 2004: "Strategies for model reduction: comparing different optimal bases". *Journal of the Atmospheric Sciences*. **61**, 2206-2217.De Swart, H. E., 1988: "Low-order Spectral Models of the Atmospheric Circulation – A Survey". *Acta Applicomdae Mathematicae*, 49-96.

De Swart, H. E., 1988: "Low-order Spectral Models of the Atmospheric Circulation – A Survey". *Acta Applicomdae Mathematicae*, 49-96.

De Swart, H. E., 1989: *Vacillation and predictability properties of low-order atmospheric spectral models*. *CWI Tract 60*, Center for Mathematics and Computer Science, Amsterdam, The Netherlands, 121 pp.

Delsole, 2001: "Optimally persistent patterns in time varying fields". *Journal of the Atmospheric Sciences*, **58**, 1341-1356.

Devaney, R. L., 1989: *An Introduction to Chaotic Dynamical Systems*. second ed. Addison Wesley, Reading, Mass., 335 pp.

Elipe, A., M. Arribas and A. Riaguas, 1997: Complete Analysis of Bifurcation in the Axial Gyrostat Problem. *Journal of Physics A: Mathematical and General*, **30,** 587-601.

Epstein, E., 1969: Stochastic dynamic prediction. *Tellus*, **21,** 739-759.

Farell, B. F. and P. J. Ioannou, 2001: "Accurate low-dimensional approximation of the linear dynamics of fluid flow". *Journal of Atmospheric Sciences*, **58**, 2771-2789.

Friedrich, R. and H. Haken, 1992: "Nonequilibrium phase transition in a system with chaotic dynamics. The ABCDE model". *Physics Letters*, A, **164**, 299-304.

Gardner, S. C., 1971: "Korteweg-de Vries Equation and Generalizations. IV. The Korteweg-de Vries Equation as a Hamiltonian system". *Journal of Mathematical Physics*, **12**, 8, 1548-1551.

Gluhovsky, A., 1982: "Nonlinear systems that are superpositions of gyrostats". *Sov. Phys. Doklady*, **27,** 823-825.

Gluhovsky, A. and E. Agee, 1997: "An Interpretation of Atmospheric Low-order Models". *Journal of the Atmospheric Sciences*, **54,** 768-773.

Gluhovsky, A. and C. Tong, 1999: "The Structure of Energy Conserving Low-order Models". *phys. Fluids*, **11,** 334-343.

Gluhovsky, A., C. Tong, and E. Agee, 2002: "Selection of Modes in Convective Low-order Models". *Journal of Atmospheric Sciences*, **59,** 1383-1393.

Gluhovsky, A, 2006: "Energy Conserving and Hamiltonian Low-order Models in Geophysical Fluid Dynamics". *Nonlinear Processes in Geophysics*, **13,** 125-133.

Guckenheimer, J., and P. Holmes, 1983: *Nonlinear Oscillilations, Dynamical Systems and bifurcation of Vector Fields*. Springer Series of Applied Mathematical Sciences, **42,** New York, 459 pp.

Haken, H., 1975: "Analogy between higher instabilities in fluids and lasers". *Physics Letters*, A. **53**. 77-79.

Hemati, N., 1994: "Strange attractors in Brushless DC motors". *IEEE Transactions on Circuits and Systems-I: Fundamental Theory and Applications*. **41**, 40-45.

Hermiz, K. B., P. N. Guozdar, and J. M. Finn, 1995: "Improved Low-order Model for Shear Flow Driven by Rayleigh-Bernard Convection". *Physical Review*, **51E,** 325-331.

Hirsch, M. W. and S. Smale, 1974: *Differential Equations, Dynamical Systems and Linear Algebra*. Academic Press, New York, 358 pp.

Holmes, P., J. L. Lumley and G. Berkooz, 1996: *Turbulence, coherent structures, dynamical systems and symmetry*. Cambridge University Press, 420 pages.

Howard, L. N. and R. Krishnamurti, 1986: "Large-scale Flow in Turbulent Convection: A Mathematical model". *Journal of Fluid Mechanics*, **170,** 385-410.

Hughs, P. C., 1986: *Spacecraft Attitude Dynamics*. Wiley, New York.

Knobloch, E., 1981: "Chaos in segmented disc dynamo". *Physics Letters*, A, **82**, 439-440.

Krishnamurti, T. N., H. S. Bedi, V. M. Hardiker and L. Ramaswarny, 2006: *An introduction to Global Spectral Modeling*. Springer Verlag, Second Edition, 317 pp.

Kuang, J., S. H. Tan, K. Arichandram and A. Y. T. Leung, 2001: Chaotic Dynamics of an Asymmetric Gyrostat. *International Journal of Nonlinear Mechanics*, 1213-1233.

Kuang, J., S. H. Tan, A. Y. T. Leung, 2000: Chaotic Attitude Motion of Satellites under Small Perturbation Torques. *Journal of Sound and Vibration*, 175-200.

Kuang, J., S. H. Tan, and A. Y. T. Leung, 2002: Chaotic Attitude Tumbling of an Asymmetric Gyrostat in a Gravitational Field. *Journal of Guidance and Control*, **25,** 804-814.

Kundu, P. K., 1990: *Fluid Mechanics,* Academic Press, 638 pages.

Kwasniok, F., 1996: "The reduction of complex dynamical systems using principal interaction patterns". *Physica D*, **92**, 28-60.

Kwasniok, F., 2001: "Low-dimensional models of the Ginsburg-Landau equation", *SIAM Journal on Applied Mathematics*, **61**, 2063-2079.

Kwasniok, F, 2004: "Empirical low-order models of barotropic flow", *Journal of Atmospheric Sciences*, **61**, 235-245.

Lakshmivarahan, S., Y. Honda, and J. M. Lewis, 2003: Second-order approximation to the 3dvar cost function: application to analysis and forecast. *Tellus*, **55A,** 371-384.

Lakshmivarahan, S., M. E. Baldwing and T. Zheng, 2006: "Further Analysis of Lorenz's Maximum Simplification Equation". *Journal of Atmospheric Sciences,* **63**, 2673-2699.

Lakshmivarahan, S. and Y. Wang, 2007a: "On the structure of the energy conserving low-order models and their relation to Volterra gyrostat". *Nonlinear Anal: Real World Appl.*, doi: 10.1016/j.nonrwa.2007.04.002.

Lakshmivarahan, S. and Y. Wang, 2007b: "On the relation between energy conserving low-order models and a system of coupled generalized Volterra gyrostats with nonlinear feedback". *Journal of Nonlinear Science* (Accepted).

Landau, L. D. and E. M. Lifshitz, 1960: *Mechanics*. Pergamon Press, 165 pp.

Legras, B. and M. Ghil, 1985: "Persistent Anomalies, Blocking and Variations in Atmospheric Predictability". *Journal of Atmospheric Sciences*, **42,** 433-471.

Leipnik, R. B. and T.A. Newton, 1981: "Double Strange Attractors in Rigid Body Motion with Linear Feed-back Control", *Physics Letters*, **86A,** 63-67.

Lewis, J. M., S. Lakshmivarahan, and S. K. Dhall, 2006: *Dynamic Data Assimilation: A least squares approach*. Cambridge University Press, Cambridge, England, chapter 32. 850 pp.

Li, Q. and Wang, H., 1998: "Has chaos implied by macrovariable equations been justified". *Physical Review*, E, **58**, R1191-1194.

Lorenz, E. N., 1960: "Maximum Simplification of the Dynamic Equations". *Tellus*, **12,** 243-254.

Lorenz, E. N., 1962: "Simplified Dynamic Equations Applied to the Rotating-Basin Experiments". *Journal of Atmospheric Sciences*, **19,** 39-51.

Lorenz, E. N., 1963: "Deterministic Non-periodic Flows". *Journal of Atmospheric Sciences*, **20,** 130-141.

Lorenz, E. N., 1982: "Low-order Models of Atmospheric Circulation". *Journal of the Meteorological Society of Japan*, **60,** 255-267.

Marsden, J. E. and T. S. Ratiu, 1999: *Introduction to Mechanics and Symmetry: a basic exposition of classical mechanical systems*, Springer, 582 pages.

Namias, J., 1950: The index cycle and its role in the general circulation. *Journal of Meteorology*, **7,** 130-139.

Obukhov, A. M., 1973: "On the Problem of Nonlinear Interactions in Fluid Dynamics", *Gerlands Beitr. Geophysics*, **82**, 282-290.

Obukhov, A. M. and E. V. Dolzhansky, 1975: In simple models for simulation of nonlinear processes in convection and turbulence. *Geophysical Fluid Dynamics*, **6,** 195-.

Pedlosky, J., 1987: *Geophysical Fluid Dynamics*, Springer Verlay, 710 pages.

Peña, M. and E. Kalnay, 2004: "Separating fast and slow modes in coupled chaotic systems". *Nonlinear Processes in Geophysics*. **11**, 319-327.

Platzman, G. W., 1962: The analytical dynamics of the spectral vorticity equation. *Journal of Atmospheric Sciences***,** 313-328.

Platzman, G. W., 1964: "An Exact Integral of Complete Spectral Equation for Unsteady One Dimensional Flow". *Tellus*, **16,** 422-431.

Rega, G. and H. Troger, 2005: "Dimension reduction of dynamical systems: Methods, Models, Application". Special Issue on Dimension Reduction of Dynamical Systems, *Nonlinear Dynamics*, **41**, 1-15.

Rinne, J., and V. Karhilla, 1975: "A spectral barotropic model in horizontal empirical orthogonal functions". *Quarterly Journal of the Royal Meteorological Society*, **101**, 365-382.

Roebber, P. J., 1995: "Climate variability in a low-order coupled atmosphere-ocean model", *Tellus*, **47A**, 473-494.

Saltzman, B., 1959: On the maintenance of large scale quasi-permanent disturbances of the atmosphere. *Tellus*, **11,** 425-431.

Saltzman, B., 1962: "Finite Amplitude Free Convection as an Initial Value Problem-I". *Journal of Atmospheric Sciences*, **19,** 329-341.

Smith, T. R., J. Moehlis and P. Holmes, 2005: "Low-dimensional modeling of turbulence using proper orthogonal decomposition: A tutorial". Special Issue on Dimension Reduction of Dynamical Systems, *Nonlinear Dynamics*, **41**, 275-307.

Starostin, E. L., 1996: "Three-dimensional shapes of looped DNA", *Meccanica*, **31**, 235-271.

Silberman, I., 1954: "Planetary Waves in the Atmosphere". *Journal of Meteorology*, **11,** 27-34.

Sparrow, C., 1982: *The Lorenz Equations: Bifurcation, Chaos, and Strange Attractors*. Vol. 41, *Applied Mathematical Sciences*, Springer Verlag, New York, 259 pp.

Thiffeault, J. L. and W. Horton, 1996: "Energy-Conserving Truncations for Convection with Shear Flow". *Physics of Fluids*, **8,** 1715-1719.

Thompson, P. D., 1957: Uncertainty of initial state as a factor in the predictability of large scale atmosphere pattern. *Tellus*, **9,** 275-295.

Tong, C. and A. Gluhovsky, 2002: "Energy-conserving Low-order Models for three–dimensional Rayleigh-Bénard Convection". *Physical Review,* **E,** 6**5,** 04306-1 to 04396-11.

Tong, X and B. Tabarrock, 1997: Bifurcation of Self-Excited Rigid Bodies Subjected to Small Perturbation Torques. *Journal of Guidance and Control*, **20,** 123-128.

Tong, X, B. Tabarrock and F. P. J. Rimroh 1995: Chaotic Motion of An Asymmetric Gyrostat in the Gravitational Field. *International Journal of Nonlinear Mechanics*, **30,** 191-203.

Uspensky, J.V, 1948: *Theory of Equations*, McGraw Hill, New York, 353 pp.

Wang, Y. and S. Lakshmivarahan, 2007: "Analysis of Bifurcation and Stability of Equilibria in Energy Conserving Low Order Models: Volterra Gyrostat", SIAM Conference on the Applications of the Dynamical Systems, Snowbird, Utah, USA, May 28 – June 1, 2007.

Wiin-Nielson, A., 1992: Comparision of low-order atmospheric dynamical systems. *Atmosfera*, **5,** 135-155.

Wittenberg, J., 1977: *Dynamics of Systems of Rigid Bodies*. B.G. Teubner, 224pp.

Zeitlin, V., 1991: "Finite-mode analogs of 2D ideal hydrodynamics: Coadjoint orbits and local canonical structure", *Physica* **D**, 49, 353-362.

APPENDIX A

Regrouping of the Nonlinear Terms in ODEs

In this Appendix, we describe the process of regrouping the nonlinear terms in $\mathbf{x}^T KA(\mathbf{x},\mathbf{x})$ using which we arrive at the conditions A1-A3 in chapter 2. Consider

$$\mathbf{x}^T KA(\mathbf{x},\mathbf{x}) = \sum_{i=1}^{n} x_i K_i \left[\mathbf{x}^T A^{(i)} \mathbf{x}\right] \tag{A.1}$$

where the quadratic form can be rewritten as the sum of two terms:

$$\begin{aligned} \mathbf{x}^T A^{(i)} \mathbf{x} &= \sum_{p,q=1}^{n} a_{pq}^{(i)} x_p x_q \\ &= \sum_{p=1}^{n} a_{pp}^{(i)} x_p^2 + \sum_{\substack{p,q=1 \\ p\neq q}}^{n} a_{pq}^{(i)} x_p x_q . \end{aligned} \tag{A.2}$$

Substituting (A.2) into the righ-hand side of (A.1), we get

$$\mathbf{x}^T KA(\mathbf{x},\mathbf{x}) = \sum_{i=1}^{n} x_i K_i \sum_{p=1}^{n} a_{pp}^{(i)} x_p^2 + \sum_{i=1}^{n} x_i K_i \sum_{\substack{p,q=1 \\ p\neq q}}^{n} a_{pq}^{(i)} x_p x_q \, . \tag{A.3}$$

The first term on the right-hand side of (A.3) can be regrouped as the sum of two terms:

$$\sum_{i=1}^{n} x_i K_i \sum_{p=1}^{n} a_{pp}^{(i)} x_p^2 = \sum_{i=1}^{n} K_i a_{ii}^{(i)} x_i^3 + \sum_{i=1}^{n} K_i \sum_{\substack{p=1 \\ p\neq i}}^{n} a_{pp}^{(i)} x_i x_p^2 \, . \tag{A.4}$$

Likewise, the second term on the right-hand side of (A.3) can be expressed as the sum of three terms:

$$\sum_{i=1}^{n} x_i K_i \sum_{\substack{p,q=1 \\ p\neq q}}^{n} a_{pq}^{(i)} x_p x_q = \sum_{i=1}^{n} x_i K_i \sum_{\substack{q=1 \\ q\neq i}}^{n} a_{iq}^{(i)} x_i x_q + \sum_{i=1}^{n} x_i K_i \sum_{\substack{p=1 \\ p\neq i}}^{n} a_{pi}^{(i)} x_p x_i + \sum_{i=1}^{n} x_i K_i \sum_{\substack{p,q=1 \\ p\neq i, q\neq i, p\neq q}}^{n} a_{pq}^{(i)} x_p x_q \ . \quad \text{(A.5)}$$

Since p and q are dummy variables, we can combine the first two terms on the right-had side of (A.5) to obtain

$$\sum_{i=1}^{n} x_i K_i \sum_{\substack{p,q=1 \\ p\neq q}}^{n} a_{pq}^{(i)} x_p x_q = \sum_{i=1}^{n} K_i \sum_{\substack{p=1 \\ p\neq i}}^{n} \left(a_{ip}^{(i)} + a_{pi}^{(i)} \right) x_i^2 x_p + \sum_{i=1}^{n} x_i K_i \sum_{\substack{p,q=1 \\ p\neq i, q\neq i, p\neq q}}^{n} a_{pq}^{(i)} x_p x_q \ . \quad \text{(A.6)}$$

Now substituting (A.4) and (A.6) into the right-hand side of (A.3) and simplifying, we obtain

$$\begin{aligned} \mathbf{x}^T K A(\mathbf{x}, \mathbf{x}) = & \sum_{i=1}^{n} K_i a_{ii}^{(i)} x_i^3 + \sum_{i=1}^{n} K_i \sum_{\substack{p=1 \\ p\neq i}}^{n} a_{pp}^{(i)} x_i x_p^2 \\ & + \sum_{i=1}^{n} K_i \sum_{\substack{p=1 \\ p\neq i}}^{n} \left(a_{ip}^{(i)} + a_{pi}^{(i)} \right) x_i^2 x_p + \sum_{i=1}^{n} K_i \sum_{\substack{p,q=1 \\ p\neq i, q\neq i, p\neq q}}^{n} a_{pq}^{(i)} x_i x_p x_q . \end{aligned} \quad \text{(A.7)}$$

Expanding the terms and collecting the like terms, we now obtain the final grouping as

$$\begin{aligned} \mathbf{x}^T K A(\mathbf{x}, \mathbf{x}) = & \sum_{i=1}^{n} K_i a_{ii}^{(i)} x_i^3 + + \sum_{i=1}^{n} \sum_{\substack{p=1 \\ p\neq i}}^{n} \left(K_p a_{ii}^{(p)} + K_i \left(a_{ip}^{(i)} + a_{pi}^{(i)} \right) \right) x_i^2 x_p \\ & + \sum_{i<p<q} x_i x_p x_q \left[K_i \left(a_{pq}^{(i)} + a_{qp}^{(i)} \right) + K_p \left(a_{iq}^{(p)} + a_{qi}^{(p)} \right) + K_q \left(a_{ip}^{(q)} + a_{pi}^{(q)} \right) \right] \end{aligned}$$

which directly leads to (2.25) in the main body of Chapter 2.

APPENDIX B

Volterra Gyrostat: An Overview

In this Appendix, we provide a succinct overview of the Volterra gyrostat and many of its special cases. For more detail refer to Wittenberg (1977), Gluhovsky and Tong (1999).

The dynamics of the Volterra gyrostat is described by a system of three coupled nonlinear (ordinary) differential equations given by

$$\left.\begin{aligned} I_1\dot{\omega}_1 &= (I_2 - I_3)\omega_2\omega_3 + h_2\omega_3 - h_3\omega_2 \\ I_2\dot{\omega}_2 &= (I_3 - I_1)\omega_1\omega_3 + h_3\omega_1 - h_1\omega_3 \\ I_3\dot{\omega}_3 &= (I_1 - I_2)\omega_1\omega_2 + h_1\omega_2 - h_2\omega_1 \end{aligned}\right\} \tag{B.1}$$

where I_i, i = 1, 2, 3 are the **principal moments of inertia**, $\boldsymbol{\omega} = (\omega_1, \omega_2, \omega_3)^T$ is the vector of **angular velocity** of the gyrostat and h is the fixed **angular momentum** caused by the relative motion of the rotor. Following Leipnik and Newton (1981) the linear terms on the right-hand side of (B.1) can also be considered as the state feed-back that controls the behavior of the gyrostat.

A fundamental property of the dynamics (B.1) is that it conserves the following quantities:

1). **Kinetic energy**:

$$E(\boldsymbol{\omega}) = \frac{1}{2}\sum_{i=1}^{3} I_i\omega_i^2 \tag{B.2}$$

2). **Square of the angular momentum**:

$$M^2(\boldsymbol{\omega}) = \sum_{i=1}^{3} \left(I_i \omega_i + h_i \right)^2 \tag{B.3}$$

3). **Phase volumes**, that is,

$$\sum_{i=1}^{3} \frac{\partial \dot{\omega}_i}{\partial \omega_i} = 0$$

It is useful to change the variables in (B.1) using

$$v_i = I_i^{1/2} \omega_i, \quad i = 1, 2, 3 \tag{B.4}$$

Substituting (B.2) into (B.1), the latter becomes

$$\left.\begin{aligned} \dot{v}_1 &= p v_2 v_3 + b v_3 - c v_2 \\ \dot{v}_2 &= q v_1 v_3 + c v_1 - a v_3 \\ \dot{v}_3 &= r v_1 v_2 + a v_2 - b v_1 \end{aligned}\right\} \tag{B.5}$$

where

$$\left.\begin{aligned} p &= J(I_2 - I_3) \quad a = J h_1 I_1^{1/2} \\ q &= J(I_3 - I_1) \quad b = J h_2 I_2^{1/2} \\ r &= J(I_1 - I_2) \quad c = J h_3 I_3^{1/2} \\ J &= (I_1 I_2 I_3)^{-1/2} \quad \text{and} \quad p + q + r = 0 \end{aligned}\right\}. \tag{B.6}$$

By exploiting the symmetries in the system, we can identify nine different special cases (Gluhovsky and Tong (1999)) which are listed in Table B.1.

By adding friction and forcing and after a linear transformation of the variables and time, the gyrostat corresponding to case 1 (r = 0; b = c = 0) in Table B.1 can be reduced to the now classic Lorenz's system of equations (Lorenz (1963)). Hence, this case is called the **Lorenz gyrostat**. Similarly, the gyrostat corresponding to case 5 (a = b = c = 0) is called **Euler gyroscope** and it also corresponds to the maximum simplification equations of Lorenz (1960). The gyrostat with two linear terms in case 6 with the addition

of friction has been shown to exhibit double strange attractor by Leipnik and Newton (1981).

Table B.1. Special cases of Volterra gyrostat

Case	Choice of parameters	Notes	Properties of the r.h.s. of (B.3)	
			# of nonlinear terms	# of linear terms
1	$r = 0$; $b = c = 0$	Lorenz gyrostat	2	2
2	$r = 0$; $c = 0$		2	4
3	$r = 0$; $b = 0$		2	4
4	$r = 0$		2	6
5	$a = b = c = 0$	Euler gyroscope	3	0
6	$b = c = 0$	Double strange attractors (Leipnik and Newton (1981))	3	2
7	$c = 0$		3	4
8	$r = 0$; $a=b=c=0$	Degenerate case	2	0
9	$r = 0$; $a = b = 0$	Degenerate case	2	2

Using these nine gyrostats as the basic building block, Gluhovsky and Agee (1997), Gluhovsky and Tong (1999), Gluhovsky et. al. (2002) and Gluhovsky (2006) have shown that several specific low-order models of interest in geophysical fluid dynamics can be synthesized (with the addition of friction and forcing) as a system of coupled gyrostats.

In Chapter 3 and Chapter 4 of this dissertation, we use only the following four gyrostats: case 5 with no linear terms, case 6 with two linear terms, case 7 with four linear terms and the general case in (B.3) with six linear terms.

Since we will be dealing with several gyrostats in the main body of the dissertation, to save space, we develop a succinct notation to represent them. Referring to the Table B.2, the Volterra gyrostat in (B.3) is represented by the triplet (1 2 3). For $i = 1$, the presence of the two linear terms corresponding to the variables v_2 and v_3 are denoted

by entries 1 and 1 in the column for $\dot{v}_i$ with $i = 1$. Notice that the Volterra gyrostat has six 1 entries in the row corresponding to the six linear terms in the Volterra gyrostat. The gyrostat for case 7 (with $c = 0$), since $\dot{v}_1$ has no linear term for v_2, it is denoted by the entry 0. Thus, case 7 has four 1 entries, case 6 has two 1 entries and case 5 has no 1 entry in it.

Table B.2. A representation of the gyrostats used in the main body

Case	Triplet (i j k) in Equation (B.3)	Linear terms in equation (B.3)					
		$\dot{v}_i$		$\dot{v}_j$		$\dot{v}_k$	
		v_j	v_k	v_i	v_k	v_i	v_j
Volterra gyrostat	(1 2 3)	1	1	1	1	1	1
Case 7 ($c = 0$)	(1 2 3)	0	1	0	1	1	1
Case 6 ($b = c = 0$)	(1 2 3)	0	0	0	1	0	1
Case 5 ($a = b = c = 0$)	(1 2 3)	0	0	0	0	0	0

APPENDIX C

Cardan's Formula For The Roots of A Cubic Polynomial

In this appendix, we provide a summary of the derivation of the roots of the cubic polynomial based on the developments in chapter 5 of the classic book by Uspensky (1948). Let

$$f(x) = x^3 + ax^2 + bx + c = 0 \tag{C.1}$$

be the cubic polynomial equation to be solved. Setting $x = y - (\frac{a}{3})$, $f(x)$ is transformed into

$$g(y) = y^3 + py + q = 0 \tag{C.2}$$

where

$$p = b - \frac{a^3}{3} \text{ and } q = c - \frac{ba}{3} + \frac{2a^3}{27}.$$

Now expressing y as a sum of two new variables u and v and requiring that $3uv = -p$, the solution of (C.2) is obtained by solving

$$u^3 + v^3 = -q \text{ and } 3uv = -p. \tag{C.3}$$

Once again setting $A = u^3$ and $B = v^3$, since (C.3) refer to the sum and products of A and B, indeed A and B are obtained as the roots of the quadratic equation

$$z^2 + qz - \frac{p^3}{27} = 0 \tag{C.4}$$

hence,

$$A = -\frac{q}{2} + \sqrt{\frac{\Delta}{108}}$$
$$B = -\frac{q}{2} - \sqrt{\frac{\Delta}{108}} \tag{C.5}$$

where the discriminant Δ is given by

$$\Delta = 4p^3 + 27q^2 . \tag{C.6}$$

Denoting the cube root of unity as

$$w = \frac{-1 + i\sqrt{3}}{2}$$

It follows that the three possible values of u and v are given by

$$u_1 = \sqrt[3]{A}, \quad u_2 = w\sqrt[3]{A} \text{ and } u_3 = w^2\sqrt[3]{A} \tag{C.7}$$

and

$$v_1 = \sqrt[3]{B}, \quad v_2 = w\sqrt[3]{B} \text{ and } v_3 = w^2\sqrt[3]{B} . \tag{C.8}$$

In constructing y, the idea is to choose u_i arbitrarily from the three possibilities in (C.7) but the choice of v_i is constrained by the requirement that $3u_iv_i = -p$. The set of all legal pairings that satisfy this requirement is given by

$$S = \{(u_1, v_1), (u_2, v_3), (u_3, v_2)\} . \tag{C.9}$$

Let $(\alpha, \beta) \in S$ be a legal pair. Then the three roots of (C.2) are given by

$$y_1 = \alpha + \beta$$
$$y_2 = w\alpha + w^2\beta \tag{C.10}$$
$$y_3 = w^2\alpha + w\beta.$$

From the properties of the roots depend on the sign of the discriminant Δ in (C.6). Three cases arise. Refer to Table C.1 for a summary.

Case 1: Δ = 0. Then $A = B = -\frac{q}{2}$ and the roots are given by

$$y_1 = 2\sqrt[3]{-\frac{q}{2}} \quad y_2 = \sqrt[3]{\frac{q}{2}} \text{ and } y_3 = \sqrt[3]{\frac{q}{2}}\,. \tag{C.11}$$

Case 2: Δ > 0. In this case, *A* and *B* are real and let *u* and *v* be denoted the real cube roots of *A* and *B*, where $u \neq v$ since $A \neq B$ and $3uv = -p$. Hence the equation (C.2) has a real root

$$y_1 = u + v$$

and the two other roots are complex conjugates given by

$$\begin{aligned} y_2 &= wu + w^2 v = \left(-\frac{1}{2} + i\frac{\sqrt{3}}{2}\right)u + \left(-\frac{1}{2} - i\frac{\sqrt{3}}{2}\right)v \\ &= -\frac{(u+v)}{2} + i\sqrt{3}\frac{(u-v)}{2} \\ y_3 &= w^2 u + wv = \left(-\frac{1}{2} - i\frac{\sqrt{3}}{2}\right)u + \left(-\frac{1}{2} + i\frac{\sqrt{3}}{2}\right)v \\ &= -\frac{(u+v)}{2} - i\sqrt{3}\frac{(u-v)}{2}. \end{aligned}$$

Case 3: Δ < 0. In this case

$$\begin{aligned} A &= -\frac{q}{2} + i\sqrt{-\frac{\Delta}{108}} \\ B &= -\frac{q}{2} - i\sqrt{-\frac{\Delta}{108}}. \end{aligned}$$

Let

$$\sqrt[3]{A} = \alpha = \eta + i\xi$$

be the cube root of A. Then the B satisfying the constraint is

$$\sqrt[3]{B} = \beta = \eta - i\xi$$

and using (C.10), we get

$$\begin{aligned}
y_1 &= 2\eta \\
y_2 &= \left(-\frac{1}{2} + i\frac{\sqrt{3}}{2}\right)(\eta + i\xi) + \left(-\frac{1}{2} - i\frac{\sqrt{3}}{2}\right)(\eta - i\xi) \\
&= -\eta - \sqrt{3}\xi \\
y_3 &= \left(-\frac{1}{2} - i\frac{\sqrt{3}}{2}\right)(\eta + i\xi) + \left(-\frac{1}{2} + i\frac{\sqrt{3}}{2}\right)(\eta - i\xi) \\
&= -\eta + \sqrt{3}\xi
\end{aligned}$$

which are all real roots. These results are summarized in Table C.1.

Table C.1 The roots of a cubic Polynomial

Roots of (C.2)	Case 1 $\Delta = 0$ (all real roots)	Case 2 $\Delta > 0$	Case 3 $\Delta < 0$ (all real roots)
y_1	$2\sqrt[3]{-\frac{q}{2}}$	$u + v$	2η
y_2	$\sqrt[3]{\frac{q}{2}}$	$-\frac{(u+v)}{2} + i\sqrt{3}\frac{(u-v)}{2}$	$-\eta - \sqrt{3}\xi$
y_3	$\sqrt[3]{\frac{q}{2}}$	$-\frac{(u+v)}{2} - i\sqrt{3}\frac{(u-v)}{2}$	$-\eta + \sqrt{3}\xi$